

BEFORE

THE PUBLIC UTILITIES COMMISSION OF OHIO

In the Matter of the Application of Duke)
Energy Ohio, Inc. to Establish its Fuel and) Case No. 07-974-EL-UNC
Purchased Power Component of its Market-)
Based Standard Service Office for the Period)
of July 1, 2007, through December 31, 2008.)

In the Matter of the Application of Duke)
Energy Ohio, Inc. to Establish its 2008)
System Reliability Tracker of its Market-) Case No. 07-975-EL-UNC
Based Standard Service Offer.)

DIRECT TESTIMONY OF

TIMOTHY J. THIEMANN

ON BEHALF OF

DUKE ENERGY OHIO, INC.

March 2, 2009

RECEIVED-DOCKETING DIV

2009 MAR -2 PM 2:18

PUCO

This is to certify that the images appearing are an
accurate and complete reproduction of a case file
document delivered in the regular course of business.
Technician Date Processed MAR 02 2009

TABLE OF CONTENTS

	<u>PAGES</u>
I. Introduction	1
II. Purpose Of Testimony	3
III. Discussion Of The Spring 2007 Zimmer Outage And The Auditor's Recommendations.....	4
IV. Conclusion	18

Attachments:

TJT-1 Memorandum to David Warren

TJT-2 Siemens Memo Date July 30, 2007.

TJT-3 Evaluation of LP Rotor Rim-Attachment Cracking
Using LPRimLife

TJT-4 Westinghouse Memos dated 9-24-84, 12-20-84 and 12-27-84

I. INTRODUCTION

1 **Q. PLEASE STATE YOUR NAME AND BUSINESS ADDRESS.**

2 **A. My name is Timothy J. Thiemann, and my business address is 139 East Fourth**
3 **Street, Cincinnati, Ohio 45202.**

4 **Q. BY WHOM ARE YOU EMPLOYED AND IN WHAT CAPACITY?**

5 **A. I am employed by Duke Energy Business Services, Inc. as General Manager,**
6 **Generation Services, Non-Regulated.**

7 **Q. PLEASE DESCRIBE YOUR EDUCATIONAL AND PROFESSIONAL**
8 **BACKGROUND.**

9 **A. I received a B.S. in Mechanical Engineering Technology from the University of**
10 **Cincinnati. In addition, during the past twenty-three years, I have attended**
11 **many seminars, workshops and forums on subject matters such as power plant**
12 **maintenance and generation-specific technical training as well as other utility**
13 **related topics. I began my career as a co-operative education student at The**
14 **Cincinnati Gas and Electric Company (CG&E) - Miami Fort Station in 1986. In**
15 **1987, I became a full-time employee in the capacity of a Cadet Engineer at East**
16 **Bend Station. Over the next several years, I was promoted through several of**
17 **the staff engineering classifications. I worked at East Bend Station for**
18 **approximately nine years. During that time, I performed various functions**
19 **including the Work Management Coordinator, Boiler and Turbine Maintenance**
20 **Liaison, Outage Coordinator, Maintenance and Operations Engineer. I also**
21 **worked at W. H. Zimmer Station in a staff engineering capacity during the unit**
22 **start up for about one year.**

1 In 1995, I was promoted to Superintendent of Production Projects at our
2 Gibson Generating Station. In this position, I was responsible for all
3 maintenance and outage projects in the plant as well as managing the contractor
4 maintenance work force. Toward the end of 1996, I was in the temporary
5 position of an Investment Engineer working on a new capital allocation and
6 justification system for the generation plants within Cinergy Corp., the parent
7 company of CG&E. During this time, I also held the position of Production
8 Coordinator at East Bend Station.

9 In 1997, I left Cinergy Corp. and took a position at Enerfab Corporation
10 where I managed an Industrial Maintenance Division. In this position, I was
11 responsible for the profitability of the division as well as providing technical
12 direction and support at various industrial sites where we performed contractor
13 work.

14 In 1999, I returned to Cinergy Corp. as a project engineer responsible for
15 rebuilding gas turbines. I was promoted to Engineering Manager in 2000, with
16 responsibility for all capital projects at the Company's East Bend Generating
17 Station, Miami Fort Station and the Combustion Turbine Fleet. In 2001, I
18 became the Production Manager at Miami Fort Station. I was responsible for
19 the safe and efficient operations of all the units at the plant. In 2004, I was
20 promoted to General Manager II at Miami Fort Station. In this position, I had
21 responsibility for the safety, financial, environmental and efficient operations of
22 the plant. In October of 2008, I became General Manager, Duke Energy
23 Business Services, Non-Regulated.

1 **Q. PLEASE DESCRIBE YOUR RESPONSIBILITIES AS GENERAL**
2 **MANAGER GENERATION SERVICES, NON-REGULATED.**

3 **A. I am responsible for managing services that support Duke Energy Ohio's (DE-**
4 **Ohio or Company) generation operations including: responsibility for long-term**
5 **maintenance outage scheduling, fleet measures development and support, work**
6 **management practices, generating station financial management and business**
7 **planning, management of long-term service contracts and responsibility for the**
8 **CD/CCD Joint Owned Units.**

9 **II. PURPOSE OF TESTIMONY**

10 **Q. WHAT IS THE PURPOSE OF YOUR TESTIMONY IN THIS**
11 **PROCEEDING?**

12 **A. The purpose of my testimony is to discuss the circumstances surrounding the**
13 **extension of the Zimmer Generation Station outage in the spring of 2007 and**
14 **explain how DE-Ohio's decision to extend the outage was reasonable and**
15 **prudent and that the replacement power costs were reasonably and prudently**
16 **incurred. This particular outage was the subject of two auditor**
17 **recommendations in the last audit of DE-Ohio's Fuel and Economy Purchased**
18 **Power Rider (Rider FPP), in Case No. 07-723-EL-UNC. As part of the**
19 **resolution of that case, the outage issue was deferred for examination as part of**
20 **the current audit. I also discuss how DE-Ohio has responded to three other**
21 **recommendations made in the audit report and agreed to in the Stipulation**
22 **resolving Case No. 07-723-EL-UNC. Specifically, I discuss changes to DE-**
23 **Ohio's maintenance practices at its Beckjord Generating Station, coal personnel,**

1 coal sampling procedures, and spare parts inventory as required by the
2 Stipulation.

3 **III. DISCUSSION OF THE SPRING 2007 ZIMMER OUTAGE AND THE**
4 **AUDITOR'S RECOMMENDATIONS**

5 **Q. PLEASE BRIEFLY SUMMARIZE THE HISTORY OF THE ZIMMER**
6 **GENERATING STATION.**

7 **A. The Zimmer Generating Station was jointly constructed by CG&E (now Duke**
8 **Energy Ohio), Dayton Power & Light (DP&L) and American Electric Power**
9 **Corporation's (AEP) utility, Columbus Southern Power Company (CSP).**
10 **Originally, Zimmer was planned as an 810 Mega-Watt (MW) nuclear generating**
11 **station. However, due to numerous delays and an order from the Nuclear**
12 **Regulatory Commission (NRC), construction of the Zimmer nuclear station was**
13 **suspended in 1982. In August of 1984, the joint owners decided to convert the**
14 **station into a 1300 MW coal-fired generating facility. American Electric Power**
15 **Service Corporation (AEPSC) managed the conversion.**

16 The selection of the AEPSC 1300 MW design resulted from an analysis
17 performed in 1984 by EBASCO Services, which examined six alternative design
18 concepts for the nuclear-to-coal conversion. This study established the
19 conceptual design basis for many of the systems, including the turbine
20 configuration and the modification of the existing turbines. AEPSC had
21 successfully managed the construction of six 1300 MW units prior to the
22 Zimmer conversion. The turbine configuration employed in Zimmer, although
23 modified from the configuration used at the other 1300 MW units, was fully

1 vetted. Even the Staff of the Public Utilities Commission of Ohio (Commission)
2 examined the conversion process and reported its findings in its "Zimmer
3 Conversion Project Staff Reconnaissance Report" dated July 1990. Specifically,
4 the Staff found the "management of AEPSC's engineering and design for
5 Zimmer coal conversion project to be effective and efficient."¹

6 The Zimmer Station began operation in 1991 as a base load coal-fired
7 station serving the three utilities, DE-Ohio, DP&L and AEP.

8 **Q. PLEASE DESCRIBE THE ZIMMER STATION OUTAGE THAT**
9 **OCCURRED IN 2007.**

10 A. Zimmer Station had a planned six-week maintenance outage that began on April
11 13, 2007 and was scheduled for completion on May 27, 2007. The scope of the
12 planned outage included boiler and turbine inspections, scrubber maintenance,
13 significant boiler tube replacement, and other boiler and balance of plant
14 maintenance. This inspection was according to normal operating procedures
15 and consistent with industry standards. During the inspection, damage was
16 found in the low-pressure turbines. DE-Ohio determined that corrective action
17 should be taken immediately rather than wait until the unit's next planned
18 outage. The planned four-week outage was extended until June 11, 2007, due in
19 part to allow for delays associated with acquiring and replacing two rows of
20 turbine blades on each of the two low-pressure turbines.

21 **Q. PLEASE EXPLAIN THE CAUSE OF DAMAGE TO THE TURBINE**
22 **BLADES THAT RESULTED IN THE EXTENDED ZIMMER OUTAGE.**

¹ *In re CG&E's Application for an Increase in Rates*, Case No 91-410-EL-AIR, (Staff Exhibit 24A, Zimmer Conversion Project, Staff Reconnaissance Report, July 1990 at 115) (Filed January 28, 1992).

1 **A.** Following the failure of the turbine blades, the Company had two metallurgical
2 studies performed to determine the cause of the blade failure. These studies
3 were requested by DE-Ohio and were provided to the Company. The first study
4 was performed internally by Duke Energy's Metallurgical Laboratory and
5 completed on May 14, 2007.. A true and accurate copy of a Memorandum
6 discussing this study is attached to my testimony as TJT-1. The second analysis
7 was performed by Siemens Power Generation, Inc. A true and accurate copy of
8 the study is included as Attachment TJT-2. I received the two reports, and I
9 have reviewed them. Based upon these two reports, the failure of the turbine
10 blades was determined to be high-cycle fatigue cracking initiated by several
11 contributing factors, including pitting corrosion and Stress Corrosion Cracking
12 (SCC) and improper welding techniques.

13 **Q.** **WHAT ARE PITTING CORROSION AND STRESS CORROSION**
14 **CRACKING?**

15 **A.** Pitting corrosion creates small shallow holes on the surface of the blade where
16 fatigue cracks can later initiate. SCC is caused by the combination of tensile
17 stress and a corrosive environment, and was observed to have occurred in some
18 of the aforementioned pits. Fatigue cracks developed at some of these SCC
19 cracks. DE-Ohio believes that the steam condition inducing pitting corrosion
20 may be one of the contributing factors to the blade damage, but it is not the only
21 contributing factor of the failures. As detailed in Attachment TJT-3, a paper
22 entitled "Evaluation of LP Rotor Rim-Attachment Cracking Using LPRimLife,"
23 two of the additional modes of failure determined in analysis after the failure are

1 the stress riser at the base of the notch for the Stellite strip and the lack of
2 penetration at the weld root in the under shroud welds on the turbine blade.

3 **Q. WAS THE TURBINE ITSELF EXAMINED AT THE TIME OF**
4 **ZIMMER'S CONVERSION FROM NUCLEAR TO FOSSIL**
5 **GENERATION TO DETERMINE WHETHER THE TURBINE COULD**
6 **WITHSTAND THE DIFFERENT STEAM CHARACTERISTICS**
7 **BETWEEN COAL-FIRED AND NUCLEAR GENERATION?**

8 **A.** Yes. As I discussed previously, AEPSC provided project management for
9 the conversion of the Zimmer nuclear plant to a coal-fired plant. AEPSC was
10 responsible for the licensing, engineering and design, procurement, construction,
11 and start-up functions for the conversion. Prior to the conversion of the plant,
12 AEPSC commissioned the Westinghouse Steam Turbine Generator Division to
13 perform a study. This study was done to ensure that the conversion of the
14 Zimmer nuclear plant to a coal-fired plant would not result in damage to the low
15 pressure turbine blades as a result of the change of the steam characteristics.
16 Attachment TJT-4 contains true and accurate copies of three Westinghouse
17 Memos dated 9-24-84, 12-20-84 and 12-27-84 discussing the compatibility of
18 the turbine for coal-fired generation. The study concluded that the conversion
19 from the nuclear steam cycle to the coal-fired steam cycle would not damage the
20 low-pressure turbine blades.

21 **Q. ARE THERE DIFFERENCES IN STEAM CHARACTERISTICS**
22 **BETWEEN THE ZIMMER STATION RUNNING AS A NUCLEAR**
23 **PLANT AND AS A COAL PLANT?**

1 **A.** **Yes. The major difference in steam characteristics between nuclear and coal-**
2 **fired generation is that a coal-fired boiler produces steam at higher pressures and**
3 **temperatures than the throttle conditions for a saturated steam nuclear turbine.**
4 **The Zimmer Station coal-fired boiler is a supercritical boiler producing steam at**
5 **3845 psig and 1010 °F. The steam generator for a typical nuclear plant**
6 **operating at 100% power is designed to produce saturated steam at 1100 psig**
7 **and 580 °F. Consequently, the steam leaving the supercritical boiler is at a**
8 **significantly higher pressure and temperature than the conditions at the throttle**
9 **of the nuclear turbine.**

10 **Q.** **WERE THOSE DIFFERENCES TAKEN INTO CONSIDERATION IN**
11 **THE DESIGN OF THE ZIMMER TURBINE AT THE TIME OF THE**
12 **CONVERSION?**

13 **A.** **Yes. In order to better match the steam conditions of the supercritical boiler, a**
14 **new BBC Brown Boveri (ABB) High Pressure/Intermediate Pressure (Reheat)**
15 **turbine was installed during the conversion. This new turbine is located**
16 **between the boiler and the nuclear cycle turbine. This turbine drives its own**
17 **generator, which provides electrical output in addition to that obtained from the**
18 **nuclear turbine generator. The Intermediate Pressure (Reheat) turbine exhaust is**
19 **transported via a very large (7 feet in diameter) and a very long (245 feet)**
20 **crossover pipe to the two original Westinghouse Nuclear Low Pressure turbines.**
21 **This design allowed for high efficiency and the utilization of the existing nuclear**
22 **turbine.**

1 Because the exhaust steam of the Zimmer Intermediate Pressure turbine
2 (118 psig and 576°F) is lower than most supercritical fossil units, Westinghouse
3 (Siemens) removed the first row turbine and generator end blades on the LP
4 rotors to better match the crossover steam conditions. The removal of the first
5 row of turbine blades better matches the initial steam pressure and allows for an
6 acceptable pressure drop across the remaining stages of the LP turbine rotor.

7 **Q. WAS THERE ANY REASON TO BELIEVE THAT THE DIFFERENCE**
8 **IN STEAM CONDITIONS BETWEEN COAL AND NUCLEAR**
9 **GENERATION WOULD NEGATIVELY IMPACT THE TURBINE**
10 **BLADES?**

11 **A.** No. Neither DE-Ohio prior to the Spring 2007 outage, nor AEPSC at the time of
12 the conversion had any indication that the difference in steam conditions
13 between nuclear and fossil generation would have any adverse impact on the
14 turbine blades. Moreover, there was no indication that an examination of
15 differing steam conditions between nuclear and coal operations should have
16 been undertaken at any time after the plant went into operation. As I discussed
17 previously, the use of the existing turbine was a significant factor, if not the
18 determining factor, in deciding to go forward with the conversion from nuclear
19 to coal generation in the mid 1980's and was analyzed before the decision was
20 made to proceed with the conversion. AEPSC retained Westinghouse to
21 examine the viability of the existing turbine for conversion to coal-fired
22 generation at the time of the conversion. As indicated in the two reports
23 attached to my testimony, the cause of the blade failure was not primarily due to

1 differences in steam conditions between nuclear and fossil generation, but due to
2 several contributing factors, none of which were preventable. The Company had
3 no reason to believe the Zimmer LP blades were fatigued or damaged at the time
4 of the planning for the Spring 2007 outage.

5 **Q. DID THE OPERATIONAL PERFORMANCE OF THE ZIMMER**
6 **STATION GIVE ANY INDICATION THAT A PROBLEM EXISTED?**

7 **A.** No. DE-Ohio is vigilant in the maintenance and operation of all its generating
8 stations, including the Zimmer Station, as evidenced by Zimmer's continued
9 efficiency and reliability. DE-Ohio performs routine inspections of the L-0
10 blades during unit outages. These inspections gave no indication that a corrosion
11 problem existed. The L-0 blades are typically associated with higher
12 maintenance due to operating in a more severe, wet condition and, accordingly,
13 are more susceptible to corrosion. Exposure to stress damage was mitigated
14 over time by continuous vibration monitoring as well as periodic balancing
15 efforts that kept the turbines operating in acceptable operating ranges. Failed
16 turbine blades have specific signs and symptoms, including but not limited to,
17 increased vibration and heat rate degradation. None of the telltale signs of failed
18 blades were apparent at the Zimmer Station.

19 As indicated in the Auditor's own report in Case No. 07-723-EL-UNC,
20 the Zimmer Station was one of DE-Ohio's most reliable stations in terms of
21 availability. Further, the Auditor's report identified the Zimmer Station as being
22 one of the most efficient units in the generating fleet, and provided historical
23 data indicating that the unit efficiency during the past three years has actually

1 improved relative to 2004 performance. The Zimmer Station did not have any
2 of the problems typically associated with blade failure.

3 **Q. WHAT WAS THE AUDITOR'S RECOMMENDATIONS REGARDING**
4 **THE ZIMMER STATION OUTAGE?**

5 A. The Auditor recommended that replacement power costs associated with the
6 Zimmer Station "unplanned extended" outage in the Spring of 2007 be excluded
7 from DE-Ohio's Rider FPP recovery.

8 **Q. PLEASE EXPLAIN LIBERTY'S RECOMMENDATION TO EXCLUDE**
9 **THE PURCHASE POWER COSTS DURING THE ZIMMER OUTAGE.**

10 A. The Auditor concluded through discussions with DE-Ohio's representatives that
11 steam parameters and water chemistry were different for a coal plant and a
12 nuclear plant and that those differences, in conjunction with the nuclear grade
13 metallurgy employed on the turbine, had caused the observed blade damage. In
14 addition, the Auditor believes that the two-week extension of the outage at
15 Zimmer could have been avoided had "an examination of the effects of differing
16 steam conditions between nuclear and coal operations"² been undertaken earlier.
17 DE-Ohio understands that the Auditor recommends that replacement power
18 costs be excluded from Rider FPP because DE-Ohio did not examine the effects
19 of differing steam conditions earlier.

20 **Q. DO YOU AGREE WITH THIS RECOMMENDATION?**

21 A. No. DE-Ohio believes that 100% of the replacement power cost associated with
22 the Zimmer outage should be included in the Rider FPP calculation. DE-Ohio

²*In re DE-Ohio's Application to Adjust its Rider FPP and SRT*, Case No. 07-723-EL-UNC, (*Final Report Management/Performance Audit, Duke Energy Ohio*, Page V-14) (Filed November 1, 2007).

1 acknowledges there is a known difference between the nuclear cycle steam
2 conditions and the fossil cycle chemistry. However, contrary to the Auditor's
3 assertion, an examination of the existing turbine materials was, in fact,
4 performed during the conversion from nuclear to fossil service nearly two
5 decades ago. The turbine materials were determined by the Original Equipment
6 Manufacturer, the Architectural Engineer, the General Contractor (AEP), and all
7 the joint owners, to be acceptable for fossil service. This configuration has
8 operated extremely reliably with minimal maintenance expense for more than 16
9 years. In addition, the reuse of this turbine was a central feature of the
10 conversion from a nuclear unit to one that burns coal. In evaluating different
11 designs for the conversion, the joint owners used three criteria: (1) maximizing
12 the utilization of existing Zimmer facilities from the nuclear design; (2)
13 utilization of a proven engineering design; and (3) achieving an acceptable heat
14 rate. The design ultimately selected was performed by AEPSC, which was also
15 chosen as the conversion project manager. If this turbine was not utilized,
16 additional tens of millions of dollars and likely additional time for construction
17 would have been required before placing this unit in service.

18 The Auditor's recommendation amounts to a hindsight prudence review
19 of a conversion that occurred nearly two decades ago and which was performed
20 under the view of the Commission.

21 **Q. WERE CONSUMERS HARMED IN ANY WAY DUE TO THE**
22 **EXTENDED OUTAGE IN APRIL 2007 THAT INCLUDED THE**
23 **TURBINE OVERHAUL?**

1 A. No. Ignoring, for a moment, all other factors determined to have contributed to
2 the Zimmer blade failure, fatigue has a dubious incubation period. It is not
3 possible to predict, with any degree of accuracy, if or when a crack will initiate.
4 Metallurgical evaluation suggests that L-2 blade failures on the Zimmer turbine
5 occurred within the last two years. Even if the corrosion, which initiated the
6 cracking, had been discovered earlier, the result would have been the same. A
7 total six-week outage would have been required to inspect and make necessary
8 repairs to the damaged turbine blades, regardless of timing of discovery.

9 DE-Ohio's standard maintenance is to schedule an annual one-week
10 outage and a biannual four-week outage for Zimmer. To inspect or repair the
11 low-pressure turbine, a minimum six-week outage is required. Had Zimmer
12 elected to utilize a six-week outage to open and inspect the low-pressure turbine
13 sooner and found the damage, two different courses of actions could have been
14 taken, but the outcome would be the same. The first option would require a
15 subsequent planned six-week outage for blade replacement. The second option
16 would require an additional and immediate two-weeks of outage time (in
17 addition to the scheduled six-week inspection outage) to replace the damaged
18 blades immediately. Each of these two options would result in purchase power
19 costs for the same incremental two-week outage period.

20 Either outcome results in a comparable incremental outage time for
21 replacement and repair of the turbine versus the events that occurred on the back
22 end of the 2007 Spring outage.

1 DE-Ohio believes that even if a more conservative approach was used to
2 determine overhaul frequencies in the range of 7-9 years ago, indications of
3 turbine failures would not have been present. Had the Company suspected the
4 existence of fatigue cracking, customers would have likely experienced either
5 more frequent outages or longer scheduled outages to allow the time to open up
6 the turbine and inspect, thereby incurring incremental purchased power costs.

7 While this two-week outage extension into June 2007 was forced due to
8 the unknown condition of the turbine, the bottom line is that it eliminated the
9 need for an additional two-week outage extension to inspect, plan and execute
10 the turbine overhaul in a more typical manner at a later time. Consequently,
11 DE-Ohio native load customers were not harmed. Customers now have a
12 refurbished turbine to serve their generation needs, at no capital costs to them.
13 Neither Rider FPP, nor any other portion of DE-Ohio's Market Based Standard
14 Service Offer (MBSSO) pricing mechanism, includes recovery for any such
15 capital expenditures or repairs related to generation plant as existed prior to
16 electric restructuring. Further DE-Ohio's rate structure does not include any
17 return of or on new investment in generation plant.

18 **Q. PLEASE DESCRIBE ANY PROCEDURES IMPLEMENTED AT THE**
19 **BECKJORD GENERATING STATION AS A RESULT OF THE**
20 **STIPULATION APPROVED IN FEBRUARY 2008.**

21 **A. An intense effort occurred in the latter part of 2007 to physically clean up the**
22 **station. Lighting was significantly improved, and various painting projects were**
23 **performed. Additional efforts have been undertaken and are underway through**

1 implementation of a "Premier Operator Program." The Premier Operator
2 Program encourages personnel to perform in the top quartile or better, relative to
3 their peer units, in regard to safety and environmental standards, financial
4 performance and operational excellence. Also, this program establishes an
5 Institutionalized Continuous Improvement Process.

6 **Q. HAS DE-OHIO COMPLETED A STAFFING REVIEW AT ITS COAL**
7 **PLANTS?**

8 **A. Yes.**

9 **Q. WHAT WERE THE RESULTS OF THAT REVIEW?**

10 **A.** In January 2008, DE-Ohio conducted a comprehensive labor study of its three
11 coal-fired stations, Beckjord, Miami Fort and Zimmer. This study addressed
12 labor needs within an Operations and Maintenance workforce strategy and
13 identified a gap in the operations area resource requirements. DE-Ohio has
14 subsequently proposed to hire additional employees for development of Control
15 Room Operators and other production positions in 2008. The maintenance area
16 will use a labor strategy of integrating the current maintenance work force with
17 contractor supplemental maintenance teams as the need for additional labor is
18 required. DE-Ohio has partnered with the Zachry Construction Corporation and
19 Enerfab Corporation for general maintenance support and the Sunbelt Insulation
20 Company for insulation and asbestos work. These companies have established
21 base crews at each of the stations. These base crews will share resources among
22 the stations as needs arise, allowing DE-Ohio to leverage available resources
23 across its Ohio generating stations. DE-Ohio's comprehensive labor study with

1 its Operations and Maintenance workforce strategy allows for continued
2 sustainable operations.

3 **Q. HAS DE-OHIO EVALUATED ITS PROTOCOL FOR TRANSPORTING**
4 **COAL SAMPLES TO THE LABORATORY?**

5 A. Yes.

6 **Q. DID THAT EVALUATION RESULT IN ANY CHANGES RELATIVE TO**
7 **THE SECURITY MEASURES EMPLOYED FOR TRANSPORTING**
8 **COAL?**

9 A. Yes. In addition to continuing the recommendations that were implemented in
10 1999, DE-Ohio developed a process to allow for the secure transport of coal
11 samples. DE-Ohio instituted a program that secures its coal samples from the
12 time they are pulled from the coal sampler until they arrive at the laboratory.
13 Coal yard personnel bag and seal the coal samples and apply an identifying label
14 to the sample bag. Next, the coal sample bags along with chain-of-custody
15 paperwork are placed in locked storage. The station lab personnel (who have the
16 only access to locked storage) retrieve the coal samples from the locked storage
17 for placement in the shipping container. After the coal samples are placed in the
18 shipping container and the chain-of-custody paperwork is placed in a plastic
19 envelope affixed to the outside of the shipping container, Lab personnel put a
20 tamper proof seal on the shipping containers. The containers are shipped by
21 internal carrier to the laboratory. When the shipping container arrives at the
22 laboratory, the seals are inspected for tampering. If a seal on a shipping
23 container is broken, the laboratory will disregard these samples and call for the

1 backup samples to be sent to ensure sampling integrity. This program provides
2 appropriate security protection of coal samples from the time they are obtained
3 at the Stations until they arrive at the laboratory.

4 **Q. HAS DE-OHIO PERFORMED AN ECONOMIC ANALYSIS TO**
5 **DETERMINE THE APPROPRIATE LEVEL AND USE OF SPARE**
6 **PARTS AT ITS GENERATING STATIONS?**

7 **A. Yes.**

8 **Q. WHAT WERE THE RESULTS OF THAT ANALYSIS?**

9 **A.** DE-Ohio's policy is that critical spare pieces of equipment are available where
10 appropriate and economically justified to ensure uninterrupted generation. Duke
11 Energy Corporation (Duke Energy), through parts storage at the many
12 generating facilities of its subsidiaries, has the ability to make readily available
13 spare parts far greater than most other utilities. The sheer size and magnitude of
14 Duke Energy's generating fleet alone makes Duke Energy stand out among
15 other utilities in the ability to offer access to spare parts and equipment. The
16 Duke Energy Warehouse supply inventory is connected electronically, providing
17 DE-Ohio the benefit of leveraging storage capability and the ability to transfer
18 parts and supplies to and from all of its locations in the Midwest and the
19 Carolinas. Material transactions between regulated and non-regulated entities
20 are conducted following the Federal Energy Regulatory Commission affiliate
21 transaction guidelines.

22 With that said, Duke Energy has taken on two initiatives around spare
23 parts. Duke Energy's warehouse organization has initiated work with a

1 benchmarking group, Scott Madden, Inc., to evaluate the Company's
2 capabilities in this area. This study will enhance the ability to expedite the
3 access to and cost of spare parts and supplies. The comparable results for other
4 utilities were published and distributed in February 2008. The Duke Energy
5 Supply Chain organization is using benchmarking information in a current
6 Redesign Project. The second initiative involves the consolidation of the item
7 catalog of items/parts across Duke Energy's Utility Operating Companies. This
8 is being done in conjunction with an Enterprise Asset Management project
9 encompassing integrated processes and systems that manage assets, work and
10 supply chain activities throughout Duke Energy. The primary information
11 technology system will be IBM's Maximo. The catalog consolidation initiative
12 started in June of 2007 and will continue throughout the Enterprise Asset
13 Management project in phases. When this initiative is finished, Duke Energy
14 will have an enterprise-wide item catalog of items/parts that again will further
15 enhance the ability to expedite access and cost of spare parts and supplies.

16 **IV. CONCLUSION**

17 **Q. DOES THIS CONCLUDE YOUR DIRECT TESTIMONY?**

18 **A. Yes.**

EVALUATION OF LP ROTOR RIM-ATTACHMENT CRACKING USING LPRimLife

Prepared for:

**Seventh EPRI Steam Turbine/Generator Workshop
August 20-23, 2001, Baltimore, Maryland**

Prepared by:

**Darryl A. Rosario, S. S. Tang, Peter C. Riccardella
Structural Integrity Associates
San Jose, CA**

**David W. Gandy, R. Viswanathan
Electric Power Research Institute
Charlotte, NC Palo Alto, CA**

EVALUATION OF LP ROTOR RIM-ATTACHMENT CRACKING USING LPRimLife

Darryl A. Rosario, S. S. Tang, Peter C. Riccardella
Structural Integrity Associates
San Jose, CA

David W. Gandy, R. Viswanathan
Electric Power Research Institute
Charlotte, NC Palo Alto, CA

ABSTRACT

Stress corrosion cracking (SCC) in the blade attachment region of low-pressure (LP) turbine rotors has emerged as one of the most significant problems affecting both nuclear and fossil steam turbines today. To assist turbine operators in evaluating the remaining life of LP rotors with known or suspected cracking, an easy-to-use PC-based computer program, LPRimLife, was developed for EPRI by Structural Integrity Associates. The first phase of development, incorporating the methodology for evaluating cracking in GE dovetail (straddle-mount) attachments, was completed in 1999 [1]. The second phase, which included evaluation of cracking in Westinghouse axial-entry (steep) attachments, was completed in 2000 [2]. The third phase, to address cracking in GE multi pin-finger attachments is currently under way.

Since initial development, the LPRimLife computer code has been successfully employed at nuclear and fossil plants, providing the basis for deferring or eliminating major unscheduled and costly repairs, such as "pressure plating" which would have significantly extended the outages. Deferring unscheduled repairs for even one more fuel cycle allows for advance planning to evaluate and select the most-effective repair/replacement option and lead time needed for procurement of appropriate materials/services. In today's competitive marketplace with ever-tightening outage schedules, timely application of LPRimLife has resulted in significant cost savings to utilities.

This paper provides a summary of the LPRimLife program methodology, software features and recent utility applications.

INTRODUCTION

Since the first discovery of stress corrosion cracking (SCC) in the blade attachment region of nuclear low pressure steam turbine disks around the late '70's, industry concern with regard to this problem has increased significantly over the last five to ten years with an increasing number of rotors requiring repair or replacement. These concerns were corroborated by an EPRI survey of U.S. nuclear and fossil utilities in 1995 [3] which reported a significant increase in the incidence of rim cracking compared with an earlier EPRI survey in 1980 [4].

Data collected by EPRI through 1995 from utility turbine operators in the United States, revealed LP rim attachment cracking in 38% of operating nuclear units (L-2 and L-3 rows most severely affected) and 26% of fossil supercritical units with once-through boilers (L-0 through L-2 rows most severely affected). The cracking mechanism reported was predominantly stress corrosion cracking, with a few instances of corrosion-fatigue and one incident of high-cycle fatigue. Based on the survey data, the incidence of cracking did not appear to be related to generator type (BWR vs. PWR), manufacturer, power rating or turbine manufacturer. Data was insufficient to establish a relationship between the incidence of rim cracking and operating variables such as operating time, number of startups, type of water treatment, oxygen levels, condenser cooling water and condenser leakage rate. Limited rim attachment crack growth data suggested that use of an equation first proposed by Clark et. al. of Westinghouse [5] to estimate crack growth rates was assessed to be adequate for the purpose of life prediction.

The application of life prediction methods to rim-attachments cracking, through 1995, was reported to be limited to a few OEM's and consultants, with several utilities expressing a strong need for a user-friendly integrated software computer program which would allow utility personnel to perform a rapid life assessment of LP rotors with known or suspected rim-attachment cracking.

In response to these utility concerns and needs, EPRI initiated Tailored Collaboration program RP4597-01 in May 1997 [6] to develop a computer code that would combine the necessary stress analysis and fracture mechanics algorithms with applicable material degradation data into an integrated methodology to assess the remaining life of LP rotors with rim attachment cracking. A description of the methodology and capabilities of the resulting computer program, LPRimLife, developed by Structural Integrity Associates (SI) for EPRI, is the subject of this technical paper.

OVERVIEW OF METHODOLOGY

The development effort for the life assessment code, LPRimLife [7], was split into two phases to separately address rim-attachment cracking for the two most common types of rim-attachment geometries in the U.S. as shown in Figure 1. Phase I, completed in 1999, included the assessment of GE straddle-mount attachments (Figure 1a). Phase II, which address cracking in Westinghouse axial-entry attachments (Figure 1b) was completed in 2000. A third phase, Phase III, is currently under way to

include the evaluation cracking of in GE multi pin-finger attachments.

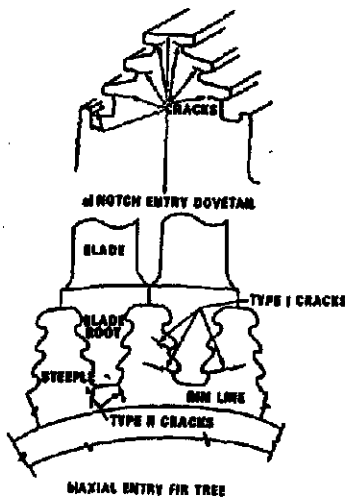


Figure 1. Schematic of rim-attachment configurations illustrating typical locations of cracking.

A flow chart of the LPRimLife computer code is provided in Figure 2.

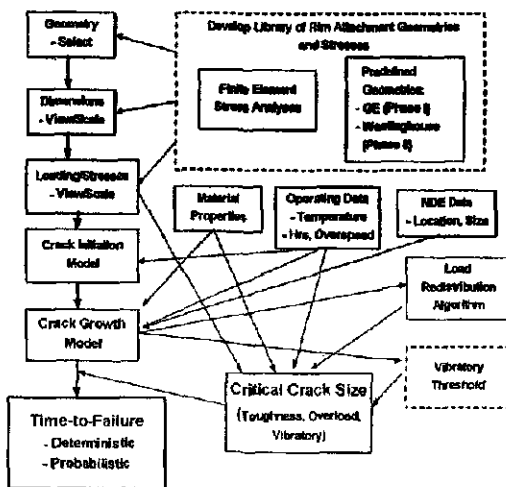


Figure 2. Flowchart of LPRimLife Software.

A brief description of the inputs and calculation procedures is given below.

(i) **Geometry/Stresses:** The user first defines the type of attachment to be evaluated (GE straddle mount or Westinghouse axial-entry). Next, the user has the option of selecting appropriate geometry and stress data from a pre-defined (built-in) library of geometry and finite element stress solutions, or, of inputting appropriate geometry and stress data for the attachment to be evaluated. In addition, pre-defined geometry and loading data can be modified to approximate the desired geometry using scale factors.

(ii) **Other Inputs:** Next the user defines various inputs required for the life assessment calculation which fall into the following major categories:

- Operating Data
- Inspection Data

- Material Properties
- Initiation and Crack Growth Data
- Calculation/Print Controls

(iii) **Calculations:** Once all the necessary inputs have been defined, the user is given the option of performing the remaining life calculations either deterministically or probabilistically.

Calculations performed include:

- Estimate initiation time (if cracking was not detected)
- Simulate growth of initiated or detected cracks due to SCC
- Account for redistribution of loading between hooks as crack growth progresses (for straddle-mount geometries)
- Check for crack arrest below defined SCC threshold
- Determine minimum critical crack size for fracture toughness limit, remaining ligament overload, or user-defined depth limit.
- Remaining life is the sum of initiation time (if applicable) and time to reach critical size.

(iv) **Results:** After the calculations are completed, detailed results are available for review in an output text file along with the option to plot key inputs/results. Results include:

- Stresses which include the effect of load scaling/redistribution factors
- Stress intensity factors (without and with scale factors and load redistribution)
- Crack size versus time
- Remaining life

Initiation and Failure Probabilistic results

Stress Analysis

The program incorporates a built-in library of finite element (FE) stress results required for evaluation of rim attachment cracking. This eliminates the complexity associated with performing typical FE analyses as shown in Figure 3a for a GE dovetail and in Figure 3b for a Westinghouse stepple.

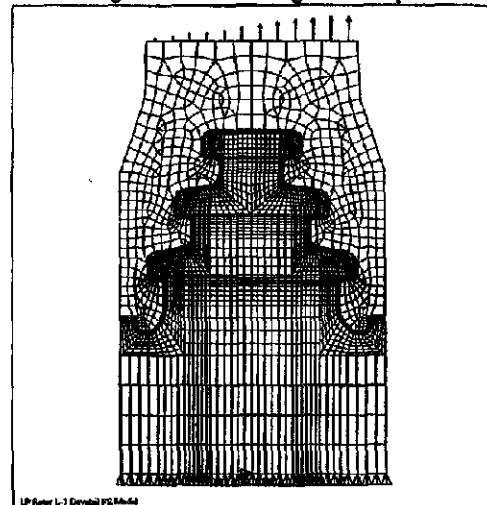


Figure 3a. Typical FE analysis model of GE dovetail and blade attachment region with non-linear contact (gap) elements.

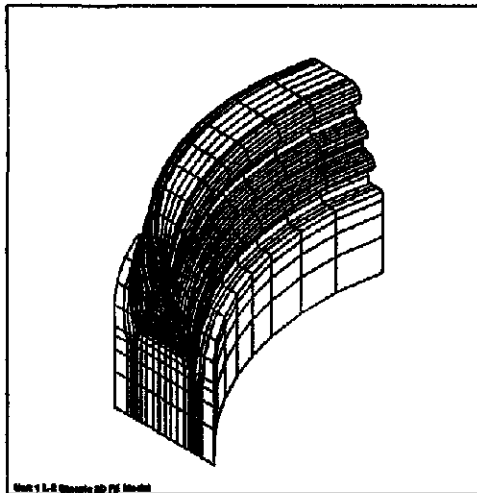


Figure 3b. Typical FE analysis model of a Westinghouse axial-entry steeple.

Stress analysis results built into the software program libraries for the Phase I dovetail geometries and Phase II axial-entry steeples are listed in Tables 1 and 2 respectively.

Table 1. Phase I Dovetail Geometries

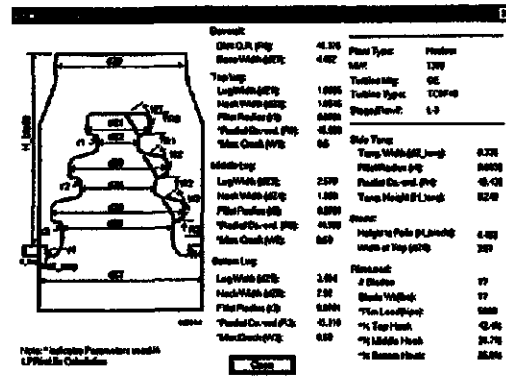
Turbine Size/Rating	LP Configuration ¹	Row
GE 920 MW	TC6F38	L-2, L-3
GE 540 MW	TC4F38	L-2, L-3
GE 642 MW	TC6F38	L-2, L-3
GE 1300 MW	TC6F43	L-2, L-3
GE 1220 MW	TC6F43	L-2, L-3
GE 830 MW	TC4F43	L-2, L-3
GE 1100 MW	TC6F43	L-2, L-3

Table 2. Phase II Axial-Entry Steeple Geometries

Turbine Size/Rating	LP Configuration ¹	Row
WH, 1160MW	TC6F44 (BB-81)	L-2 (Curved)
WH, 1160MW	TC6F44 (BB-81)	L-3 (Skewed)
WH, 1160MW	TC6F44 (BB-81)	L-4 (Skewed)
WH, 944 MW	TC4F44 (BB-281)	L-0 (Curved)
WH, 944 MW	TC4F44 (BB-281)	L-1 (Curved)
ABB 900 MW	TC6F52	L-0 (5-hook Curved)
ABB 900 MW	TC6F52	L-1 (3-hook Straight)

Key geometry and loading information are incorporated in the built-in library as shown in Figures 4 and 5 for dovetail and axial-entry style attachments. Appropriate stress gradients normal to the plane of cracking are also built into the library (Figure 6). Local stress increases such as at the notch-entry position must be accounted for using a "Load/Stress Scale Factor" which can be modified by the user. For example, to increase stresses by 50%, this factor must be changed to 1.5. A separate "Library" module allows the user to expand the existing library to include additional attachment geometry/loading/stress data.

¹ TC6F38 = Tandem-Compound, 6-Flows (3 LPs), with 38-inch last blades.



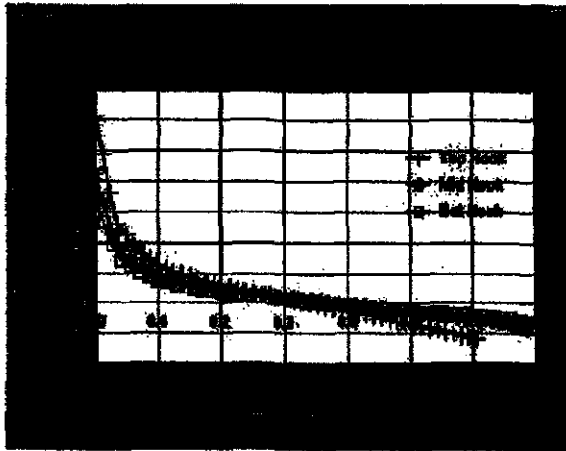


Figure 6. Stress gradients normal to crack plane incorporated in built-in library of FE stress results.

The methodology for crack initiation and growth is the same for both dovetail and axial-entry attachments and is described below.

Crack Initiation and Growth

An industry review of available SCC initiation data and models is given in [8]. Since there is currently no quantitative model to predict SCC initiation as a function of the principal governing material, stress and environment variables, the software allows the user to specify an industry-experienced-based statistical probability of initiation as a function of total operating time for a given fleet or design of LP rotor.

Crack growth due to stress corrosion cracking (SCC) is the dominant crack growth mechanism simulated within the software. Low cycle fatigue due to unit start/stops is typically very small relative to SCC growth rates. The most widely accepted model for SCC crack growth rate is given by Clark et al. of Westinghouse [5], expressed by the following equation:

$$\ln\left(\frac{da}{dt}\right) = C_1 - (7302/T) + 0.0278 \sigma_y \quad (1)$$

where, C_1 is a material constant with a mean value of -4.968 and a standard deviation of 0.587, T is the operating temperature of the disk in °R (°F+460), σ_y is the yield strength in ksi, and, da/dt is the growth rate in inches/hour.

The 1995 EPRI survey of rim-attachment cracking [3] has shown that this equation also provides reasonable estimates of crack growth rates for disk rim attachments. Data presented by Holdsworth [9] and Speidel [10] at the most recent EPRI Steam Turbine Stress Corrosion Cracking Conference in March 1997, also confirms that SCC growth rates, for typical disk steels with yield strengths below 160 ksi, are a function of only yield strength and temperature.

To allow flexibility in defining the SCC growth rate, the following generic form of Equation (1) is incorporated in the software program:

$$\ln\left(\frac{da}{dt}\right) = C_1 - (C_2/T) + C_3 \sigma_y \quad (2)$$

where, the material constants C_1 , C_2 and C_3 can be defined by the user.

SCC Growth Threshold (K_{ISCC})

Equation (1) applies to the SCC growth region called the "plateau region" which is independent of stress intensity factor [10]. However, for stress intensity factors below the threshold (K_{ISCC}), which is in the range of 10 to 20 ksi $\sqrt{\text{inch}}$, crack growth is insignificant [10]. With load redistribution, stress intensity factors may fall below the threshold and SCC crack growth will cease. To incorporate this effect, SCC crack growth is terminated when, $K_I < K_{ISCC}$. To activate this threshold effect the user must define a mean and standard deviation for K_{ISCC} ; this feature can be deactivated by setting both mean and standard deviation values to zero.

Critical Crack Size

The critical crack size computed by the software is the minimum value for the following failure criteria: (i) the applied stress intensity factor (K_I) exceeds the material toughness (K_{IC}), (ii) plastic overload of the remaining ligament and (iii) the crack depth exceeds a user-specified limit. In future software releases, a vibratory limit will be included to address the possibility of terminal high cycle fatigue failure. A flow diagram for critical crack size determination is shown in Figure 7.

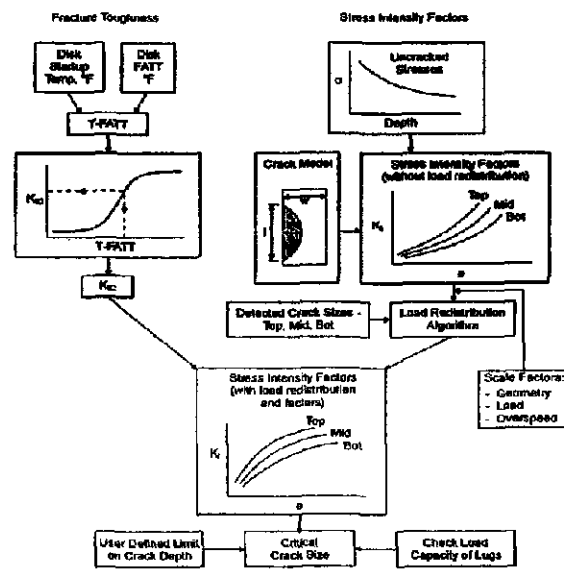


Figure 7. Critical crack size determination flow diagram.

Stress intensity factor solutions for a semi-elliptic surface-connected cracks were compiled from [11] along with 3D FE crack front modeling for more complex axial-entry steep cracks using the ALT3D computer program [12]. Any combination of user-specified depth (a) and length (l) can be evaluated. Unit-specific disk fracture toughness values can be specified by the user or default values in the software code from literature data [13] can be used. Lower bound disk toughness values are estimated based on a startup temperature for the disk, which is input by the user. Plastic overload of the remaining ligament (from [14]) is calculated based on the combined membrane, bending and shear stresses in the ligament and compared with the material flow stress (half disk yield+ultimate strength).

Load Redistribution: An algorithm to account for load redistribution between the hooks due to cracking has been developed and incorporated into the software program for the

Phase I dovetail geometries. This algorithm will be expanded to include axial-entry attachments in future releases.

Remaining Life (Deterministic versus Probabilistic)

For a deterministic analysis, remaining life (t_{rem}) is computed using the following relationship:

$$t_{rem} = t_{ini} + \frac{a_{cr} - a_i}{da/dt} \quad (3)$$

where, t_{ini} is remaining initiation time (if applicable), a_i is the initiated or detected crack size, a_{cr} is the critical crack size and da/dt is the crack growth rate. Because of the non-linear dependency of load redistribution on crack size, crack growth simulations must be performed in small increments of crack size and critical size determined when one of the above failure criterion is met.

Deterministically predicted remaining lives typically yield a large scatter in results for worst-case versus mean data, suggesting that variability in modeled data cannot be adequately characterized deterministically. The use of worst-case assumptions stacks conservatism on conservatisms, resulting in an overly pessimistic estimate of remaining life, which does not represent a realistic outcome. It is unlikely that all of the worst case conditions would occur simultaneously, and therefore a probabilistic analysis that considers position in the scatterband can provide a more realistic assessment of remaining life.

A probabilistic evaluation requires identification of appropriate random variables and determination of a statistical distribution associated with each variable. The generation of probabilistic results can then be accomplished using a technique such as Monte Carlo which involves successive deterministic remaining life calculations using randomly selected values of inputs.

In LPRimLife probabilistic calculations are performed using the Monte Carlo technique for a user-specified number of iterations. A summary of random variables, which can be defined using the various sub-menus under the "Input" main menu option, is provided below.

- (1) Scale factor for load/stresses (normal distribution)
- (2) Overspeed level (normal distribution)
- (3) Disk startup temperature (normal distribution)
- (4) Disk steady-state operating temperature (normal distribution)
- (5,6,7) Crack depth (normal distribution) - top, middle, bottom
- (8,9,10) Crack length (normal distribution) - top, middle, bottom
- (11) Yield strength (normal distribution)
- (12) Lower Bound Fracture Toughness (normal distribution)
- (13) FATT (normal distribution)
- (14) Fracture Toughness (normal distribution) vs. (T-FATT)
- (15) Crack initiation time (user-defined tabular)
- (16) SCC Growth Rate Constant, C_1 (lognormal distribution)
- (17) SCC Growth Threshold, K_{ISCC} (normal distribution)

LPRimLife Software Description

The LPRimLife software program was written in Microsoft C++ for operation on a personal computer (PC) in a Windows environment (Figure 8).

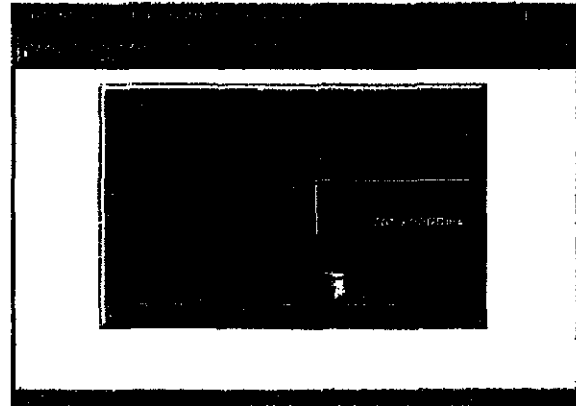


Figure 8. LPRimLife splash screen and main menu options.

The software program incorporates an easy-to-use graphical user interface with comprehensive on-line help. Main menu options, shown in Figure 8, are as follows.

The "File" Option should be selected by the user when the program is first executed to define whether a new analysis is to be performed or an existing analysis file is to be opened.

The "Edit" Option is currently limited to searching for text (using Find) in the standard output file once an analysis has been performed.

The "Input" Option contains all of the necessary inputs that must be defined by the user prior to performing an analysis.

The "Analysis" Option offers the user the choice of performing a deterministic or probabilistic analysis and starts the calculations.

The "View" Option allows the user to view the output of the analysis in text or graphical form.

The "Library" Option is a special tool that allows the user to add-to or modify items in the default library of geometry and stress data.

The "Help" Option allows the user to access "Help Topics" which cover the entire content of the User's Manual provided with the software, and to invoke the "About LPRimLife" pop-up window which provides details about the version number of the program and software support. Context-specific help can also be accessed using the "F1" function key from any dialog box.

A typical solution procedure, consisting of defining inputs, selecting an analysis type and viewing results, is illustrated in Figure 9.

Inputs → Analysis → View Results



Figure 9. Typical solution procedure.

Inputs: Separate dialog boxes are provided for each of the input categories, shown in Figure 9. An example of one such input data dialog box is shown in Figure 13 for "Calculation and Print Controls".

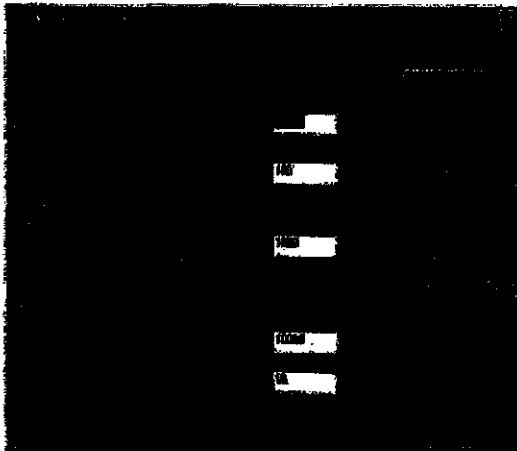


Figure 10. "Calculation and Print Controls" data input.

Before proceeding to the "Analysis" option the user must define the calculation and print controls shown in Figure 10. The "Total Simulation Time" is the total number of operating hours into the future over which remaining life calculations will be performed. A "Calculation Increment" of 100 to 500 hours is recommended for accuracy because the failure criteria and SCC threshold features are non-linear functions of crack size. To limit the size of the output file, a "Print Increment" in excess of 1000 hours should be used. For a probabilistic analysis, the number of iterations should be at least one order of magnitude greater than the reciprocal of the desired failure probability level i.e., to demonstrate a failure probability less than 10^{-3} , the number of iterations should be at least 10^4 .

Analysis: A deterministic analysis takes only a few seconds to run on a personal computer with a Pentium processor, while a probabilistic analysis with 10^4 iterations runs in about 5 to 10 minutes.

Results: After an analysis is completed, results can be viewed either in a detailed output text file or in graphical format. Sample output file results for deterministic and probabilistic analysis runs are shown in Figures 11a and 11b below. The failure simulation capability for dovetail attachments has been extended to include successive failure of all three dovetail hooks, as shown in Figures 11a, 11b and 12.

Parameter	Value	Unit	Comment
Simulation Time	10000	Hours	
Calculation Increment	100	Hours	
Print Increment	1000	Hours	
Number of Iterations	10000		
Failure Probability	0.0001		
Simulation Results	10000	Hours	
Failure Time	10000	Hours	
Failure Location	10000	Hours	
Failure Mode	10000	Hours	
Failure Description	10000	Hours	
Failure Time	10000	Hours	
Failure Location	10000	Hours	
Failure Mode	10000	Hours	
Failure Description	10000	Hours	

Figure 11a. Deterministic analysis results "Output".

Parameter	Value	Unit	Comment
Simulation Time	10000	Hours	
Calculation Increment	100	Hours	
Print Increment	1000	Hours	
Number of Iterations	10000		
Failure Probability	0.0001		
Simulation Results	10000	Hours	
Failure Time	10000	Hours	
Failure Location	10000	Hours	
Failure Mode	10000	Hours	
Failure Description	10000	Hours	
Failure Time	10000	Hours	
Failure Location	10000	Hours	
Failure Mode	10000	Hours	
Failure Description	10000	Hours	

Figure 11b. Probabilistic analysis results "Output".

Various key inputs and results can also be plotted using graphics built into the software code. The user can modify any of the plot elements such as title, legend, markers etc. by clicking the "Right" mouse button anywhere within the plot. As an example, the tabular probabilistic analysis results shown in Figure 11b are plotted in Figure 12 using the "Failure Plot" option from the "View" main menu.

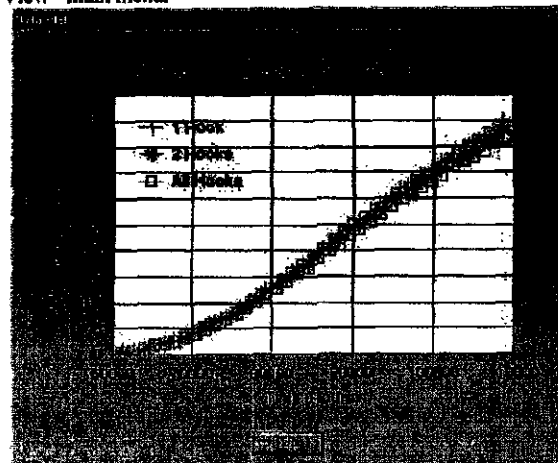


Figure 12. Cumulative probability of "Failure Plot" option from the "View" main menu.

RECENT UTILITY APPLICATIONS

Since initial development, the LPRimLife software has been successfully applied at about ten utilities. Most utilities have acquired the software, received site-specific software customization and training, and performed analyses of various cracking scenarios to prepare in advance for a scheduled outage. A few utilities, who did not include LPRimLife in pre-outage planning, have also successfully applied the software in "crisis" mode during an outage, with assistance from Structural Integrity. Two recent applications are summarized below to illustrate the benefits to utility end-users.

Millstone Nuclear Plant: Subsequent to attending an EPRI-sponsored LPRimLife training workshop in August 2000, Northeast Utilities (NEU) acquired the software and received additional training for in-house engineering staff, in preparation

for a Spring 2001 Unit 3 outage. The LPB and LPC rotors were removed and a phased-array ultrasonic inspection was performed by GE to assess the severity of cracking in the L-2 (5G, 5T) and L-3 (4G, 4T) dovetails, which had been inspected during prior outages. For the LPB rotor, indications up to 0.2-inch in depth were detected, and critical-path decisions to be made included (i) whether to pull buckets to verify depth and (ii) whether cross keys were necessary to distribute load. Several deterministic and probabilistic analyses, performed using LPRimLife, provided the justification that a reasonable margin of safety existed to defer bucket removal and cross-keying for one more fuel cycle of operation. With dovetail indication depths of up to 0.3-inch reported by the phased-array UT in the LPC rotor, the critical issue was whether to pull buckets to confirm depth/length by grinding. LPRimLife calculations indicated that bucket removal could be deferred for one more cycle. Based the findings in the LPB and LPC rotors, and past inspection results for the LPA rotor, LPRimLife calculations were performed to assess whether the LPA rotor should also be inspected. These calculations indicated an increased risk of dovetail failure if inspection of the LPA rotor were deferred by one more cycle. NEU therefore made the decision to inspect the LPA rotor, and significant cracking, up to 0.6-inch depth in the L-2 row and up to 0.5-inch depth in the L-3 row, was uncovered. LPRimLife calculations indicated a significant risk of L-2 row failure for operation as-is. NEU therefore elected to install "long-shank" blades (buckets) thereby completely eliminating the risk of dovetail failure, and the loss of MW associated with installation of a "pressure-plate". NEU estimated that use of the LPRimLife software saved at least five (5) days of critical-path outage time, equating to a cost saving of several million dollars (\$).

Nine Mile Point Nuclear Plant: Niagara Mohawk Power Corporation (NMPC) sought Structural Integrity's assistance during their Unit 1 Spring 2001 outage, in "crisis" mode, following the discovery of dovetail cracking in both the L-1 and L-2 rows of the LPC rotor. With phased-array UT crack depths of up to 0.21-inch in the L-1 row, a decision had to be made whether bucket removal was warranted to confirm depth/length for safe operation. LPRimLife calculations indicated a very low risk of L-1 dovetail failure associated with deferring bucket removal for one more cycle (2 years) of operation. Crack depths up to 0.17-inch in one of the L-2 rows, led to a "pressure-plate" recommendation by GE. NMPC requested Structural Integrity to provide an independent assessment of whether a "pressure-plate" was warranted for this L-2 row. Deterministic and probabilistic calculations, performed using LPRimLife indicated a very low risk of dovetail failure for one additional cycle of operation, without "pressure-plate" installation or additional bucket removal to confirm indication size. Because of timely availability of "long-shank" blades for this row, and fatigue cracking that was also discovered the L-2 blades, NMPC elected to machine and install these new blades, to eliminate both the disk SCC cracking and the blade cracking problems. Like NEU, NMPC also estimated saving several days of outage time, equating to a cost saving of several million dollars (\$).

SUMMARY AND FUTURE DEVELOPMENTS

Successful application of the Windows-based personal computer software program, LPRimLife to assess remaining life of GE dovetails and Westinghouse axial-entry attachments with cracking has been demonstrated at several utilities. With the completion of the first two phases of software development, the capabilities of the software program have been enhanced to include successive hook failures for GE dovetail attachments and the assessment of complex 3D crack shapes/profiles in axial-entry disk rim attachments. The code combines the necessary stress analysis, fracture mechanics algorithms and material degradation data into an easy-to-use software tool to predict the appropriate failure mode and remaining life of rim attachments affected by stress corrosion cracking. With comprehensive on-line help, and built-in graphics/plotting capability, the program facilitates rapid life assessments which can be performed by non-experts within a short time of being introduced to the software.

The next (third) phase, to evaluate cracking in GE multi-finger pinned root (finger dovetail) attachments is currently under way. Future developments will include expanding the software capabilities/library to evaluate cracking in fossil super-critical units which continue to experience this problem at an alarmingly increasing rate.

ACKNOWLEDGMENTS

The authors would like to thank all the tailored collaboration utility participants who funded this program and provided valuable input, guidance and feedback from the initial stages of the program development through the testing and release of the of the current software version. Special thanks are also due to Bruce Roy of DNC² and Chris Contard of NMPC for providing a utility perspective on outage time and cost savings realized from recent application of LPRimLife.

REFERENCES

1. D. A. Rosario, P. C. Riccardella, S. S. Tang, R. Viswanathan, D. W. Gandy, "Development of an LP Rotor Rim-Attachment Cracking Life Assessment Code (LPRimLife)," Proceedings of the Sixth EPRI Steam Turbine/Generator Workshop, August 17-20, 1999, St. Louis, Missouri.
2. D. A. Rosario, P. C. Riccardella, S. S. Tang, D. W. Gandy, R. Viswanathan, "Development of an LP Rotor Rim-Attachment Cracking Life Assessment Code (LPRimLife), Phase II - Evaluation of Westinghouse Axial-Entry Attachments," Fourth International EPRI Conference on Welding & Repair Technology for Power Plants, June 7-9, 2000, Naples, Florida.
3. D. A. Rosario, C. H. Wells, G. J. Licina, "LP Rotor Rim-Attachment Cracking Survey of Utility Experience," EPRI Research Project 9005-01, Final Report TR-107088, January 1997.
4. EPRI Report NP-2429, "Steam Turbine Disk Cracking Experience," Volumes 1 through 7, Research Project 1398-5, June 1982.

² Dominion Nuclear Connecticut, Inc. is the current owner/operator of the Millstone Nuclear Plant.

5. W. G. Clark, B. B. Seth, and D. M. Shaffer, "Procedures for Estimating the Probability of Steam Turbine Disc Rupture from Stress Corrosion Cracking," presented at Joint ASME/IEEE Power Generation Conference, October 1981.
6. "LP Rotor Rim-Attachment Cracking - Development of a Life Assessment Code," Project Agreement WO4597-01 between Electric Power Research Institute (EPRI) and Structural Integrity Associates, Inc. (SI), May, 1997.
7. "LP Rotor Rim-Attachment Cracking Computer Code (LPRimLife) Software User's Manual," prepared for EPRI by Structural Integrity Associates, Inc. (SI), Report No. SIR-97-111, Rev.C, October 2000.
8. D. A. Rosario, R. Viswanathan, C.H. Wells and G. J. Licina, "Stress Corrosion Cracking of Steam Turbine Rotors," 1998 NACE International, CORROSION- Vol.54, No. 7, pp. 531-545.
9. S. R. Holdsworth, et al, "Laboratory Stress Corrosion Cracking Experience in Steam Turbine Disc Steels," Proceedings of the EPRI Steam Turbine Stress Corrosion Cracking Workshop, March 1997.
10. M. O. Speidel and R. Magdowski, "Major Influences on the Growth Rates of Stress Corrosion Cracks in Steam Turbine Rotor and Blade Materials," Proceedings of the EPRI Steam Turbine Stress Corrosion Cracking Workshop, March 1997.
11. pc-CRACK™ for Windows, Version 3.0-3/27/97, Structural Integrity Associates, 1997.
12. ALT3D Version 2.1, Copyright 1989-1995, Computational Mechanics, Inc.
13. R. C. Schwant and D. P. Timo, "Life Assessment of General Electric Large Steam Turbine Rotors," EPRI CS-4160, Proceedings of the Seminar on Life Assessment and Improvement of Turbo-Generator Rotors for Fossil Plants, September 12-14, 1984, Raleigh, North Carolina.
14. A. G. Miller, "Review of Limit Loads of Structures Containing Defects," Int. Journal of Pressure Vessels and Piping 32 (1988) pp. 197-327.

SIEMENS

Siemens Power Generation, Inc.

TGME 07-107

To: Todd Anderson.

From: Ravi Angal

Date: July 30, 2007

Subject: L-2R fractured blades evaluation and L-3R blade root fracture evaluation from Duke Energy Ohio, Inc. Zimmer (ST) Unit 1

Siemens Confidential

Copyright © 2007 Siemens Power Generation, Inc.
All Rights Reserved

INTRODUCTION

LP-A L-2R fractured blades #49 and #175 and LP-B L-2R fractured blades #103 and #141 from Duke Energy Ohio, Inc. Zimmer Station (ST) Unit 1 were submitted to Siemens Materials Engineering for metallurgical evaluation of the fracture. The LP-A L-3R #4 blade was also submitted for metallurgical evaluation of the fracture in the blade root. This was the first complete disassembly and inspection performed on these LPs since they went into operation in 1991.

CONCLUSIONS

1. The fracture surface of the blades LP-A L-2R #49 and #175 and LP-B L-2R #103 and #141 was obliterated due to exposure to oxidizing atmosphere for a long period. No interesting fracture features were found. No clear origin of the crack was found. Microstructure of the cross section of the fracture surface indicates that the crack propagated in a transgranular fashion, typical of high cycle fatigue.
2. The hardness and chemistry of the blades LP-A L-2R #49 and #175 and LP-B L-2R #103 and #141 meets the specification requirements of Siemens material specification. The microstructure of the core of the blades consists of tempered martensite and delta ferrite. The percentage of delta ferrite is approximately 15% (5% maximum per internal specification) in the core of the blade LP-B L-2R #14. Pitting was found below the reddish brown deposits of blade LP-B L-2R #103. Delta ferrite phase greater than 5% did not contribute into the fracture of the blades as fracture also occurred in blades having less than 5% as per the specification.
3. The chemical and X-Ray Diffraction analysis of reddish brown deposit on the blades LP-A L-2R #49 and #175 and LP-B L-2R #103 and #141 revealed up to 71% amorphous SiO_2 and

SIEMENS

24% Fe₂O₃. The chemical and XRD analysis of black deposit revealed iron oxides of hematite and magnetite.

4. The fracture surface of the LP-A L-3 #4 blade showed a number of secondary crack origins and these cracks propagated in a transgranular fashion. The beach / arrest marks were found to be consistent with a fatigue fracture. Primary crack originated at the trailing edge and propagated towards the leading edge. Pitting was found in the blade root grooves and around the fracture surface.
5. The chemical analysis of the weld filler metal of the undershroud welds of blades LP-A L-2R #175 and LP-B L-2R #141 was typical 17-4PH stainless steel.
6. The lack of penetration at the weld root was found in both the undershroud welds of LP-A L-2R #175 and LP-B L-2R #141 blades. Shrinkage porosity was found in the weld bead of LP-B L-2R #141 blade. Hydrogen cracking due to low preheat temperature was found in the weld bead of LP-B L-2R #141 blade.

DETAILS OF EVALUATION:

The LP-A L-2R fractured blades #49 and #175 and LP-B L-2R fractured blades #103 and #141 in the as received condition are shown in Figures 1 – 8. All the blades were covered with a reddish brown deposit on the convex side. The fracture surface of the blades was covered by oxide deposits.

Deposit from all the blades were collected and analyzed for chemical composition, compound identification and corrosive ionic elements using inductively coupled plasma – optical emission spectroscopy (ICP-OES), X-Ray Diffraction and Ion Chromatography. No corrosive elements were found in the deposit sample. The results of the analysis of deposit indicated presence of amorphous SiO₂ and iron oxides (hematite and magnetite). Refer to chemical analysis report attached as Appendix 1. The chemical composition of the L-2R blades meets the Siemens material specification. Refer to the chemical analysis report attached as Appendix 2.

After ultrasonic cleaning to remove the oxide deposits, the macro fractography of the L-2R blades was done to find the origin of the primary crack and direction of crack propagation. The macro fractographs are shown in Figures 10-13. The fracture surface of the L-2R blades comprises of a smooth flat surface starting from the leading edge and merging into the overload fracture area towards the trailing edge. The fracture surface of L-2R blades was obliterated and no interesting fracture features were found. The exact origin of the crack could not be confirmed. The

SIEMENS

Scanning Electron Microscope (SEM) evaluation of the fracture surface did not reveal any useful information as the surface was badly oxidized.

A cross section normal to the flat fracture surface was metallographically prepared for evaluation under the optical microscope. The micrographs are shown in the Figures 14-17. From the micrographs it seems like the crack in L-2R blades propagated in a transgranular fashion consistent with the fatigue mode, most likely high cycle fatigue. The microstructure at the fracture surface of L-2R blades consists of uniform tempered martensite.

Metallographic samples and hardness measurements were taken from the core of L-2R blades. The micrographs are shown in Figures 18-21. The microstructure of the L-2R blades #49, #175 and #103 consists of tempered martensite and delta ferrite (<5%). The microstructure of L-2R blade #141 consists of tempered martensite and delta ferrite, the delta ferrite content is greater than 5% (~15%). The measured hardness values for L-2R blades are shown in Table 1. The hardness of the L-2R blades meets the Siemens materials specification requirements (262-321 BHN).

The as received pictures of the L-3R #4 cracked blade are shown in the Figure 9. The fracture surface was covered with oxide deposits. After ultrasonic cleaning to remove the oxide deposits, the macro fractography of the LP-A L-3R #4 blade was done to find the origin of the primary crack and direction of the crack propagation. The macro fractograph is shown in Figures 23 & 24. Numerous secondary crack origins were found. Secondary cracks propagated in a transcrystalline mode as shown by the black arrows. Beach / arrest marks were found consistent with fatigue fracture. Primary crack originated at the trailing edge and propagated towards leading edge consistent with fatigue fracture. Pits due to corrosion were found around the fracture surface. The SEM fractography of the fracture surface revealed beach marks in the secondary crack consistent with fatigue fracture (Figures 23 & 24). The microstructure (Figure 22) of L-3R blade consists of tempered martensite and delta ferrite greater than 5% (~10%). The measured hardness values for L-3R blade are shown in Table 1. The hardness of the L-3R blade meets the specification requirements of Siemens material specification (262-321 BHN). The chemical analysis of the blade also meets the specification requirements. Refer to the attached Appendix 2.

A cross section of the undershroud weld of LP-A L2-R #175 and LP-B L2-R #141 was mounted for optical microscope evaluation. Refer to Figures 24 and 25. Lack of penetration at weld root was found in both the blades. Shrinkage porosity and crack originating at the interface of the heat affected zone and fusion zone was found in the weld bead of the LP-B L2-R #141. The crack is consistent with "hydrogen cracking" that can be attributed to low preheat

SIEMENS

temperatures. Semi - quantitative elemental chemical analysis via X-ray energy dispersive spectroscope (EDS) was performed on the undershroud weld beads of both blades. The chemical analysis of weld filler material was typical of grade 17-4PH stainless steel.

SIEMENS

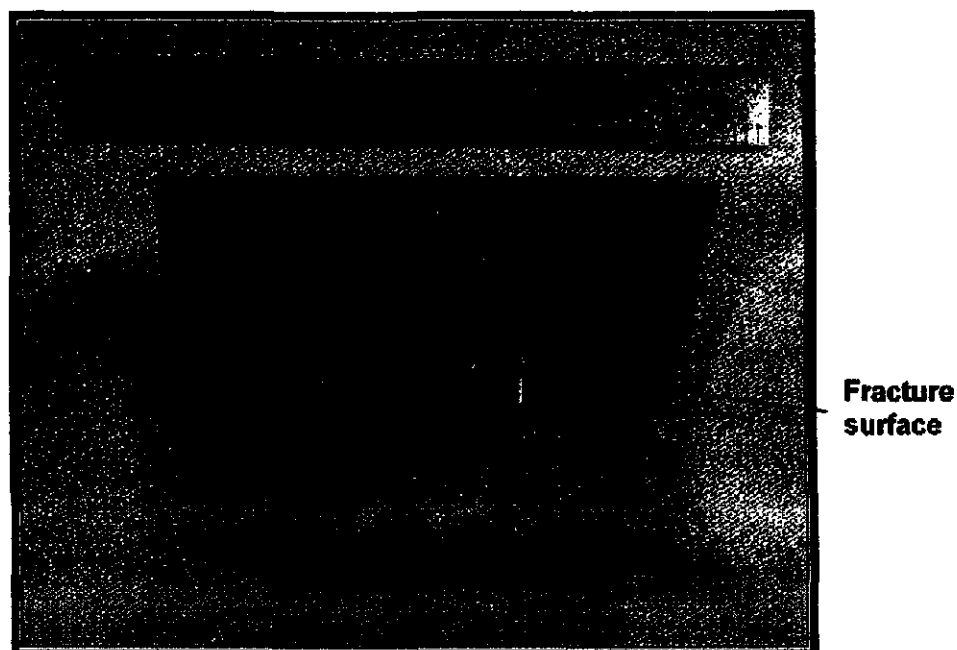


Figure 1: As received LP-A L-2 #49 blade concave side.

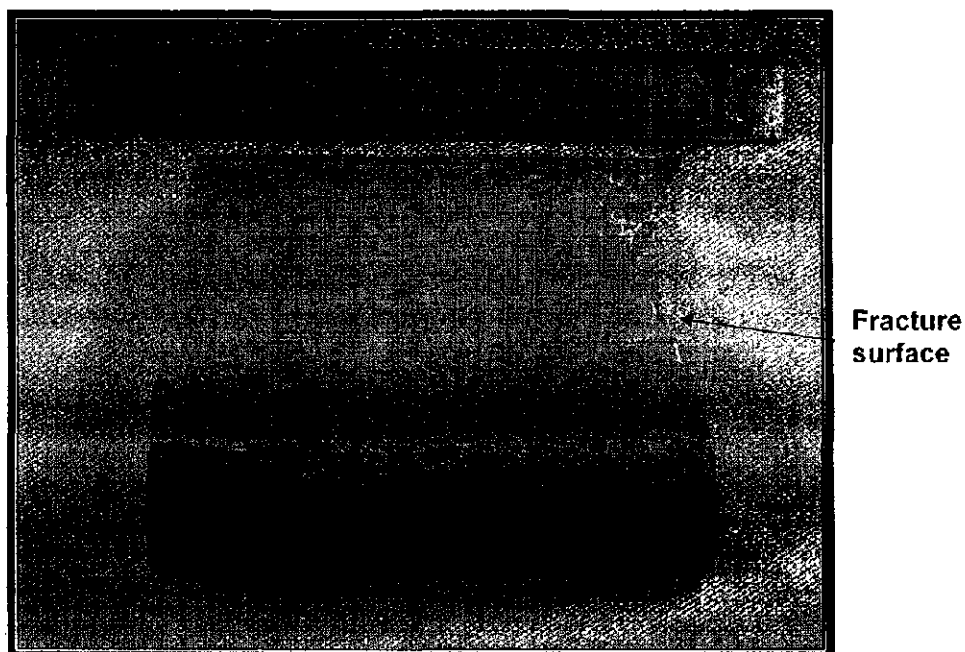


Figure 2: As received LP-A L-2 #49 blade convex side. Reddish brown deposit is seen on the convex side.

SIEMENS

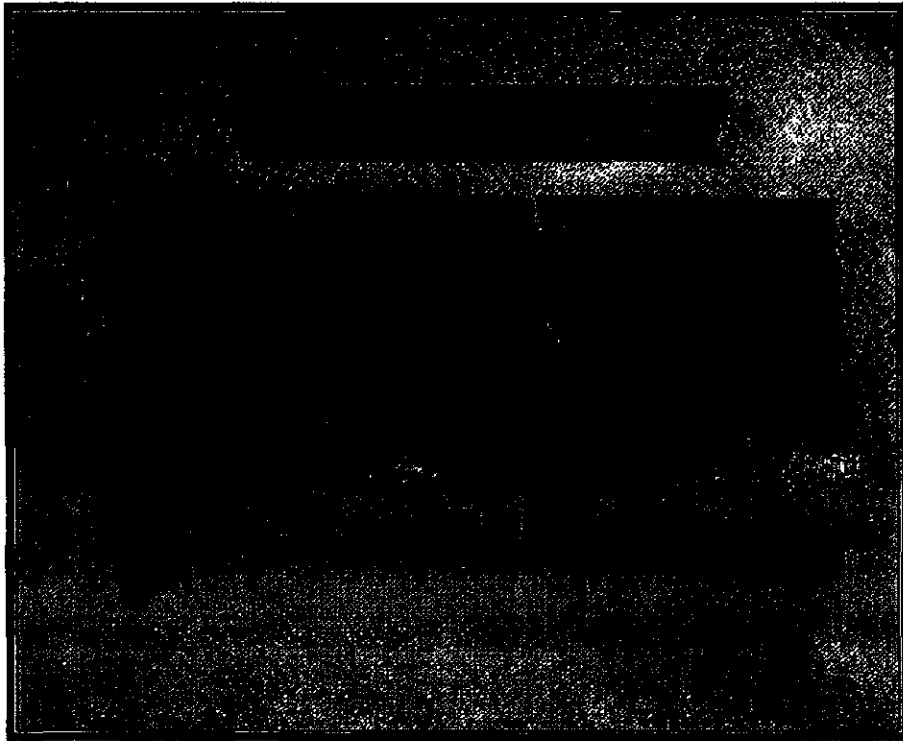


Figure 3: As received LP-A L-2 #175 blade concave side

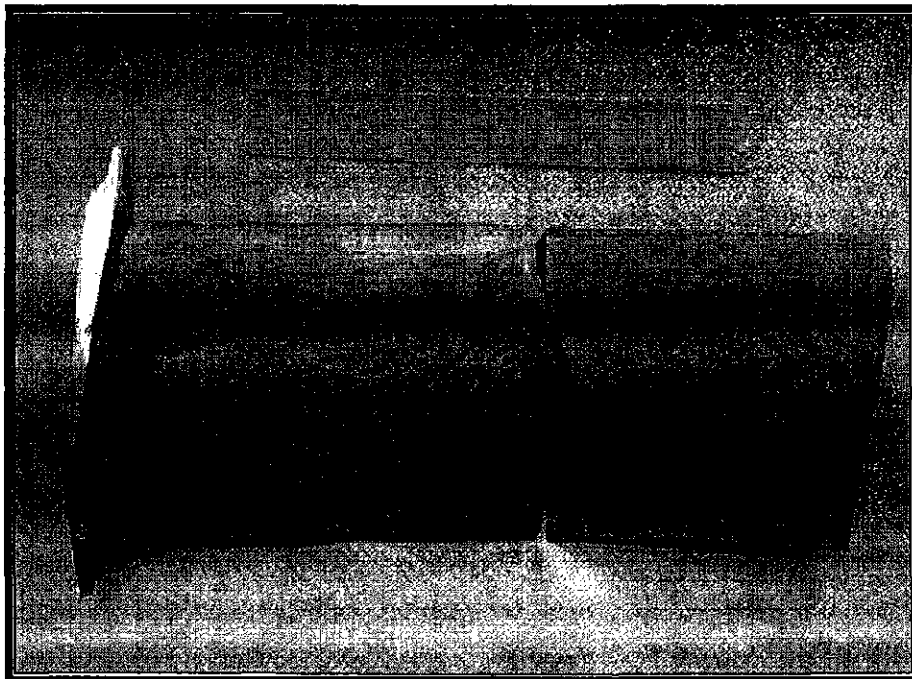


Figure 4: As received LP-A L-2 #175 blade convex side. Reddish brown deposit is seen on the convex side.

SIEMENS

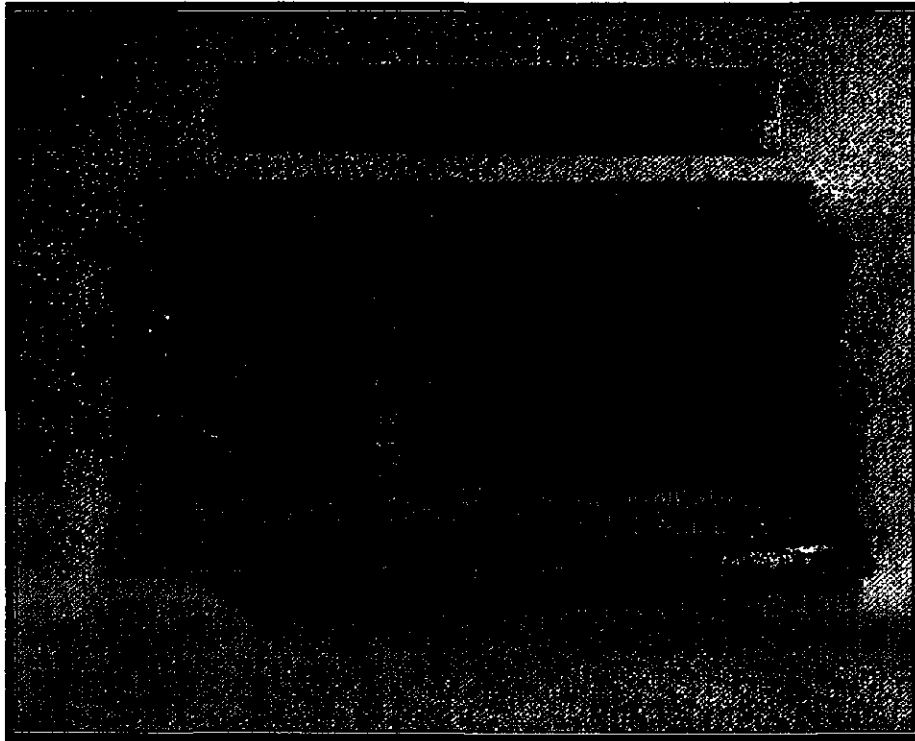


Figure 5: As received LP-B L-2 #103 blade concave side

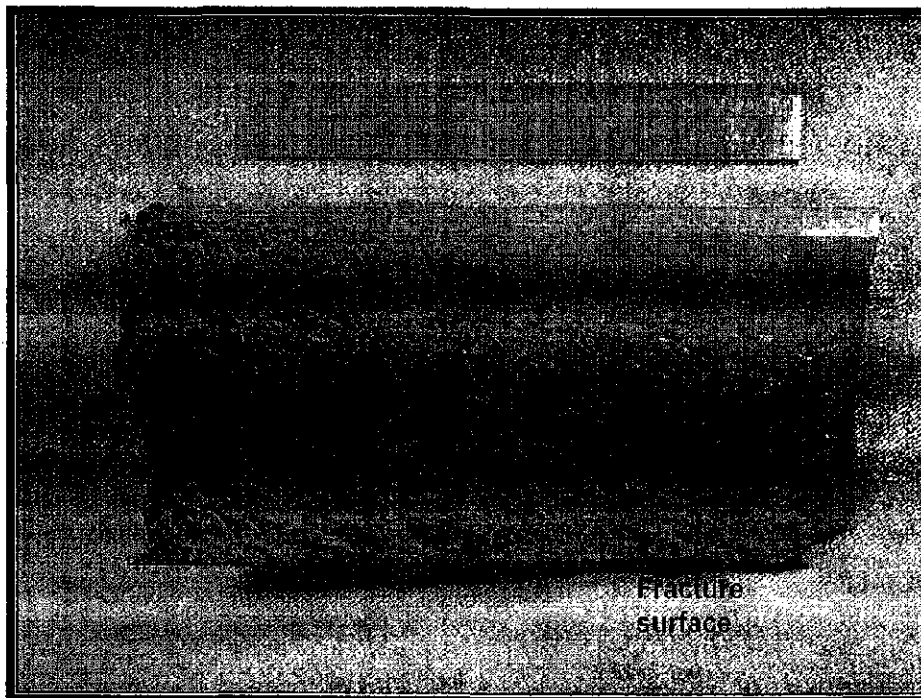


Figure 6: As received LP-B L-2 #103 blade convex side. Reddish brown deposit is seen on the convex side.

SIEMENS

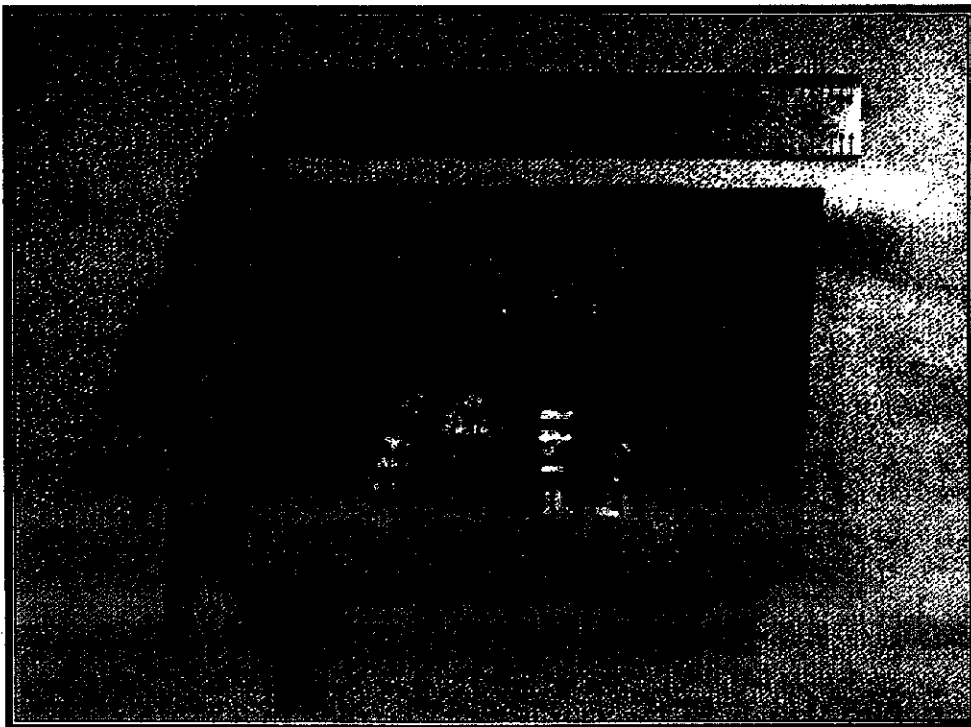


Figure 7: As received LP-B L-2 #141 blade concave side

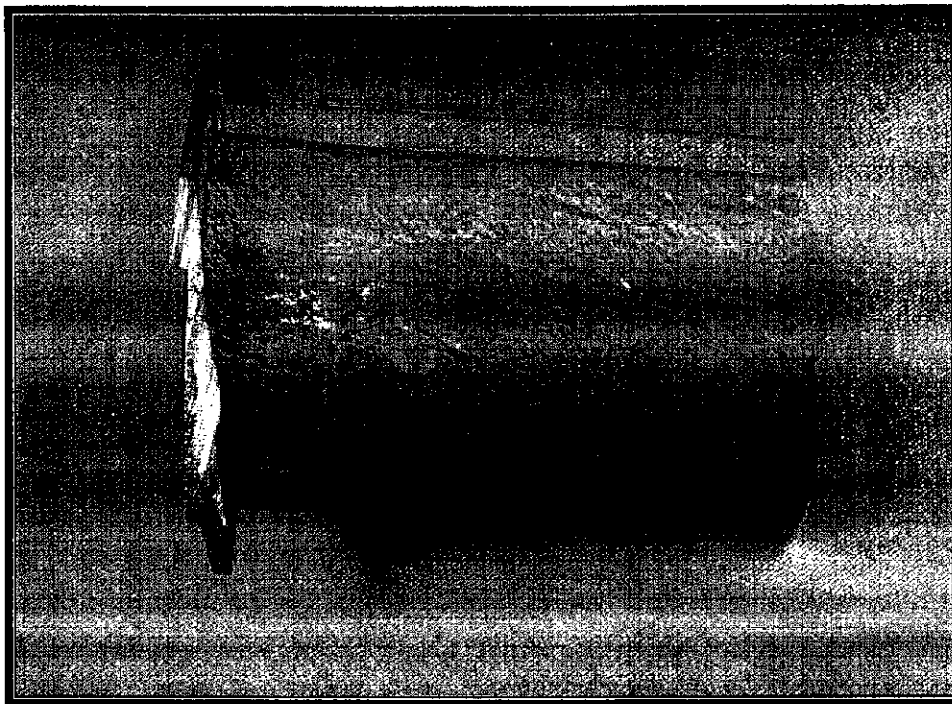


Figure 8: As received LP-B L-2 #141 blade convex side. Reddish brown deposit is seen on the convex side.

SIEMENS

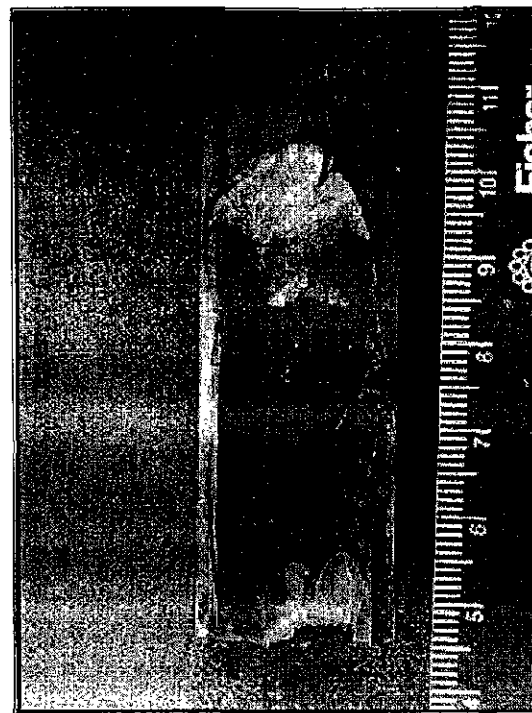
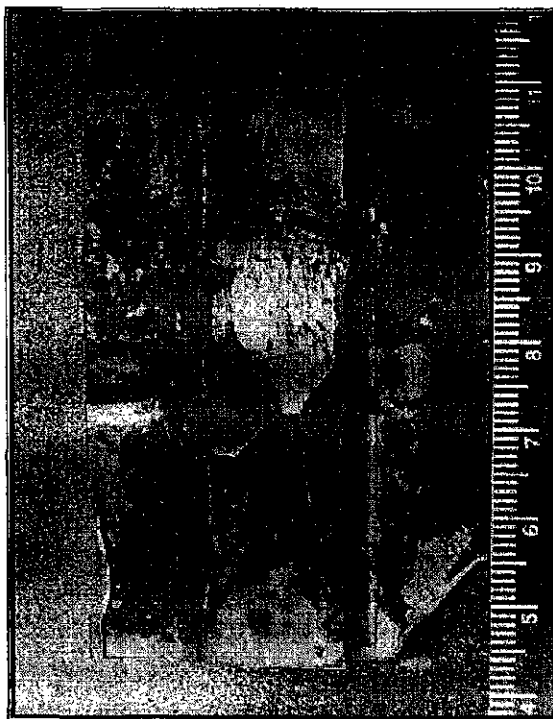
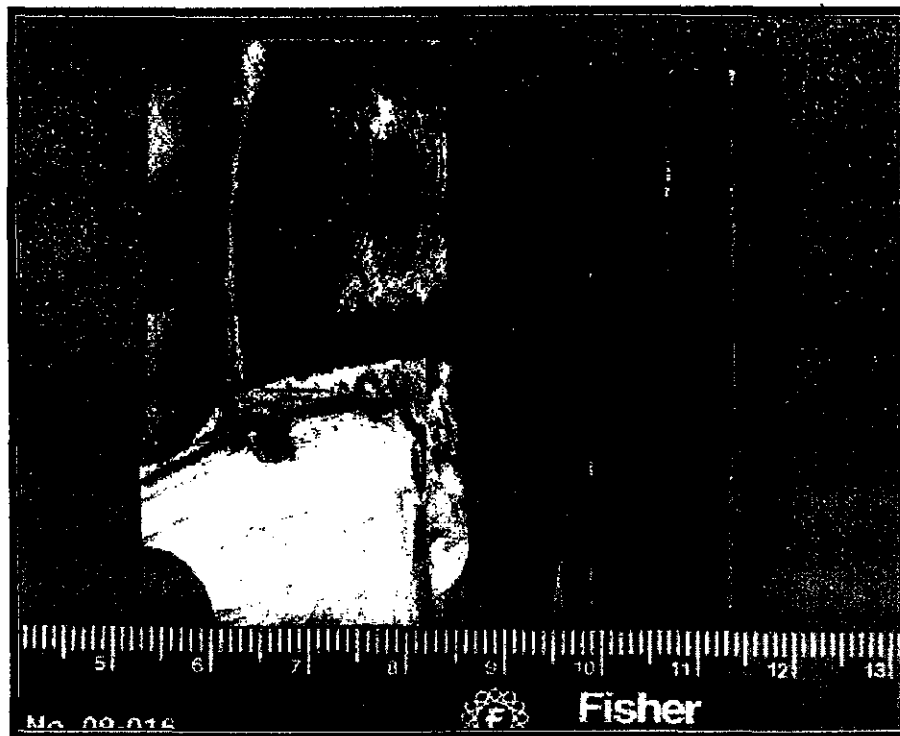


Figure 9: As received LP-A L-3 #4 blade cracked in the root. Fracture surface is covered by reddish brown oxide deposits.

SIEMENS

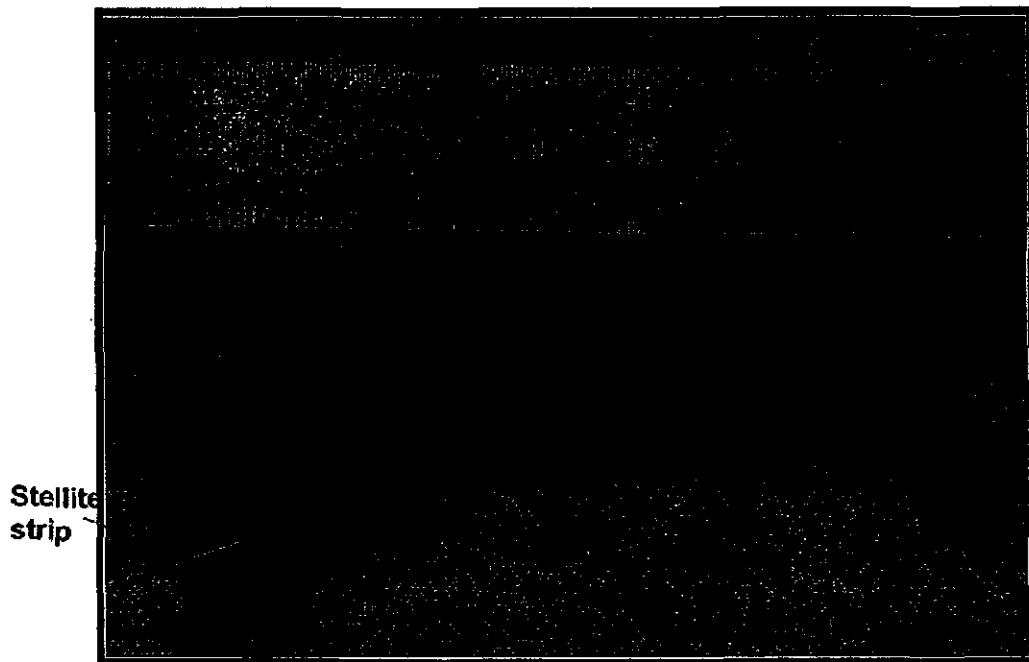


Figure 10: Macro photograph of fracture surface of LP-A L-2 #49 blade. Fracture surface was cleaned to remove thick oxide deposit. Flat fracture surface can be seen from the leading edge continuing into a fracture surface due to overload towards the trailing edge.

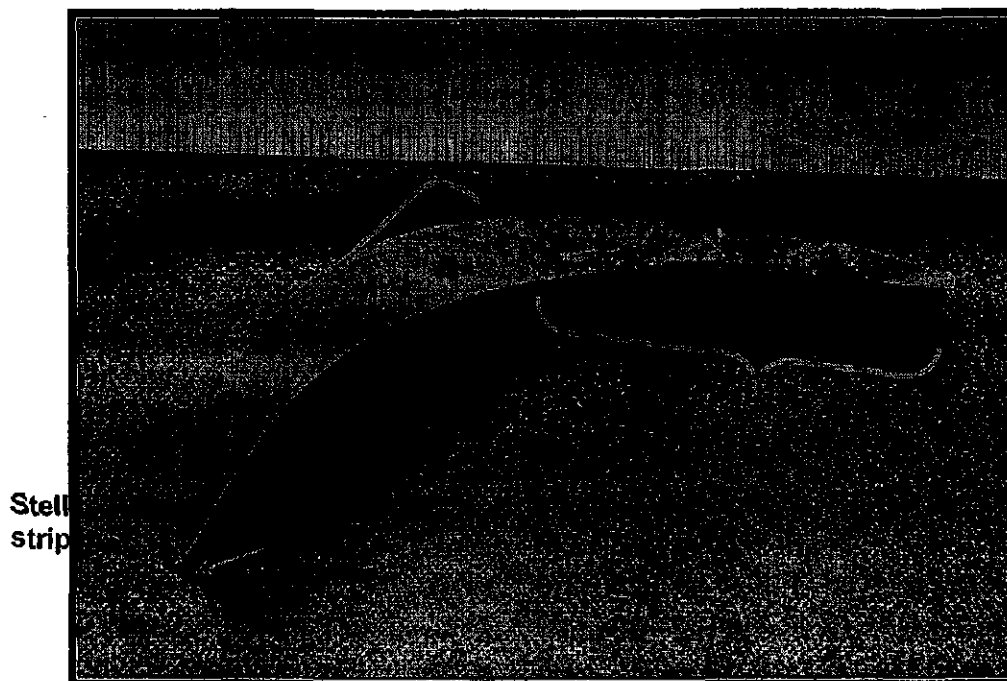


Figure 11: Macro photograph of fracture surface of LP-A L-2 #175 blade. Fracture surface was cleaned to remove thick oxide deposit. Flat fracture surface can be seen from the leading edge continuing into a fracture surface due to overload towards the trailing edge

SIEMENS

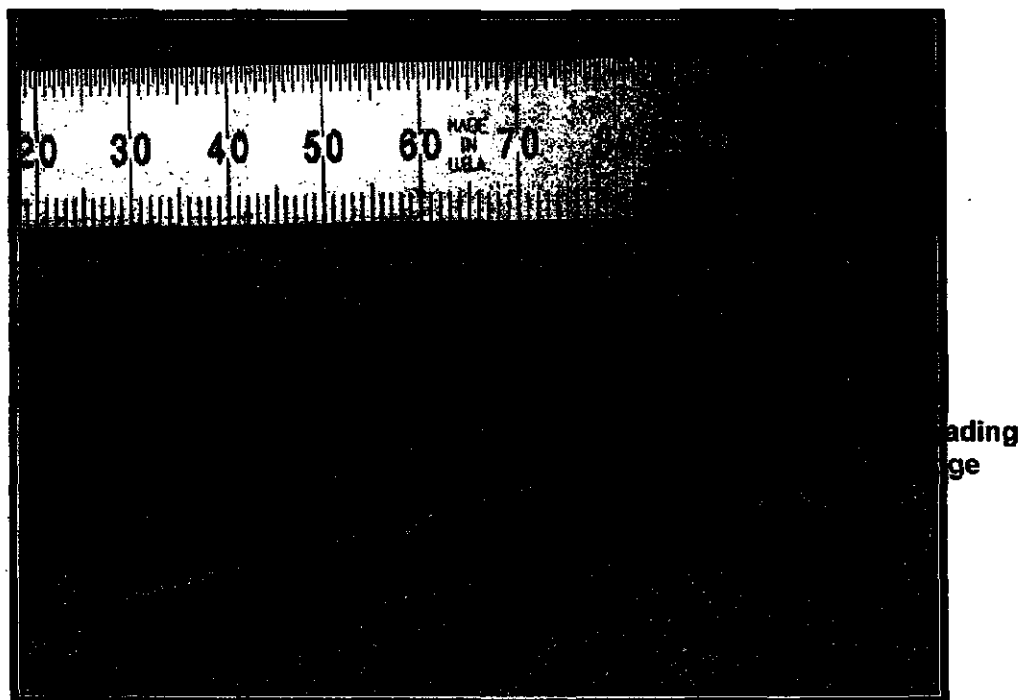


Figure 12: Macro photograph of fracture surface of LP-B L-2 #103 blade. Fracture surface was cleaned to remove thick oxide deposit. Flat fracture surface can be seen from the leading edge continuing into a fracture surface due to overload towards the trailing edge.

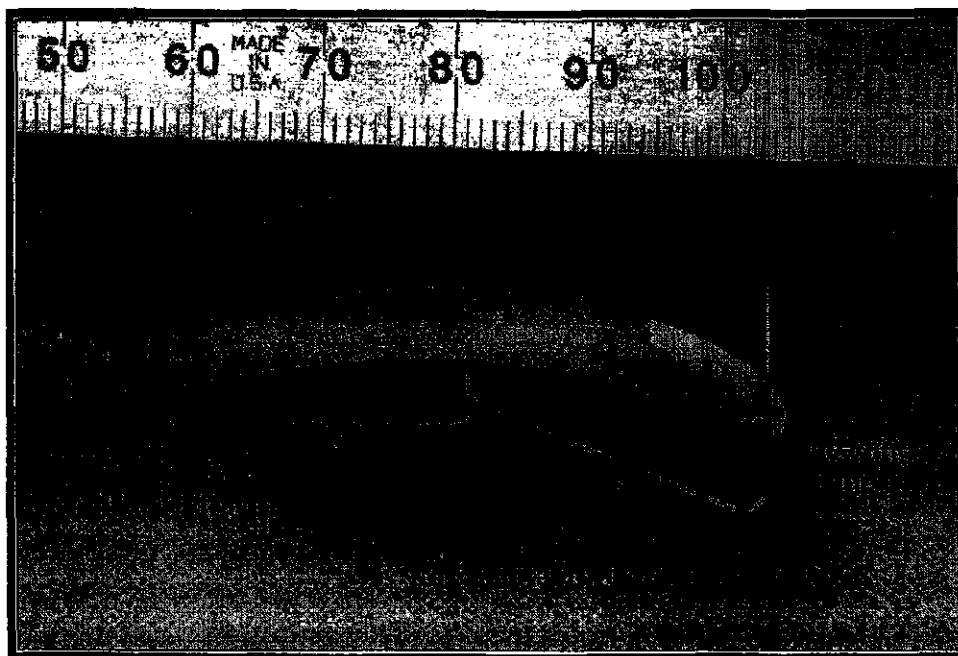


Figure 13: Macro photograph of fracture surface of LP-B L-2 #141 blade after opening the crack. Fracture surface was cleaned to remove thick oxide deposit. Flat fracture surface can be seen from the leading edge continuing into a fracture surface due to overload towards the trailing edge.

SIEMENS

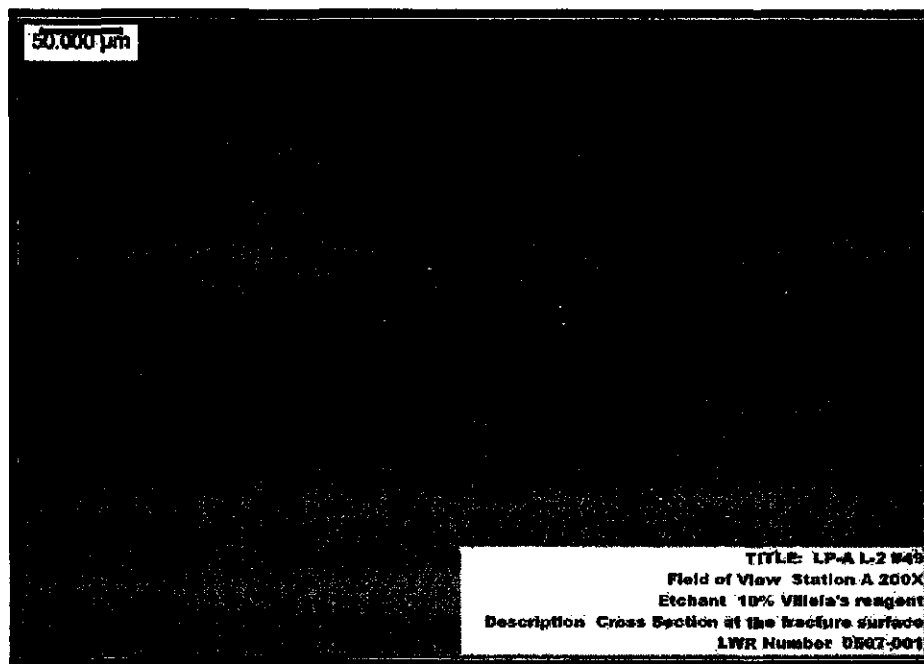


Figure 14: Photomicrograph of the cross section of the flat fracture surface of LP-A L-2 #49 blade. Microstructure indicates that the crack propagated in a transgranular fashion. The microstructure consists of tempered martensite.

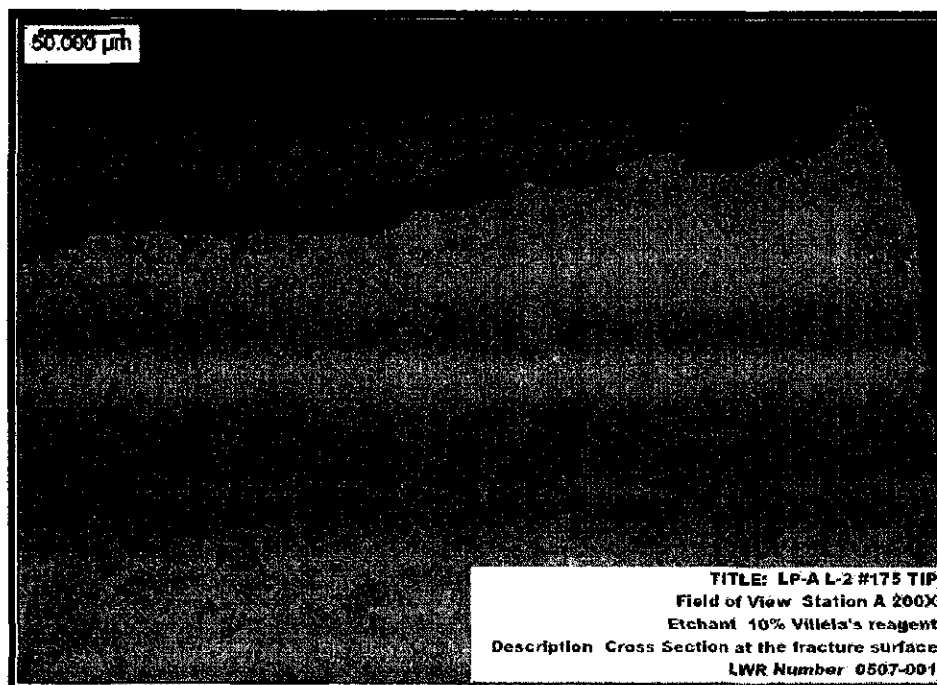


Figure 15: Photomicrograph of the cross section of the flat fracture surface of LP-A L-2 #175 blade. Microstructure indicates that the crack propagated in a transgranular fashion. The microstructure consists of tempered martensite.

SIEMENS

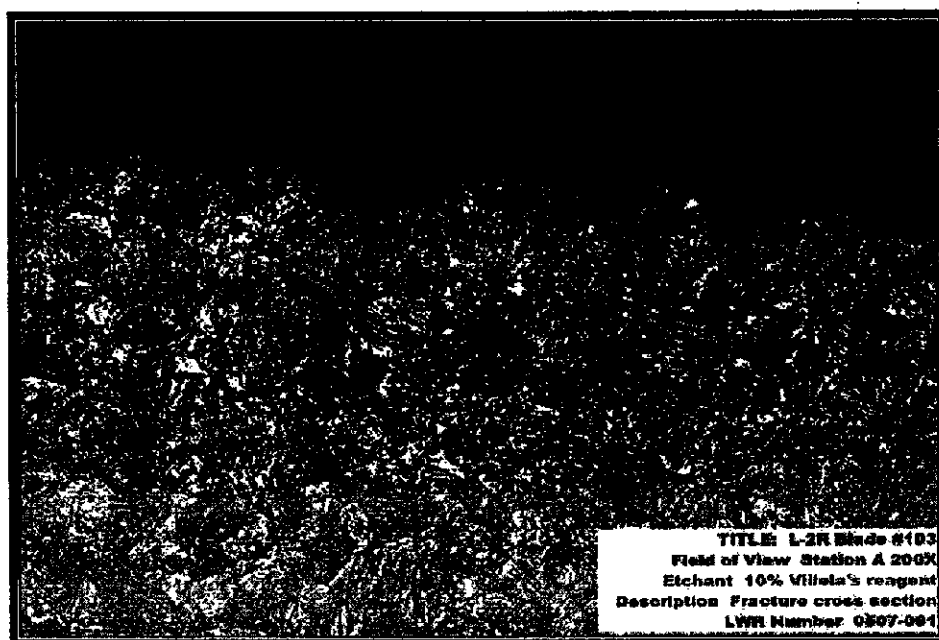


Figure 16: Photomicrograph of the cross section of the flat fracture surface of LP-B L-2 #103 blade. Microstructure indicates that the crack propagated in a transgranular fashion. The microstructure consists of tempered martensite.

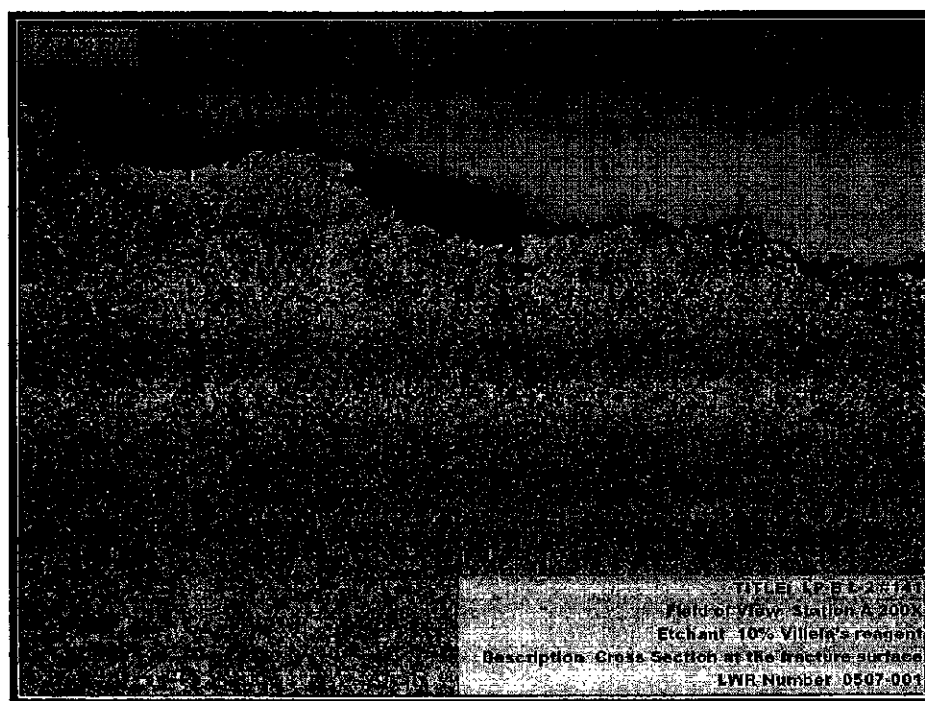


Figure 17: Photomicrograph of the cross section of the flat fracture surface of LP-B L-2 #141 blade. Microstructure indicates that the crack propagated in a transgranular fashion. The microstructure consists of tempered martensite and delta ferrite.

SIEMENS

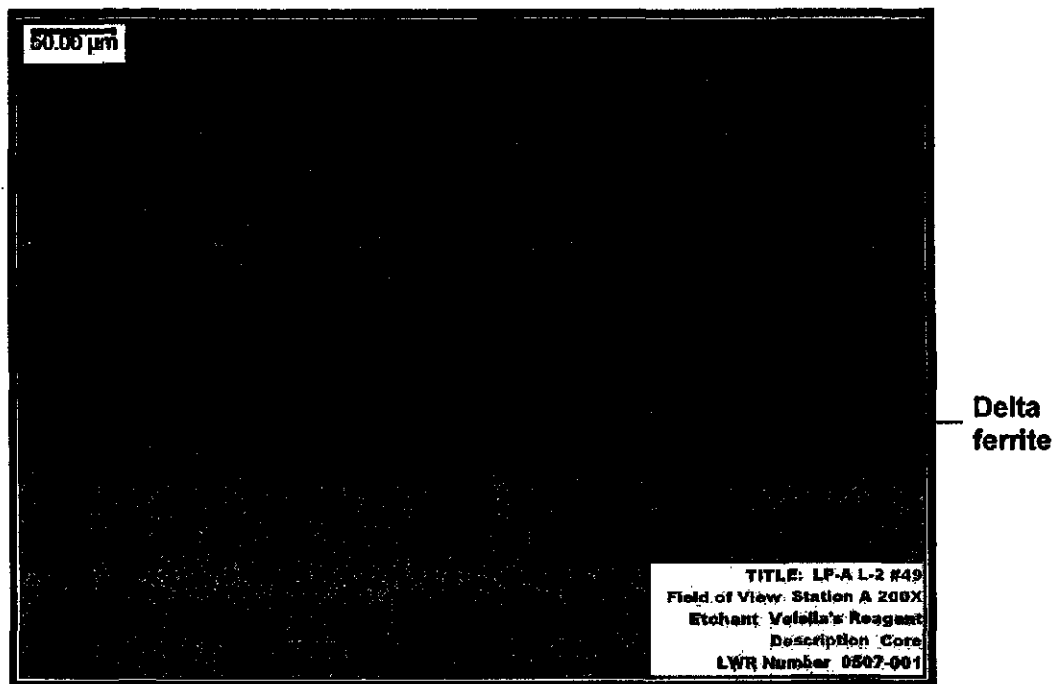


Figure 18: Photomicrograph of the core of LP-A L-2R #49 blade. The microstructure consists of tempered martensite and delta ferrite (<5%).

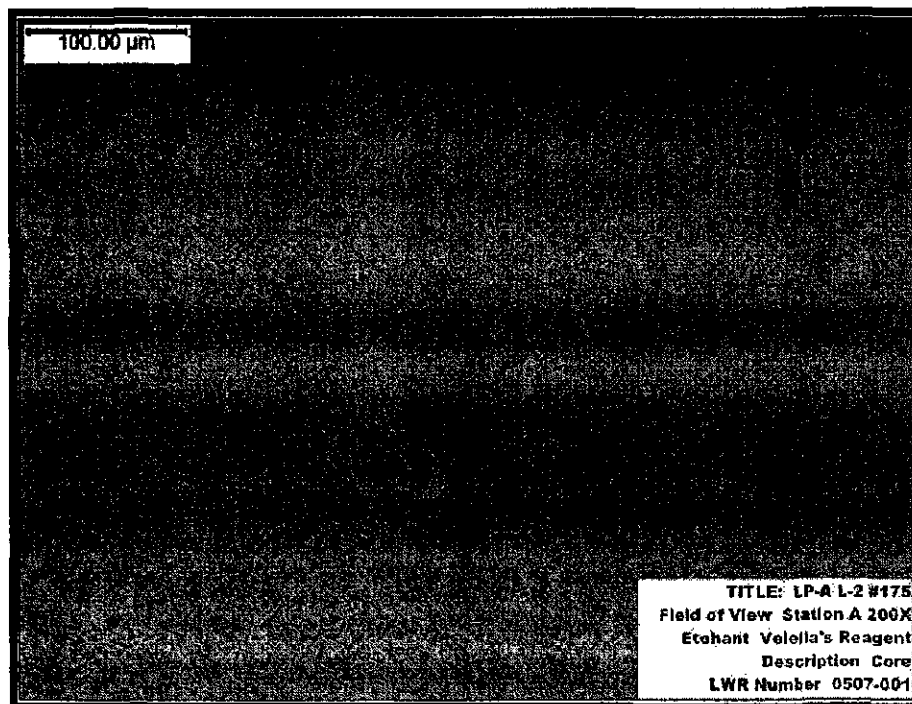


Figure 19: Photomicrograph of the core of LP-A L-2R #175 blade. The microstructure consists of tempered martensite and delta ferrite (<5%).

SIEMENS

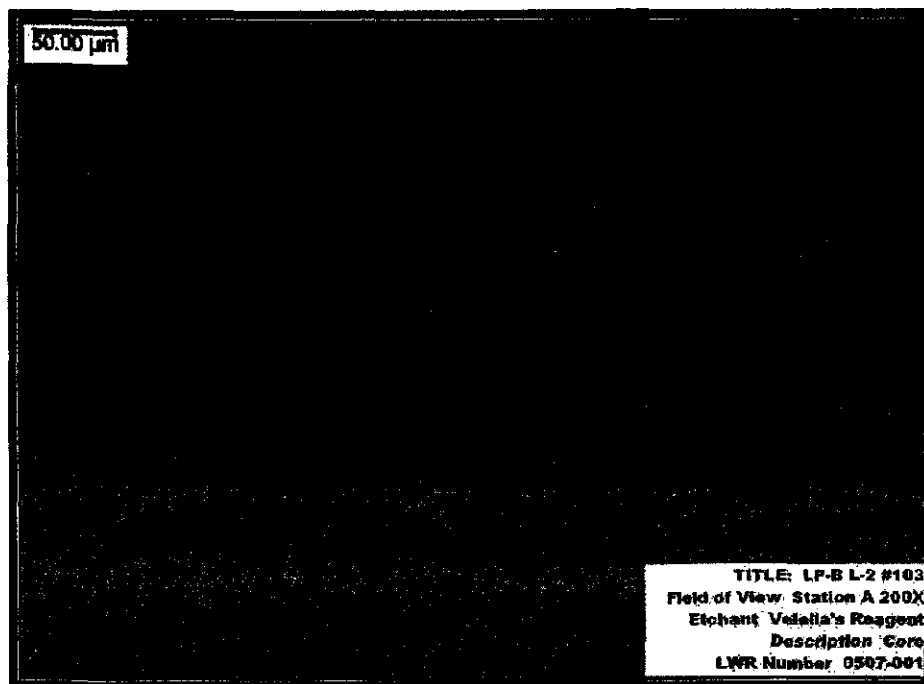


Figure 20: Photomicrograph of the core of LP-B L-2R #103 blade. The microstructure consists of tempered martensite and delta ferrite (<5%).

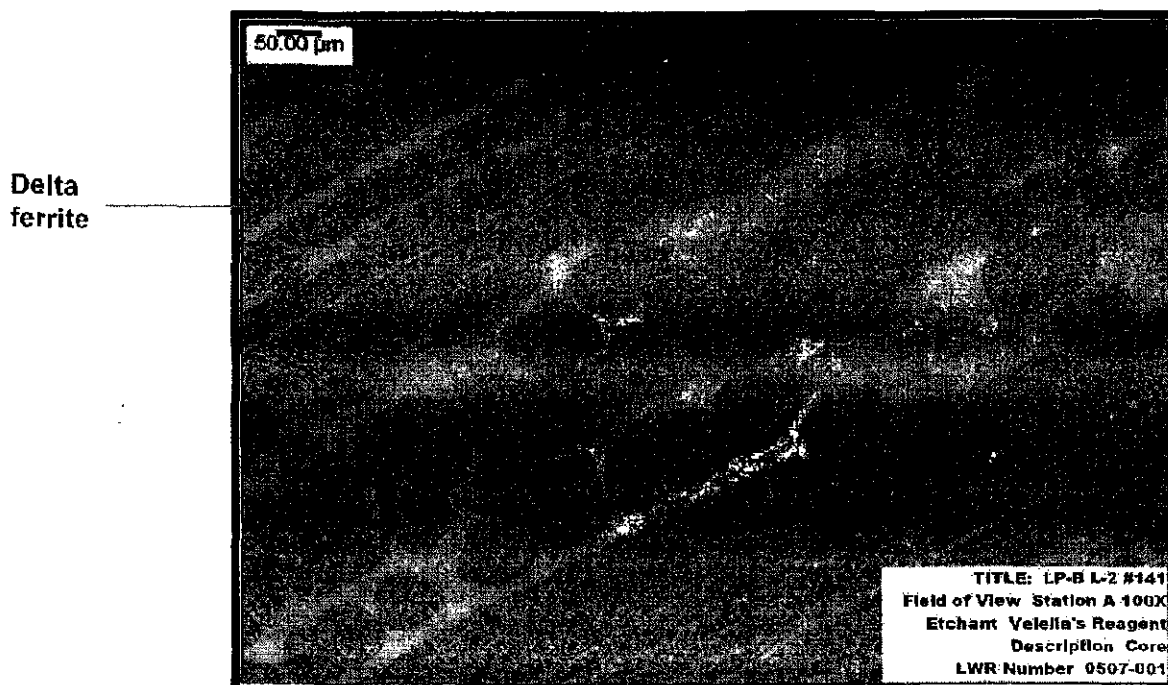


Figure 21: Photomicrograph of the core of LP-B L-2R #141 blade. The microstructure consists of tempered martensite and delta ferrite (~15%).

SIEMENS



Figure 22: Photomicrograph of the core of LP-B L-2R #141 blade. Microstructure consists of tempered martensite and delta ferrite (~10%).

Sample No.	Measurement No	Hardness (HRC)	BHN (converted)
LP-A L-2 #49	1	30.3	309
	2	31.9	319
	3	32.3	319
LP-A L-2 #175	1	31.7	315
	2	32.1	319
	3	31.7	315
LP-B L-2 #103	1	30.5	305
	2	29.6	301
	3	29.6	301
LP-B L-2 #141	1	30.6	305
	2	30.9	309
	3	30.9	309
LP-A L-3 #4	1	30.3	309
	2	30.5	309
	3	31.2	311

Table 1: Measured hardness values of the L-2R blades and L-3R blade

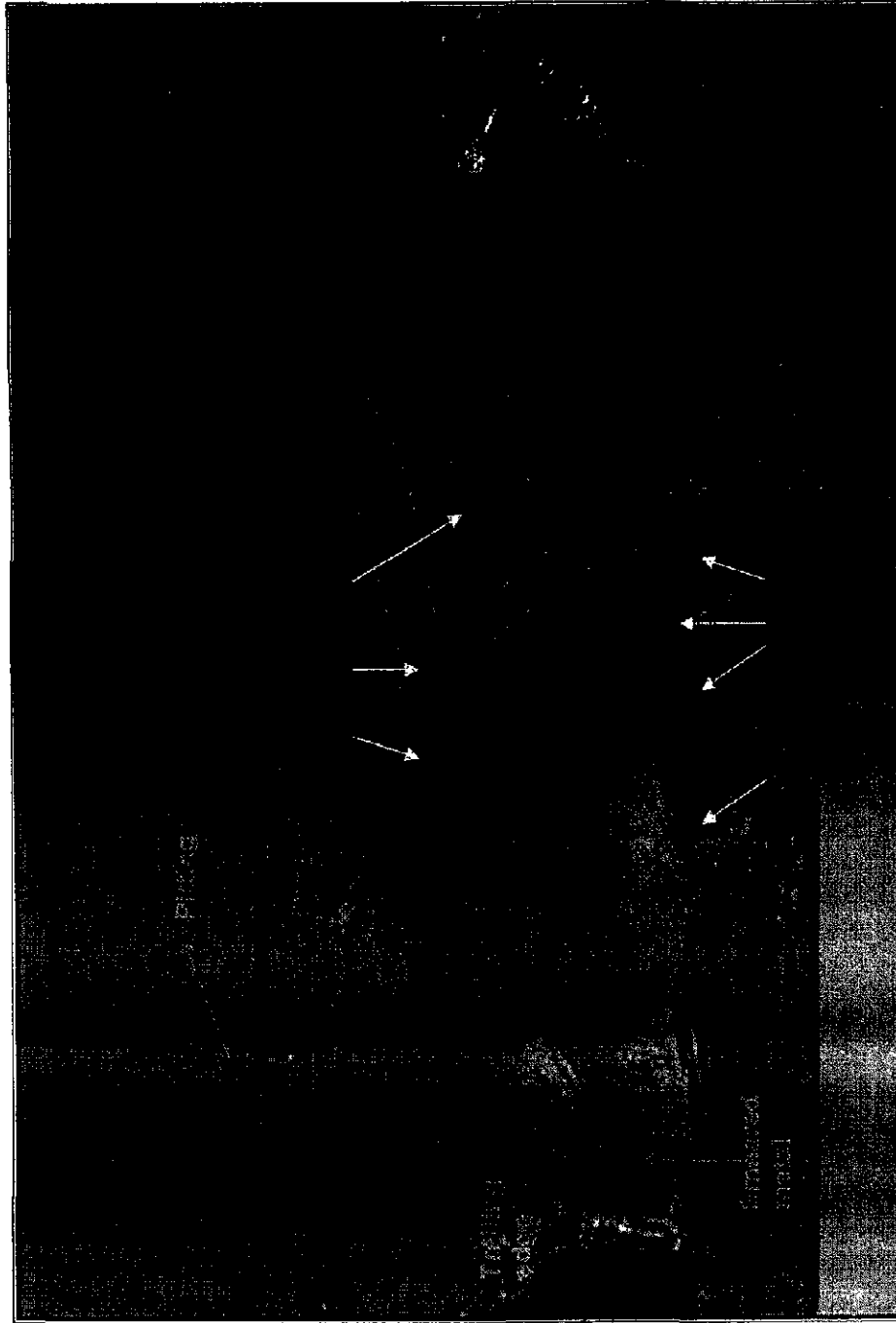


Figure 23: Macrograph of the lower half of the L-3 #4 blade root after cleaning. Numerous secondary crack origins (red arrows) were found. Secondary cracks propagated in transcrystalline mode as shown by the yellow arrows. Beach / arrest marks (dashed red lines) can be seen consistent with fatigue fracture. Primary crack propagates from the trailing edge to the leading edge as shown by the blue arrows.

SIEMENS

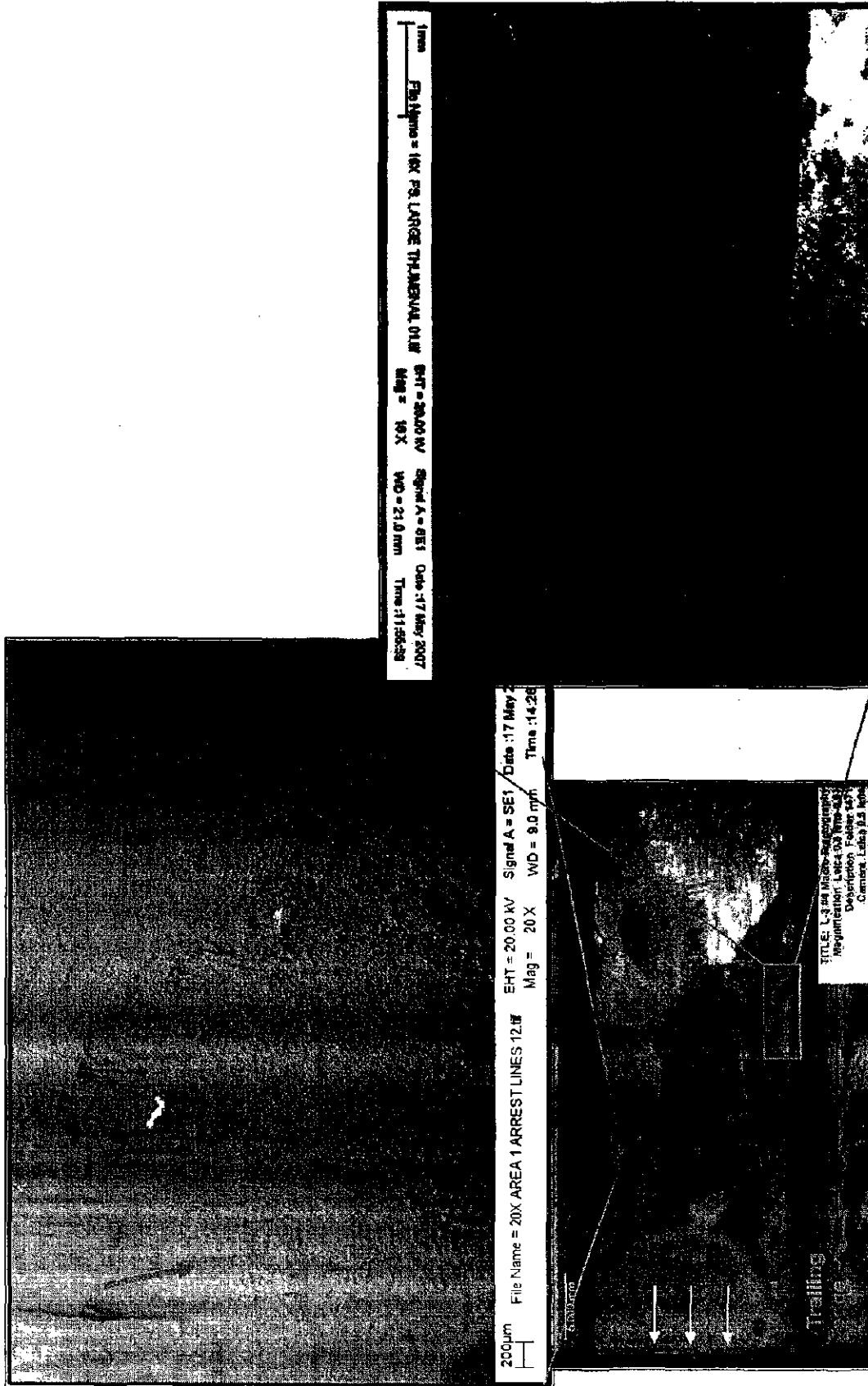


Figure 24: Macrograph of the upper half (tip side) of the L-3 #4 blade root after cleaning. SEM fractographs of the secondary cracks are shown taken at two different locations. Secondary cracks propagated in transcrystalline mode as shown by the red arrows. Beach / arrest marks (dashed red lines) can be seen consistent with fatigue fracture. Smooth thumb nail print area at the trailing edge indicates that primary crack originated at the at the trailing edge shown by yellow arrow and propagated towards leading edge as shown by blue arrow.

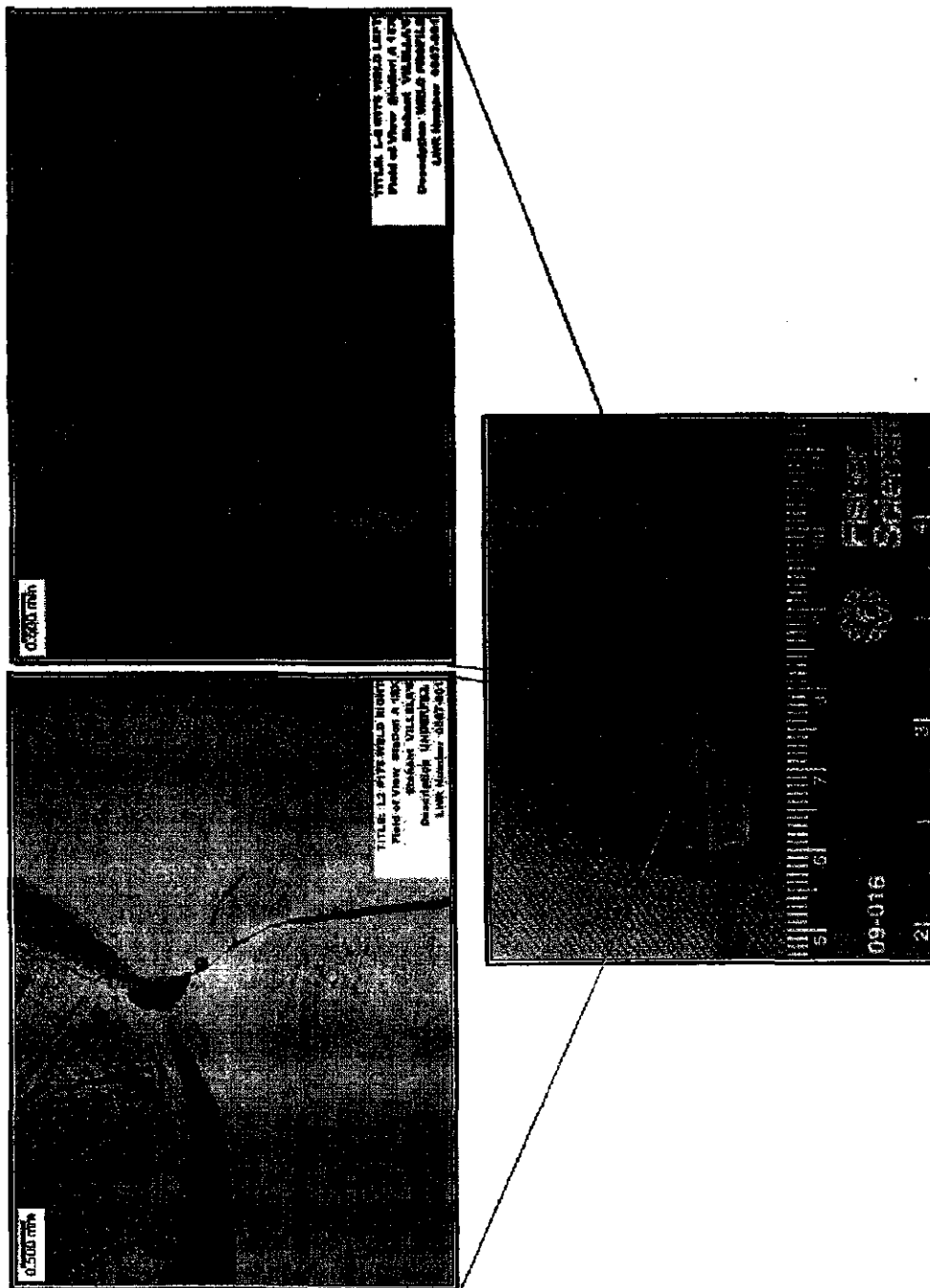


Figure 25: Micrographs of undershroud welding joint of LP-A L-2R #175 blade. Lack of penetration at the weld root was found on both sides of the blade.

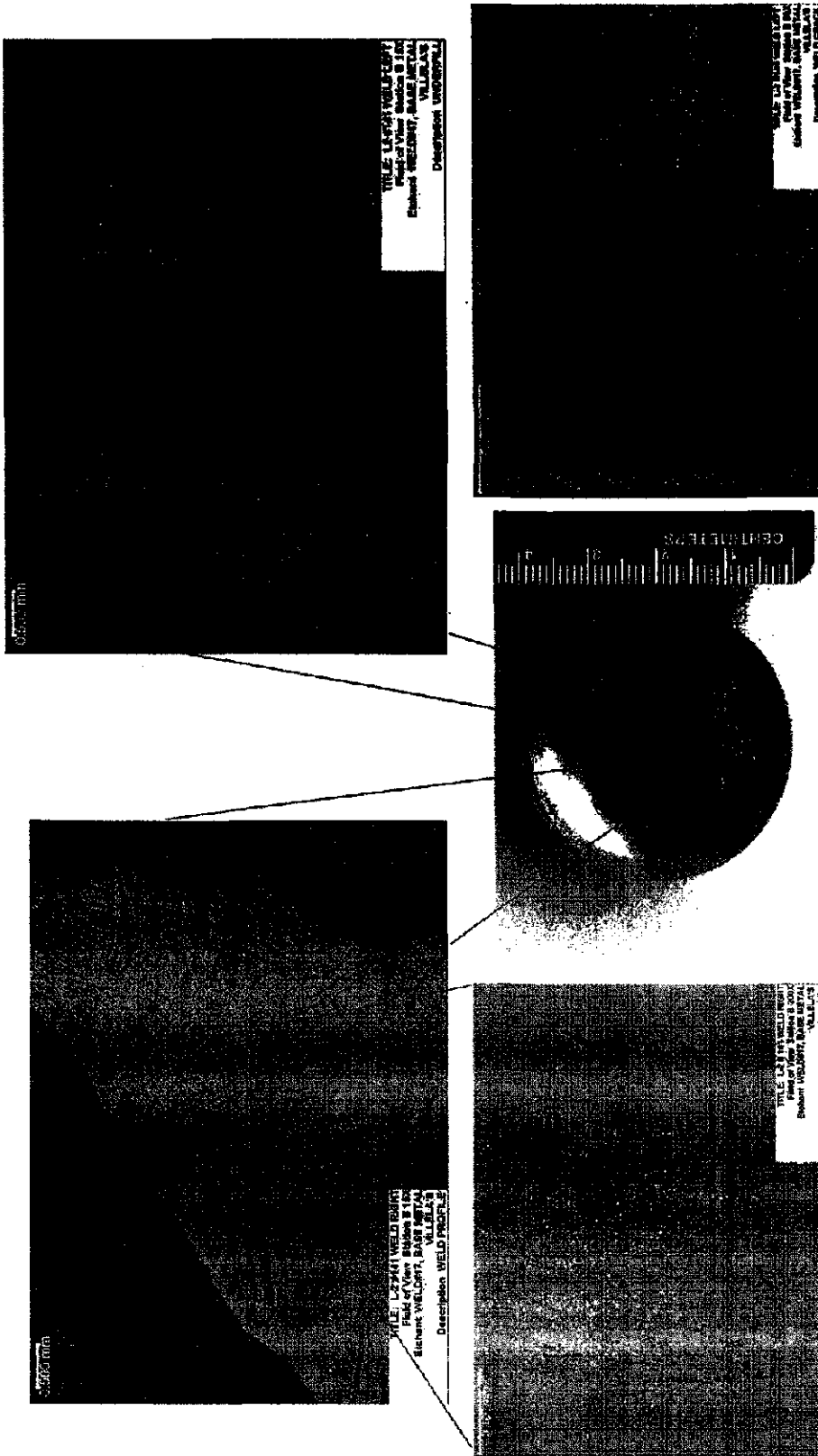


Figure 26: Micrographs of undershroud welding joint of LP-B L-2R #141 blade. Lack of penetration at the weld root was found on both sides of the blade. Shrinkage porosity was found in the left side weld and crack originating at the interface of fusion and heat affected zone was found in the right side weld. The crack propagated along the grain boundary.



Nuclear Generation

Materials Engineering & Lab Services

May 14, 2007

Memorandum to: David Warren, Turbine SMEs, Duke Energy Corporation
C.T. Alley Jr., Nuclear Generation, Duke Energy Corporation

Subject: Evaluation of Failed Turbine Blades from Zimmer Station
Metallurgy File #3791

Introduction

A total of four failed low pressure turbine blades were received in the Metallurgy Laboratory for evaluation of failure mode. Two from LPA L-2 were fractured and one from LPB L-2 was severely cracked. The fourth from LPA L-3 had cracks in the peened end of the tenon and a crack in the shroud (cover band). Information received with the blades included the following:

The L-2 governor end blade failures on LP1 (or LPA) failed approximately 4-3/4" to 5-1/2" from the tip of the blade. Two blades from this row were submitted for laboratory evaluation. The L-2 generator end blade failures on L-2 (or LPB) failed approximately 1" from the tip. One failed blade from this location was submitted for laboratory evaluation. Both rows had been undershroud welded. All failed blades are reported to be type 403 stainless steel. Both LPs had fairly heavy deposits on the L-2 blades. The failed blades were in service for 16 years and some of the failures may have occurred as long as two years ago. At the time the blades were removed for examination, visual examination had confirmed twelve failed L-2 blades on the governor end of LP1 And seven failed L-2 blades on the generator end of LP2.

Visual Examination

The most striking characteristic of the three L-2 blades was the adherent brown deposit on the convex side of each. The deposit lay over the blades in a pattern that suggests condensation ran from the root end of the blade outward toward the tip depositing material and producing erosion-corrosion grooves oriented along the radial axis of each blade (Figures 1, 2 and 3). The blade that was not completely fractured shown in Figures 3 and 4 had a complex crack pattern that did not appear to be particularly related to the direction of the stresses that would be expected to occur during operation. Figure 4 also serves to illustrate the typical surface condition of all three blades. Each had thin discontinuous black deposits also oriented in a radial deposition pattern on the concave side of the blade. Figure 5 shows the multi-directional looping crack pattern extending through the thickness of the blade.

The portion of the fracture faces near the leading edge of the two broken blades shown in Figure 6 have the macroscopic characteristics of fatigue. Some portions of each face is relatively deposit free suggesting that the final fracture probably occurred recently. Further toward the trailing edge, the fracture surface is much rougher (stepped) and has more deposit which suggests corrosion rather than fatigue.

The results of macroscopic examination indicate both corrosion and mechanical fatigue were associated with the failures of the blades from LPA L-2. The complex crack pattern on the LPB blade does not rule out mechanical fatigue but suggests corrosion as the predominant mechanism.

Figure 7 illustrates the as-received condition of the L-3 blade. The face of the crack in the shroud of this blade was covered with a tenacious brown deposit similar to that seen on the convex surface of the other blades. No secondary or branch cracking was observed either on the shroud or on the tenon. The shroud and tenon were cut to separate the parts for further



Nuclear Generation

Materials Engineering & Lab Services

examination. The crevice between the two parts was tightly packed with debris. A strong solvent smell emanating from the area of the deposits was noted. Later conversations with the turbine SME suggested this odor might come from the penetrating oil used when the blade was removed from the rotor. SiliKroil was suggested as one of the possible solvents used. The crack in the tenon was longer on the flank of the tenon than on the peened end which suggests it initiated in the crevice and propagated toward the outer surface.

Scanning Electron Microscopy (SEM)

Adherent deposits obscured much of the fracture faces of the L-2 blades but the cleaner areas had evidence of fatigue propagation of the fractures (Figures 8, 9 and 10). Other than the heavy deposits in the region of the trailing edge, no indications of intergranular or transgranular corrosion were found.

The entire surface of L-3 blade shroud crack was covered with the adherent brown deposit that could not be successfully removed without damaging the underlying fracture features. No useful SEM information was obtained. A part of the crack in the tenon was opened and examined by SEM. The features near the end of the crack were more consistent with corrosion than with fatigue (Figure 11). The deposits analyzed by EDS are discussed below.

Metallography

Sections through the blade from LPB and one of the blades from LPA were prepared for microscopic examination by grinding and polishing. The first crack examined (Figure 12) was from LPB and ran in a direction consistent with through thickness loading. It is mixed intergranular and transgranular consistent with a corrosion driven crack. Figure 13 shows a pit on the convex surface of one of the LPA blades. It has a network of stress corrosion cracks growing from the bottom of the pit. The convex surface illustrated in Figure 14 shows that metallic copper is associated with many of the pits. The metallographic results indicate corrosion pitting on the surface of the L-2 blades was widespread and that copper is associated with most of the pits. Not all pits have stress corrosion cracks emanating from the bottom of the pit but many do.

A section through the crack in the tenon of the L-3 blade revealed a crack on a plane parallel to the tenon axis that turned 90 degrees as it approached the peened head of the tenon (Figure 15). There were numerous small secondary cracks at right angles to the main crack (cracking on planes normal to the tenon axis). These cracks were multi-branched and filled with corrosion deposit (Figure 16).

Deposit Characterization

As noted above, the L-2 blades had an adherent brown deposit on the convex surface. Some of the material was scraped from the surface and examined by energy dispersive spectroscopy (EDS) to determine if any specific corrosive species could be detected (Figures 17 and 18). The bulk of the deposit consists of a silicon compound. No elements were detected that might commonly be associated with silicon as a silicate, therefore, it appears that the bulk of the deposit is silica. Several other elements such as copper, aluminum and nickel were also detected in the deposit. Nickel and aluminum were not uniformly dispersed among the particles examined but copper appeared in almost every spectrum. No chlorides or sulfur compounds were detected in any of the deposits. One analysis by Nalco (below) confirmed the presence of these elements.



Nuclear Generation

Materials Engineering & Lab Services

Silicon as (SiO₂) 68 %
Iron as (Fe₂O₃) 22 %
Chromium as (Cr₂O₃) 1 %
Copper as (CuO) 1 %
Nickel as (NiO) 1 %
Total From XRF: 93 %

*The results for the XRF analysis were normalized to Loss at 925° C
Thus, XRF + L925 = 100%*

Deposits scraped from the blade in the Metallurgy Laboratory found detectable quantities of calcium, chromium, copper, magnesium, nickel, phosphorus, potassium and sodium. These elements were present in quantities much less than the detectable limits for the EDS. This analysis is consistent with the Nalco analysis and with the EDS analysis.

EDS analysis of the deposits from the crevice between the tenon and shroud on the L-3 blade contained essentially the same chemical elements as the surface deposits on the L-2 blades except chlorine and sulfur compounds were detected (Figure 19). These two elements may have been present from service but are more likely the result of contamination with penetrating oil noted during macroscopic examination.

A small quantity of black magnetic deposit was also seen under the shroud (Figure 20). The angular appearance of the fragments and EDS analysis indicate these are magnetite deposits.

Base Material Characterization

The base material was reported to be type 403; however, hardness and quantitative chemical analysis indicate the blade material is 17-4PH or similar precipitation hardening material. The microstructure evaluated during metallography is tempered martensite as expected for a turbine blade. Hardness of all blades is Rockwell C 30 to 34 (see tables below). The characteristics are consistent with hardened 17-4PH stainless steel sometimes used for turbine blades. The specified hardness is not known.

Table 1 Rockwell C Hardness

LPA #115	LPA #58	LPB #150	L-3 Row
30	32	33	34
33	33	32	33
31	34	31	34
31	33	31	33

Table 2 Chemical Analysis (wt%)

(1)	C	Mn	P	S	Si	Ni	Cr	Mo	Cu	Nb	Ta
L2-3	0.04	0.31	0.013	0.015	0.71	4.30	16.53	0.06	3.13	0.46	0.03
LPA-L2-2	0.04	0.31	0.016	0.015	0.73	4.39	16.44	0.07	3.10	0.49	0.02
LPA-L2-1	0.04	0.29	0.015	0.015	0.71	4.11	16.98	0.06	3.15	0.46	0.02
LPA-L3	0.06	0.34	0.010	0.006	0.62	4.21	15.75	0.19	3.07	0.49	0.01

- (1) LP-3—Blade no. 58 from LP A
L2-2—Blade no. 115 from LP A
L2-1—Blade no. 150 from LP B
LPA-L3—Unidentified blade from L-3 row of low pressure turbine A



Nuclear Generation

Materials Engineering & Lab Services

Discussion and Conclusions

The data indicate that both corrosion and mechanical fatigue are participating in the blade failures. The pitting corrosion and stress corrosion cracking appear to be more severe on the half of the blade toward the trailing edge. The most common corrosive species, chlorides and sulfur compounds were not detected in the deposits but these are generally very soluble and may have been reduced to undetectable levels by condensate leaching of the surface. The association of the copper with pits suggests that plating of this element from solution may have been the primary driving force for pitting. The dissolution of the blade alloy and diffusion of anions due to charge balance considerations within the pits would then create the acidic conditions conducive to stress corrosion cracking at the bottom of the pit.

In summary, it appears that the most likely failure scenario is pitting and stress corrosion cracking initiated first and then fatigue drove crack extension from these small stress concentrations.

The presence of copper suggests that copper components such as condenser tubes elsewhere in the boiler are experiencing significant corrosion. High copper contents in the feedwater could be contributing to problems elsewhere including in the waterwalls of the boiler. Silica and alumina found in the deposits are likely carry over in the feedwater. The magnetite deposits may suggest significant exfoliation is occurring in the superheater and reheater sections of the boiler.

If the Metallurgy Lab can be of further assistance, please call us at (704)875-5275.

A handwritten signature in black ink, appearing to read 'C.R. Frye'.

C. R. Frye, P.E.
Senior Engineer
Materials, Metallurgy & Piping

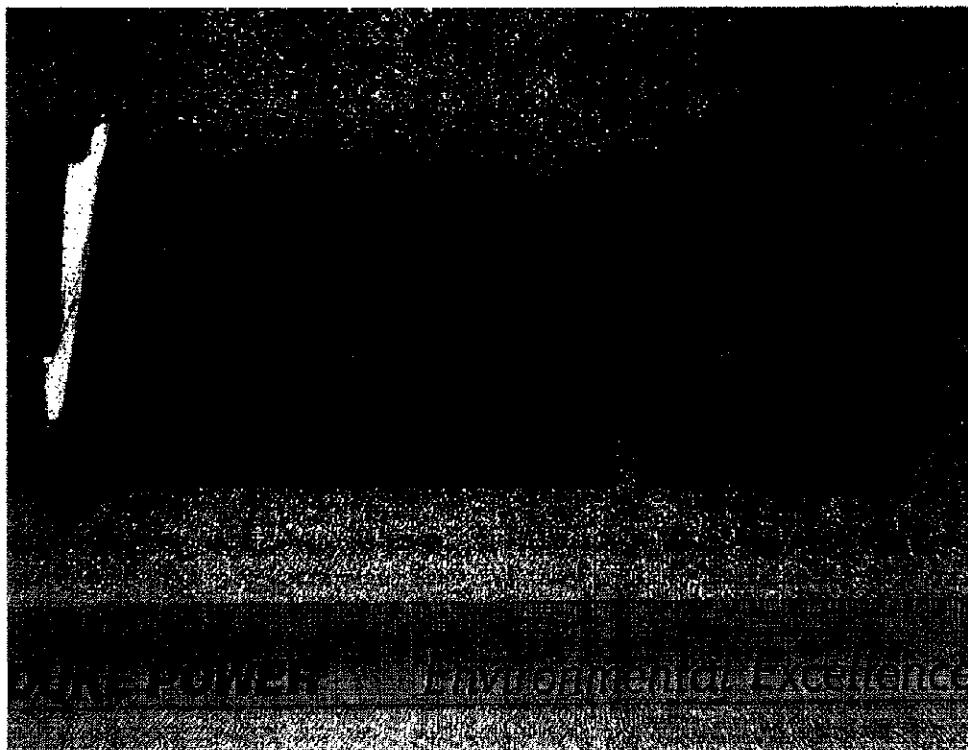


Figure: 1 LPA blade 115, number 4 in group.

Macro 01

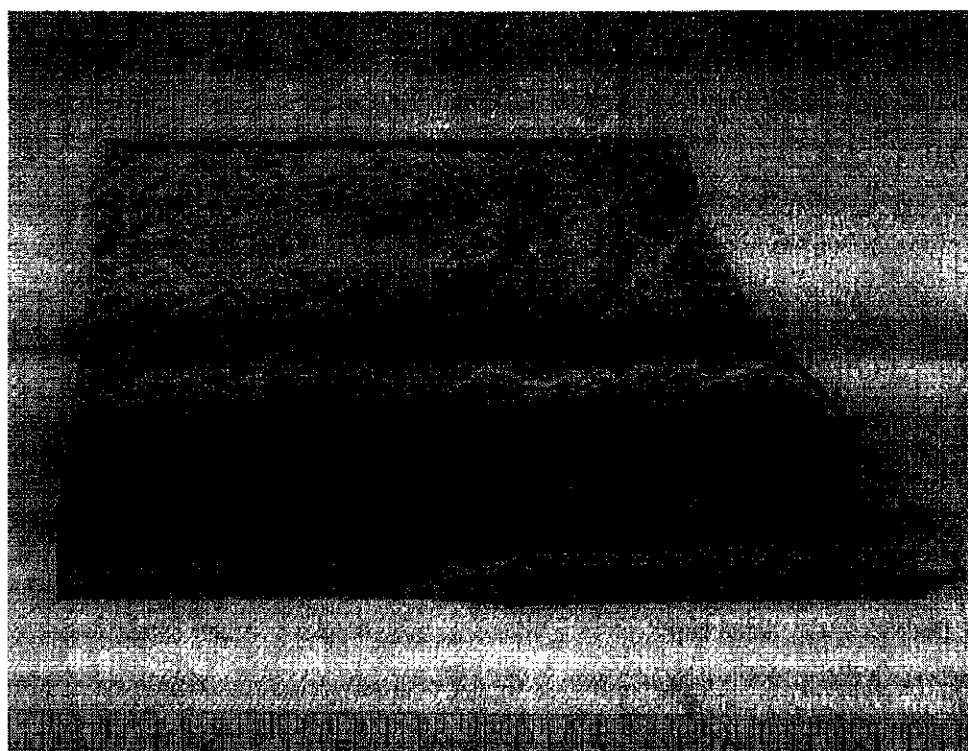


Figure: 2 LPA blade 58, start of group.

Macro-06

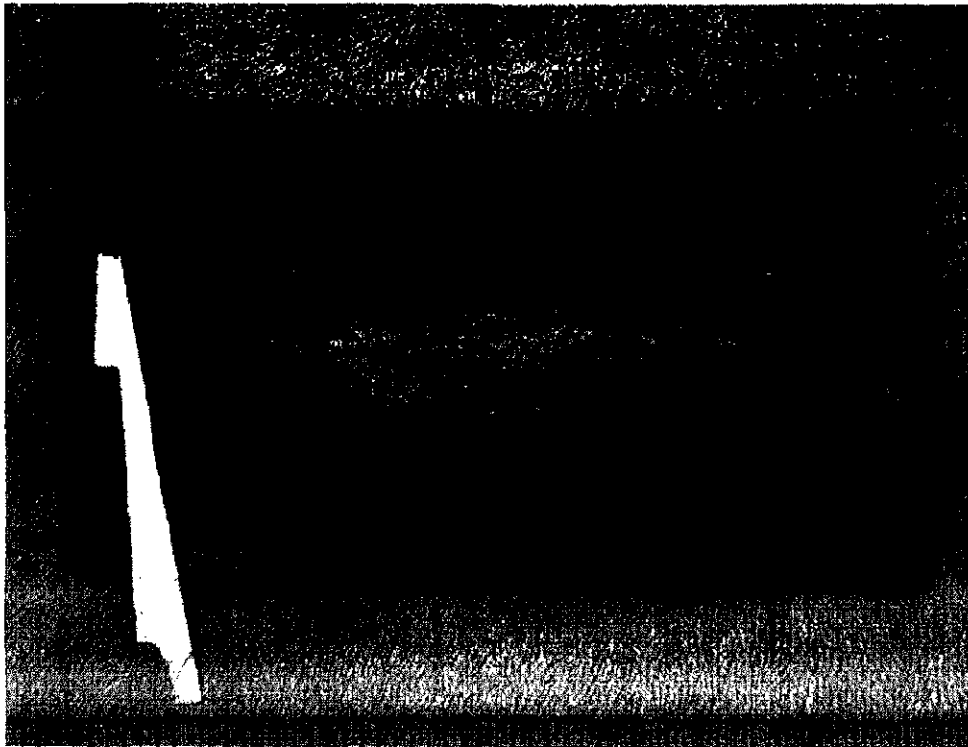


Figure: 3 LPB blade 150, third in group.

Macro -04

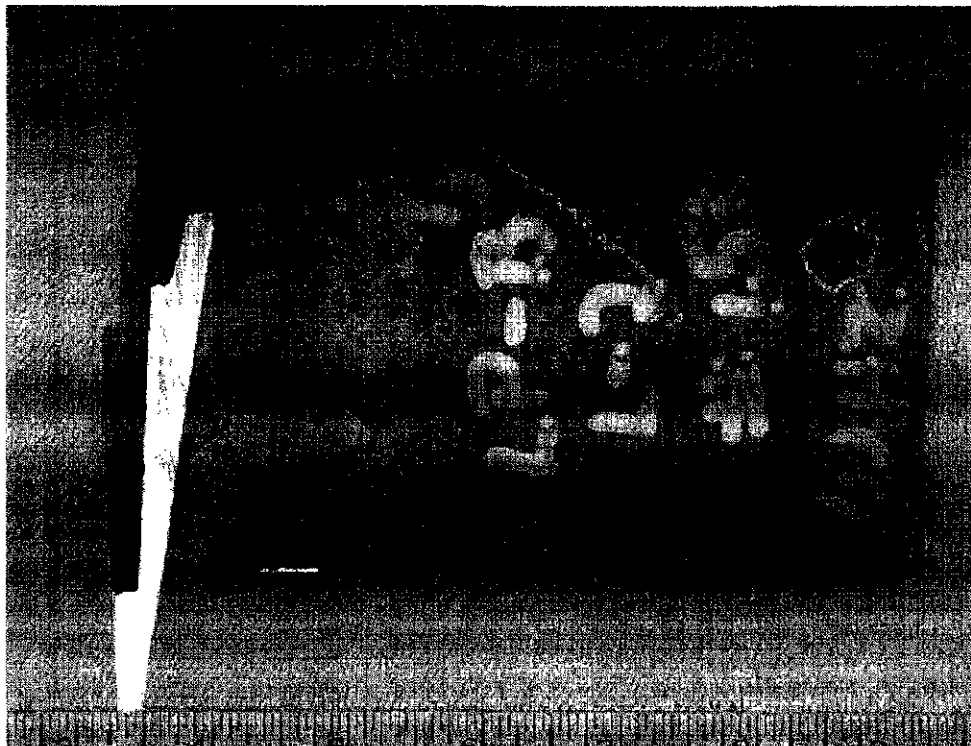


Figure: 4 LPB blade 150, third in group. Enlarged View of cracks looking on concave side (opposite side of Figure 3)

Macro-05

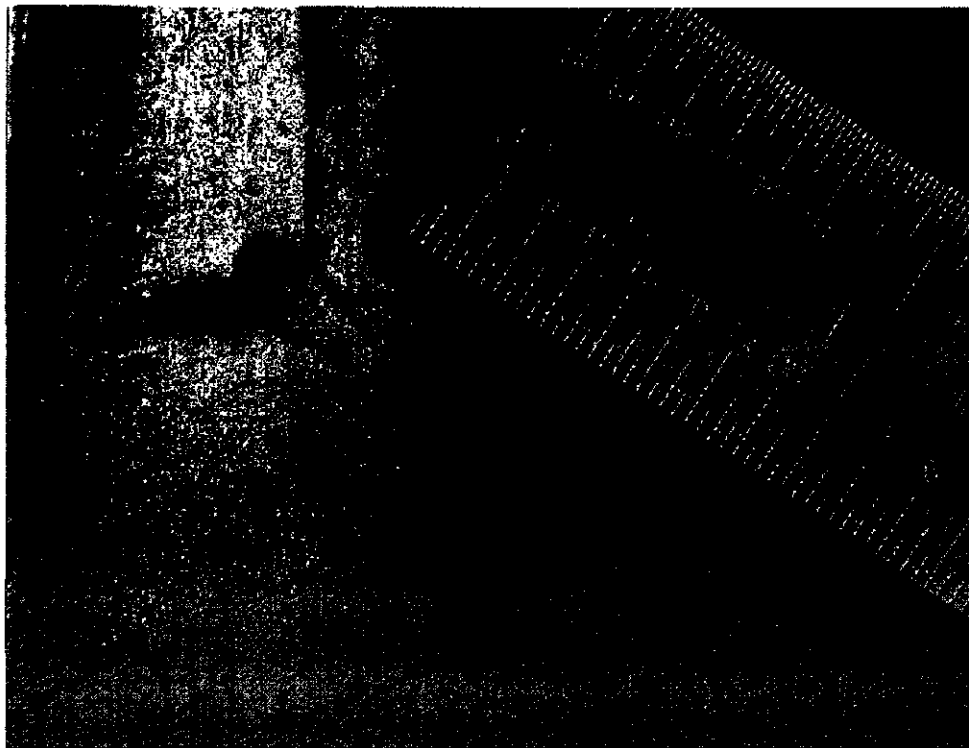


Figure: 5 LPB blade 150, third in group. Enlarged View of cracks looking on concave side (opposite side of Figure 3)

Macro-08



Figure: 6 Fracture surfaces from LPA-115 (left) and LPA-58 blades that were broken as received in laboratory.

Macro-12
Macro-14

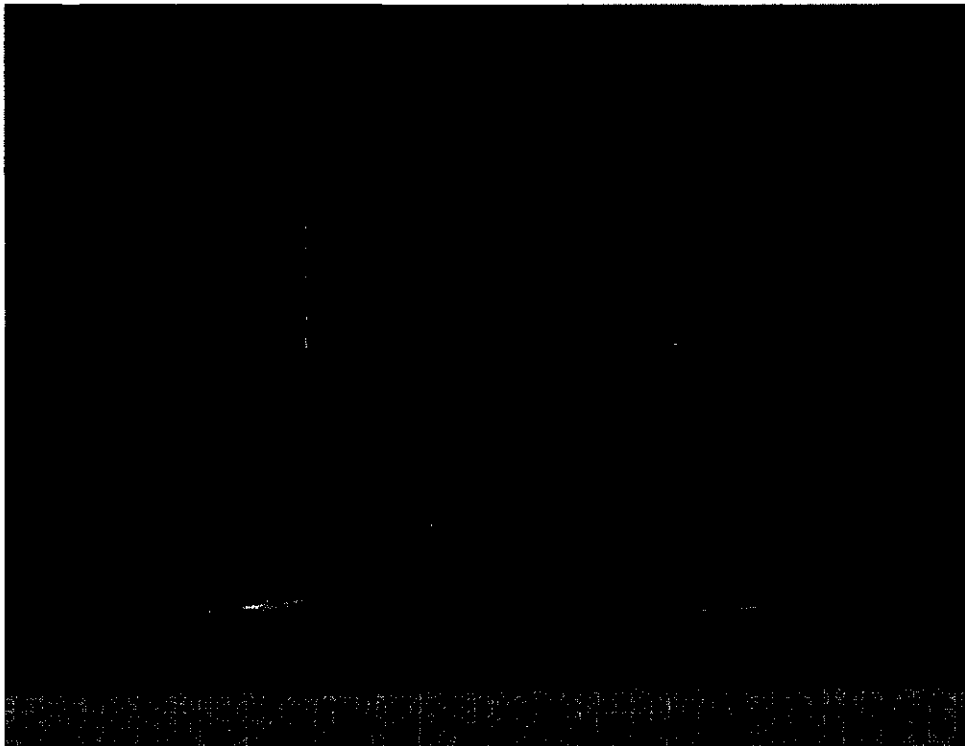


Figure: 7 .L-3 blade as-received. Note crack in shroud aligned with crack in tenon.

Macro-16

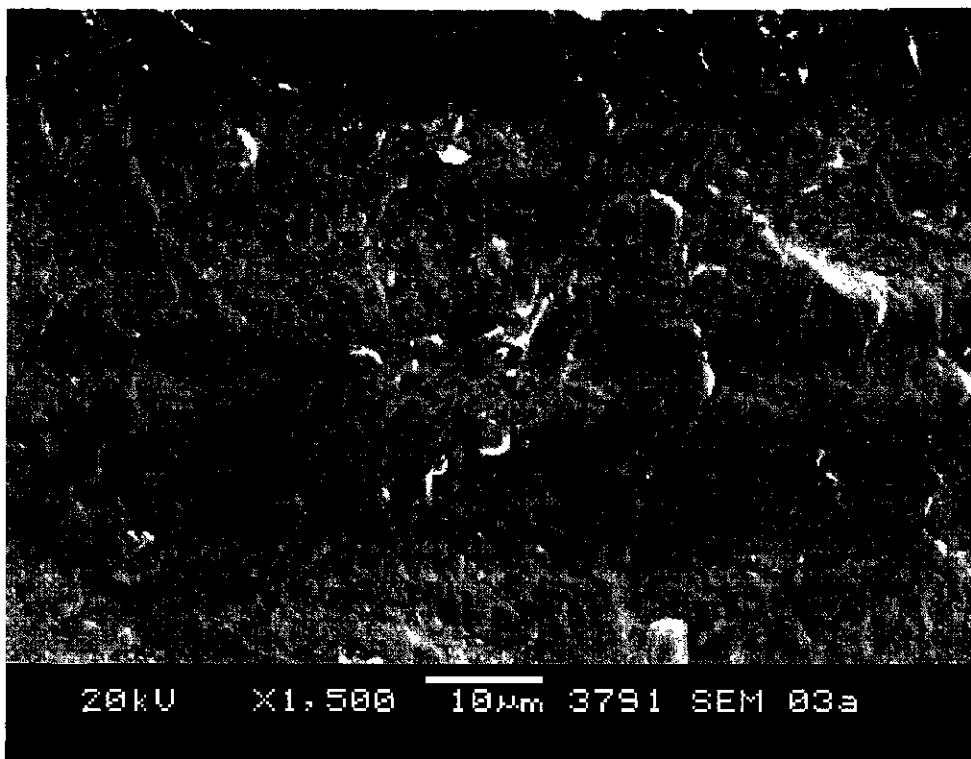


Figure: 8 SEM micrograph of fracture face near leading edge of blade from LPA. Features are characteristic of striated fatigue.

SEM-3a
SEI

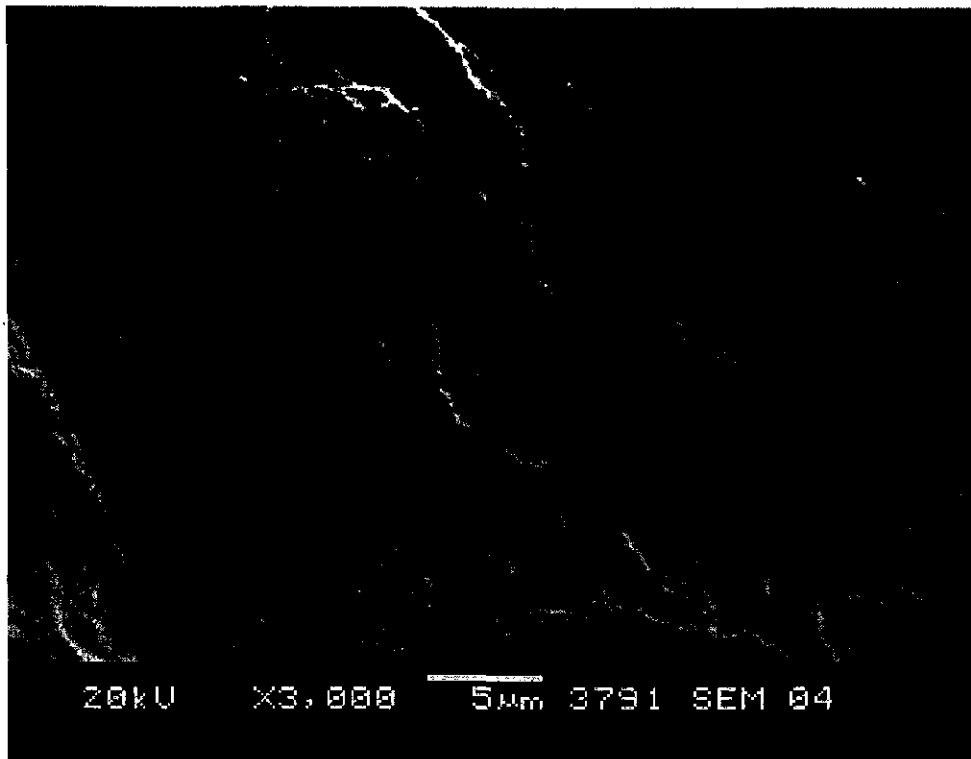


Figure: 9 SEM micrograph of fracture face near trailing edge of blade from LPA. Features are characteristic of striated fatigue.

SEM-04
SEI

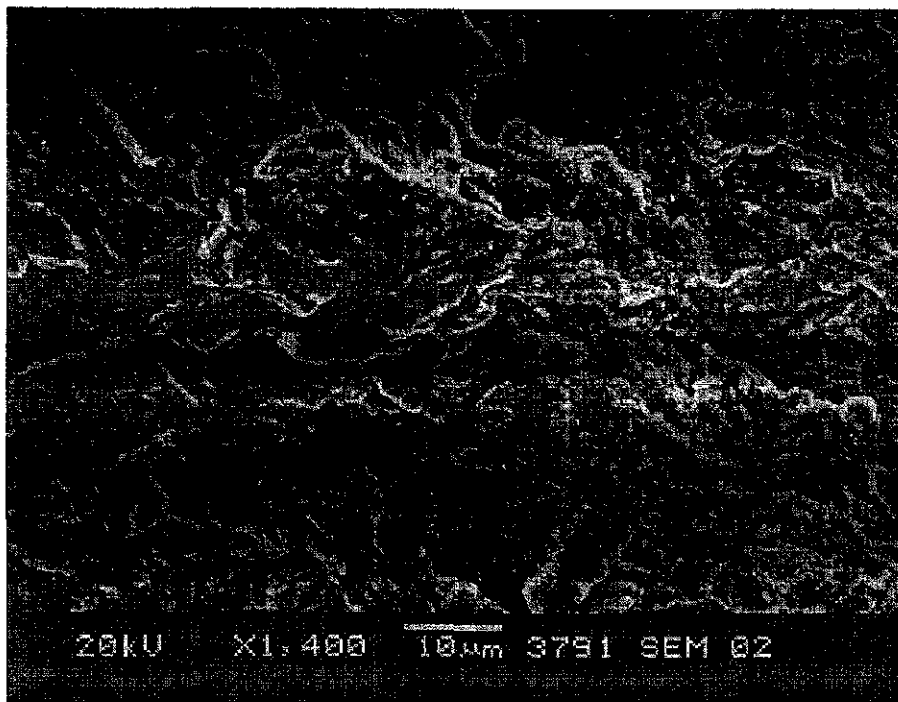


Figure: 10 SEM micrograph of opened crack near leading edge of blade from LPB. Features are characteristic of striated fatigue.

SEM-02
SEI

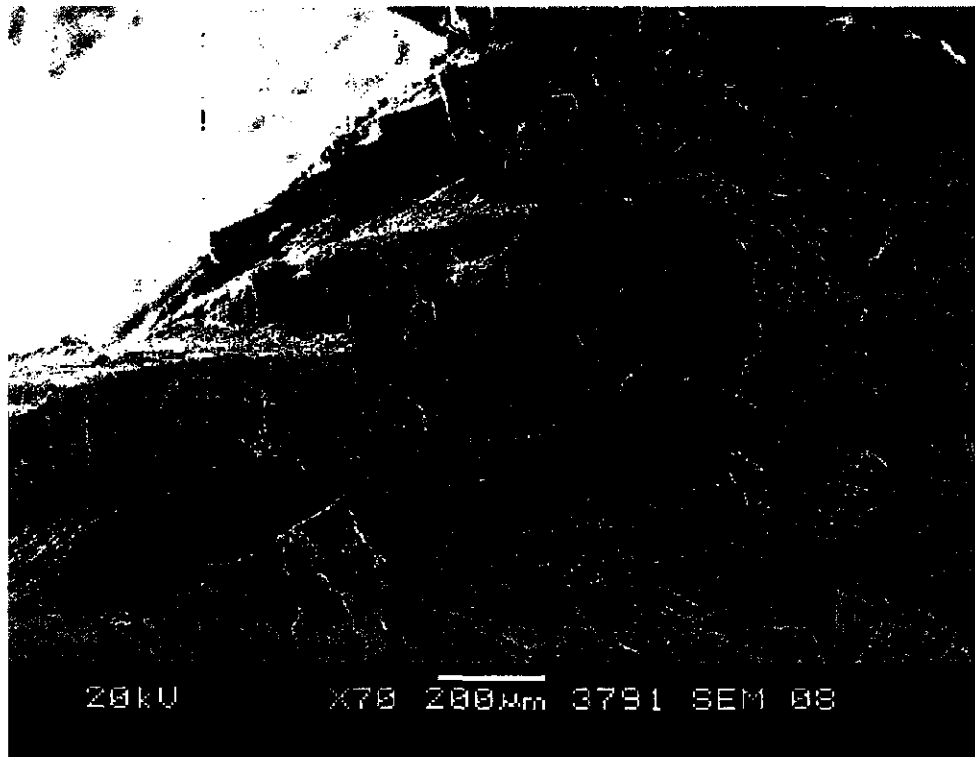


Figure: 11 Fracture produced in lab by opening crack in tenon. Note secondary cracking at top edge of picture

SEM-08
SEI

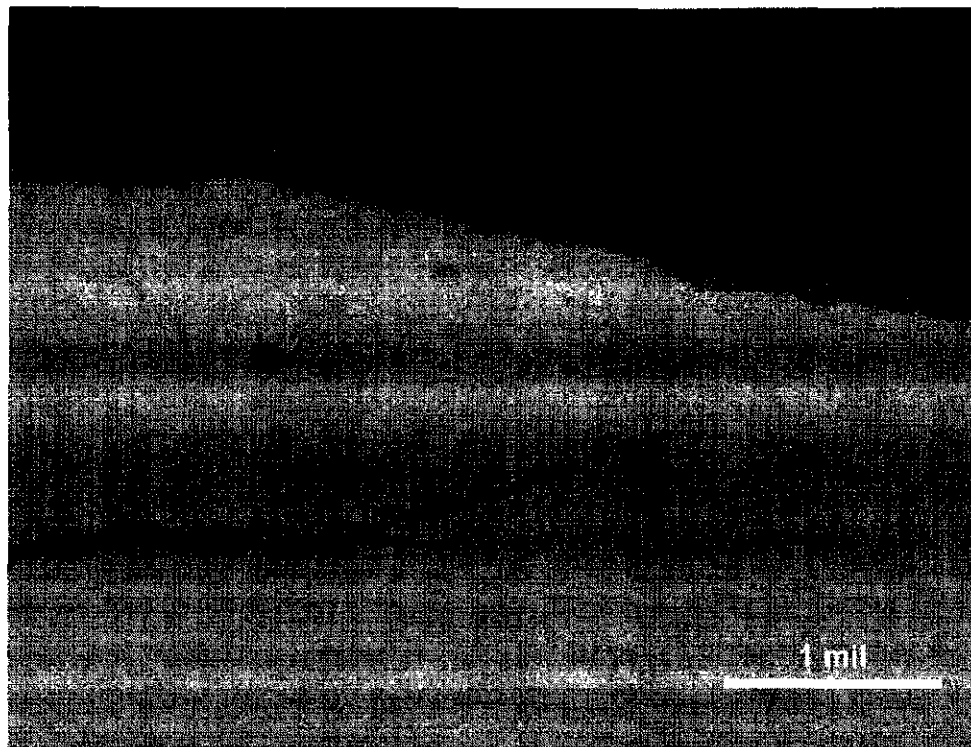


Figure: 12 Transverse cross section through crack in LPB blade (axis of blade runs into paper). Cracking is mixed transgranular and intergranular.

Micro-01a
Vilela's etch

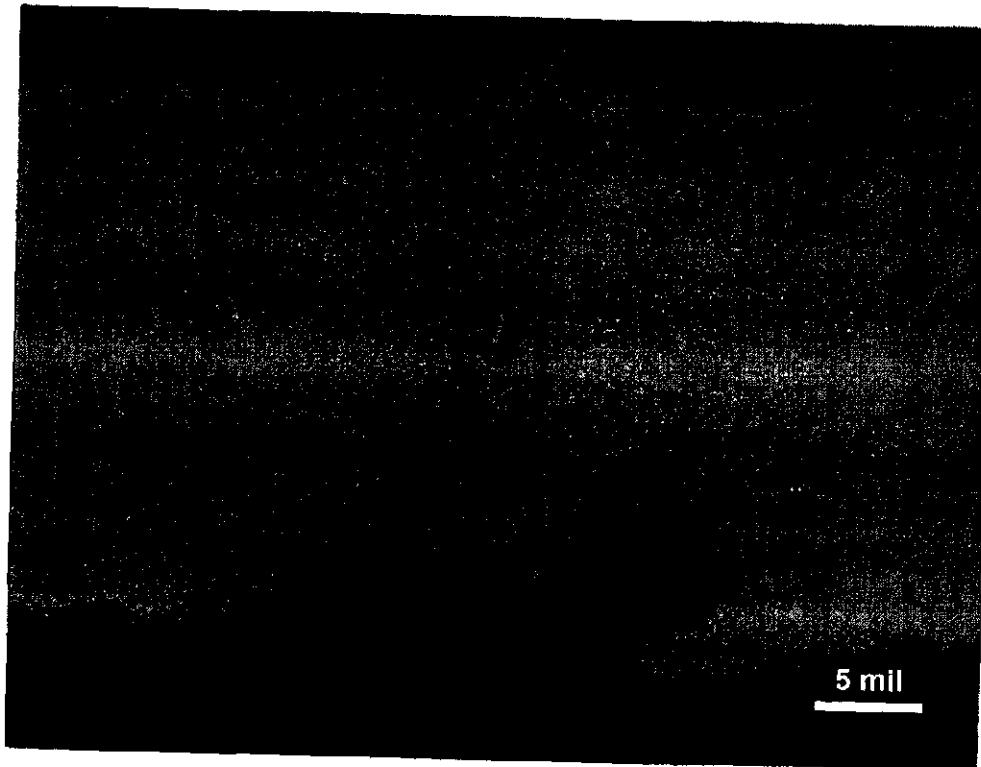


Figure: 13 Stress corrosion cracking at base of a pit on convex surface.

Micro-03
Villega's etch

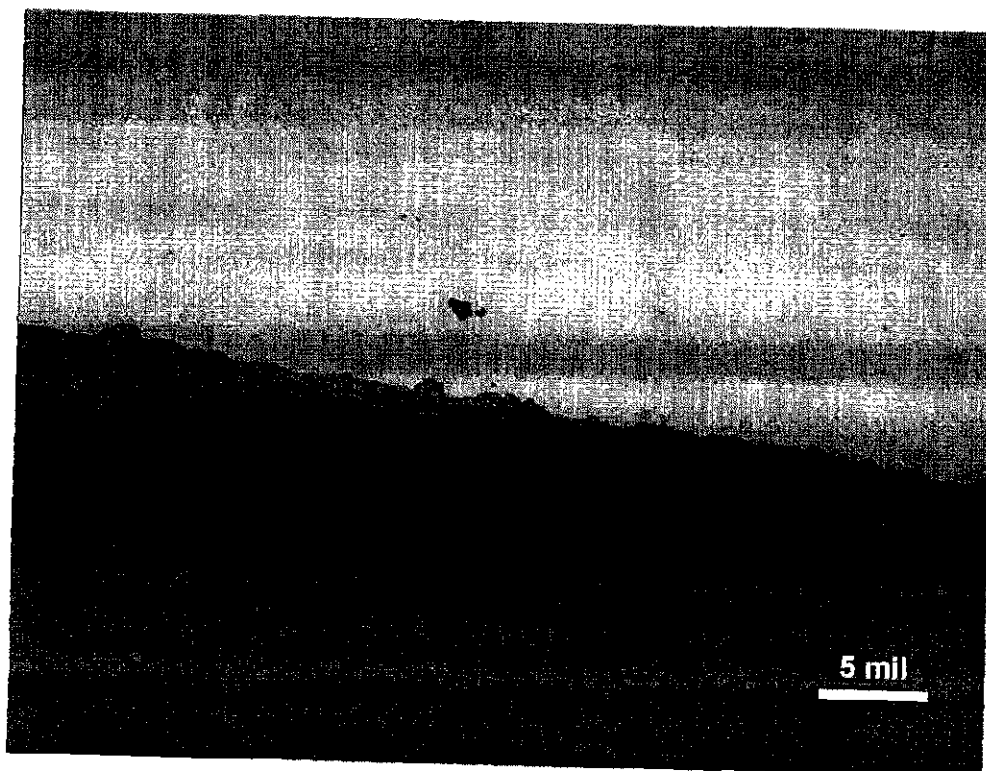


Figure: 14 Cross section through typical deposit on convex face.
Note copper association with pits.

Micro-04
Unetched



Figure: 15 Section through crack in tenon. Axis of tenon is parallel to crack. Peened head is at upper left.

Micro-09
Unetched

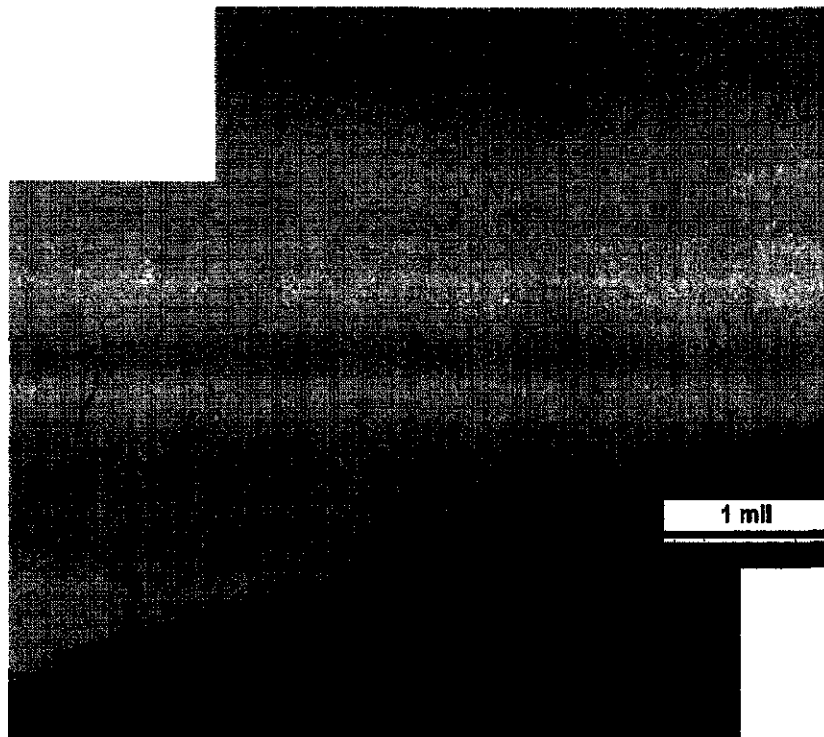


Figure: 16 Secondary cracking along main crack in tenon. Edge at bottom of photo is surface of main crack parallel to tenon axis.

Micro-14
Villega's etch

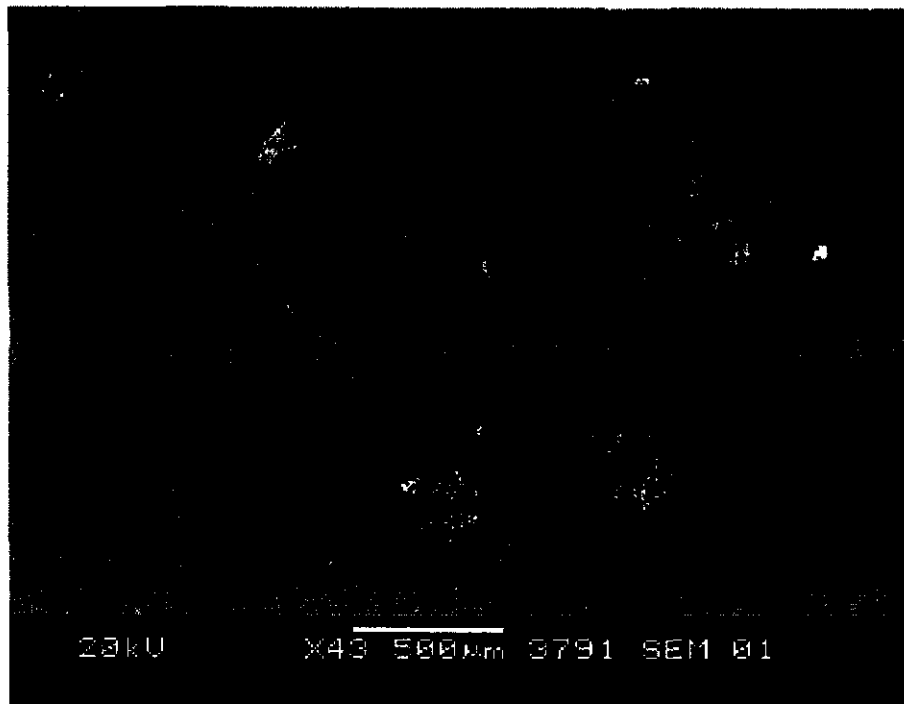


Figure: 17 Deposit particles scraped from the surface of one of the LPA L-2 blades. Lighter areas indicate the presence of heavier elements such as copper, iron, chromium and nickel.

SEM-01
BEI

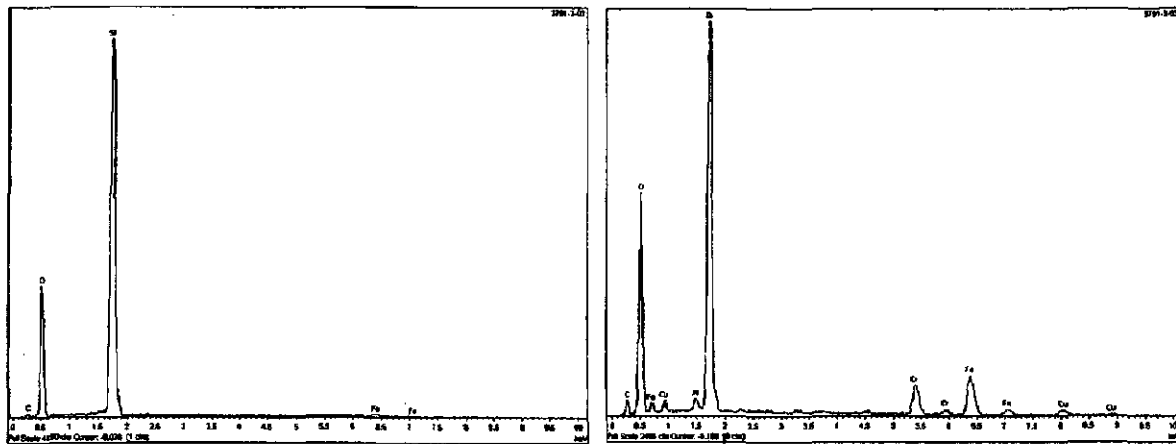


Figure: 18 EDS spectra of particles at left and bottom of Figure 13. Composition variation is typical from particle to particle.

3791-3-02
3791-3-03

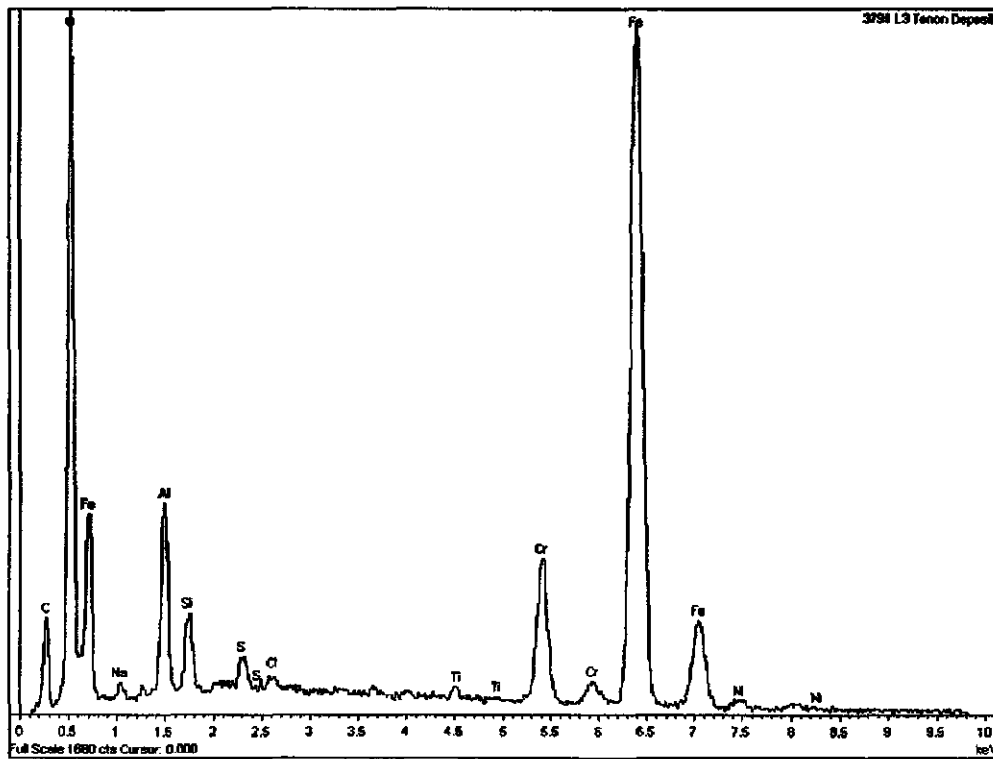


Figure: 19 EDS spectrum of material in L-3 tenon crevice.

3791-L3

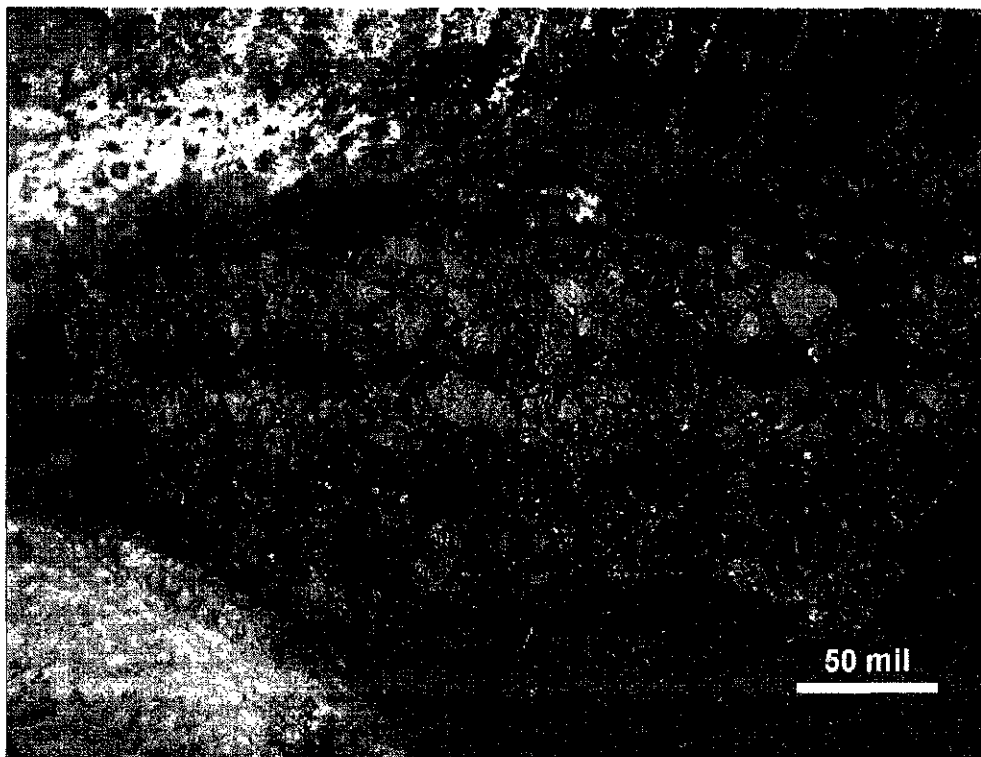


Figure: 20 Angular magnetic deposits under shroud.

Stereo-03



DEC 31 1984

Westinghouse
Electric Corporation

840 Williams Avenue
Columbus Ohio 43212

(614) 297-6223
December 27, 1984

American Electric Power Service Corp.
One Riverside Plaza
P. O. Box 16631
Columbus, Ohio 43216-6631

Attn: Mr. ~~W~~ Lodge

Subject: Zimmer Generating Plant - Study of
Shrink Fit and Eccentric Loading of LP Rotors

Dear Steve:

Enclosed is the report detailing the results of the subject studies on the Westinghouse LP rotor at Zimmer. A summary of this information was sent to you last week. This completes the work scope authorized in your order 06566-610-4N, our CNE-92003.

Please let us know if you have any additional questions.

Very truly yours,

A handwritten signature in cursive script that reads "P. L. Weissman".

P. L. Weissman
Special Sales Representative

PLW/sr
Encl.

AMERICAN ELECTRIC POWER

ZIMMER UNIT

CNE 92003 (23A4162)

12/20/84

Abstract: This study was commissioned to analyze the feasibility of changing the LP inlet steam conditions from a nuclear cycle to a fossil cycle.

The results indicate the conversion is feasible and that up to 700°F inlet temperature is acceptable.

SUMMARY

The following highlights are the findings regarding whether or not the LP's on CG&E's Zimmer #1 unit, could be changed from nuclear cycle steam conditions (typical 493°F LP inlet) to fossil cycle steam conditions (700°F LP inlet):

1. The stationary components have been reviewed and were found to have no problem at 700°F inlet temperature. Actual stress values were compared to temperature dependent allowable stresses that have been developed for the materials used. All values pass easily.
2. The rotating components were analyzed and the only area of concern was the shrink fit on the first disc on the LP shaft. The following highlights the findings:
 - a. The disc #1 has .102" shrink fit on dia. at 0 RPM. Note: disc bore is 40.000 dia. nominal.
 - b. At 1800 RPM, the disc loses .062 fit due to CF alone, not including temperature effects, leaving .040 residual fit.
 - c. Thermal gradients during a cold start, assuming 672°F inlet temperature (see Table 1 for projected worst case radial temperature gradients), are projected to cause a loss of fit of .035. This adds to the CF loss of fit, leaving .005 final fit. Any value exceeding .000 is acceptable.
 - d. Thermal gradients during a cold start, assuming 700°F inlet temperature causes a loss of fit of .0365, (leaving .0035 final fit. This is more marginal than 2(c) but is acceptable.
 - e. Removing row 1R increases disc neck stresses due to eccentric loading, but they are acceptable. Table 2 summarizes stresses at several critical locations. All stresses can be found in the computer output located in the Appendix. Shrink fit is adversely impacted by an additional .0003, but this should not be a problem since the inlet temperature will be much lower with row 1R removed (i.e. 582°F), hence negating a concern regarding shrink fit.

One might be concerned that the .0035 fit remaining due to a 700°F inlet may be within the calculation accuracy, specifically regarding projecting thermal gradients. A more exacting calculation is available, but additional design effort would require approximately four weeks. It also requires, as input, a time history of flows and temperatures.

However, the .0035 fit remaining due to a 700°F cold start is conservative since it resulted from an analysis at the disc centerline. Since the disc outlet is significantly cooler than the disc centerline, it will have additional fit. As long as there is fit remaining at any disc bore location, there will be no problem.

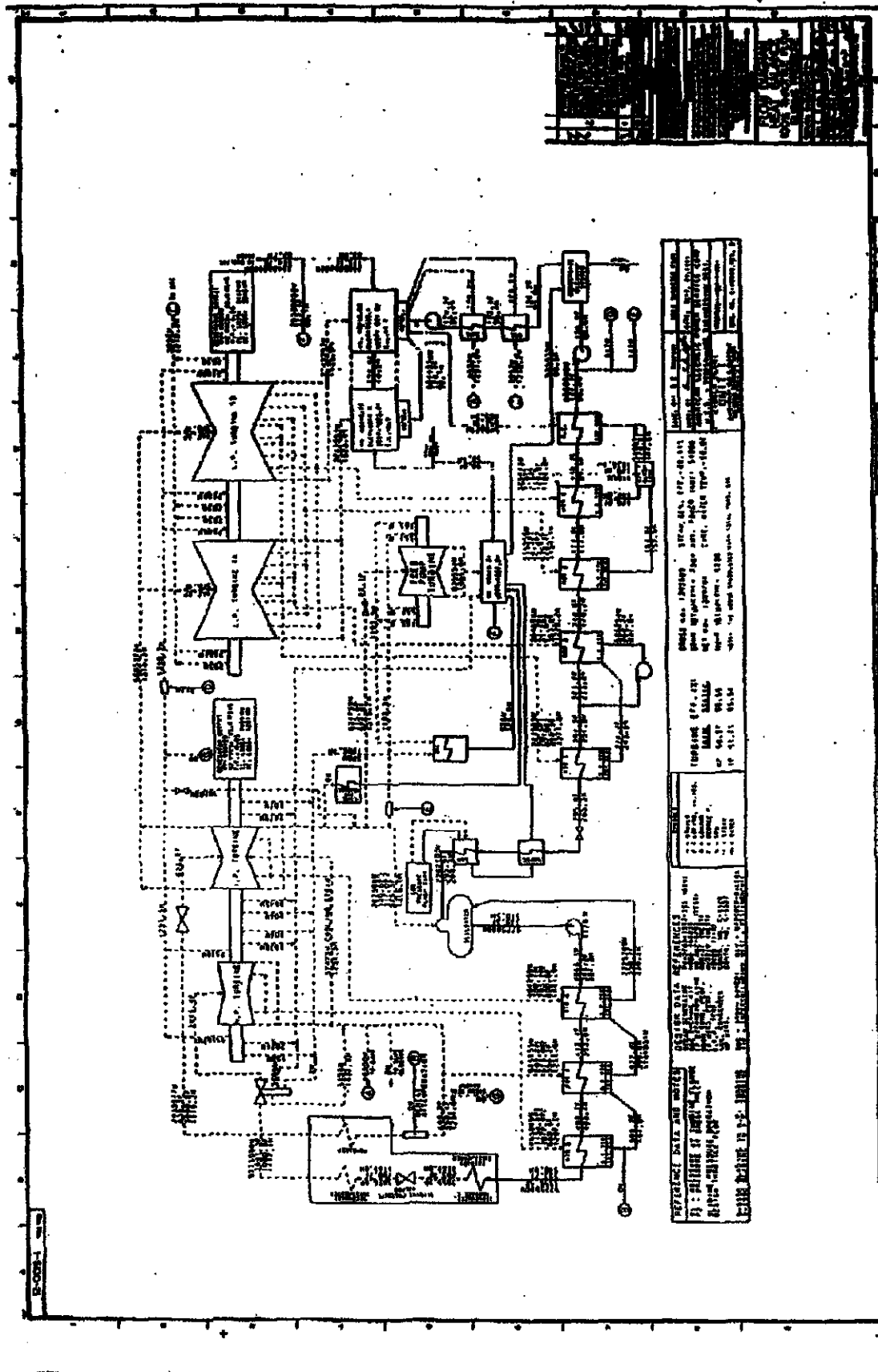
Page 2

A point worth mentioning is that loss of fit, if it happened, would be a temporary condition. For example, during a cold start, the disc might lose fit 2 hours into the start up, but regain it 4 hours into the cycle as the rotor temperature "catches up" to the disc temperature. See Figure 1 for an analysis on a nuclear LP rotor similar to CGSE. At steady state, the shrink fit is probably close to .015.

The bottom line is that a 700°F inlet temperature is acceptable. Sufficient margin exists in all analyses and, therefore, no additional studies are recommended.

Mike Lloyd

Robert M. Lloyd
Charlotte Product Engineering
Westinghouse-Steam Turbine Division



1. TITLE: STEAM ENGINE		2. DATE: 10/1/1918		3. DRAWN BY: J. H. HARRIS		4. CHECKED BY: J. H. HARRIS		5. APPROVED BY: J. H. HARRIS	
6. SCALE: 1/2" = 1"		7. MATERIAL: STEEL		8. FINISH: POLISHED		9. WEIGHT: 100 LBS.		10. PRICE: \$100.00	
11. PARTS LIST:		1. STEAM ENGINE		2. VALVE		3. PISTON		4. CYLINDER	
5. CRANK		6. CONNECTING ROD		7. BEARING		8. SHAFT		9. GEAR	
10. BELT		11. PUMP		12. VALVE		13. PISTON		14. CYLINDER	
15. CRANK		16. CONNECTING ROD		17. BEARING		18. SHAFT		19. GEAR	
20. BELT		21. PUMP		22. VALVE		23. PISTON		24. CYLINDER	
25. CRANK		26. CONNECTING ROD		27. BEARING		28. SHAFT		29. GEAR	
30. BELT		31. PUMP		32. VALVE		33. PISTON		34. CYLINDER	
35. CRANK		36. CONNECTING ROD		37. BEARING		38. SHAFT		39. GEAR	
40. BELT		41. PUMP		42. VALVE		43. PISTON		44. CYLINDER	
45. CRANK		46. CONNECTING ROD		47. BEARING		48. SHAFT		49. GEAR	
50. BELT		51. PUMP		52. VALVE		53. PISTON		54. CYLINDER	
55. CRANK		56. CONNECTING ROD		57. BEARING		58. SHAFT		59. GEAR	
60. BELT		61. PUMP		62. VALVE		63. PISTON		64. CYLINDER	
65. CRANK		66. CONNECTING ROD		67. BEARING		68. SHAFT		69. GEAR	
70. BELT		71. PUMP		72. VALVE		73. PISTON		74. CYLINDER	
75. CRANK		76. CONNECTING ROD		77. BEARING		78. SHAFT		79. GEAR	
80. BELT		81. PUMP		82. VALVE		83. PISTON		84. CYLINDER	
85. CRANK		86. CONNECTING ROD		87. BEARING		88. SHAFT		89. GEAR	
90. BELT		91. PUMP		92. VALVE		93. PISTON		94. CYLINDER	
95. CRANK		96. CONNECTING ROD		97. BEARING		98. SHAFT		99. GEAR	
100. BELT		101. PUMP		102. VALVE		103. PISTON		104. CYLINDER	
105. CRANK		106. CONNECTING ROD		107. BEARING		108. SHAFT		109. GEAR	
110. BELT		111. PUMP		112. VALVE		113. PISTON		114. CYLINDER	
115. CRANK		116. CONNECTING ROD		117. BEARING		118. SHAFT		119. GEAR	
120. BELT		121. PUMP		122. VALVE		123. PISTON		124. CYLINDER	
125. CRANK		126. CONNECTING ROD		127. BEARING		128. SHAFT		129. GEAR	
130. BELT		131. PUMP		132. VALVE		133. PISTON		134. CYLINDER	
135. CRANK		136. CONNECTING ROD		137. BEARING		138. SHAFT		139. GEAR	
140. BELT		141. PUMP		142. VALVE		143. PISTON		144. CYLINDER	
145. CRANK		146. CONNECTING ROD		147. BEARING		148. SHAFT		149. GEAR	
150. BELT		151. PUMP		152. VALVE		153. PISTON		154. CYLINDER	
155. CRANK		156. CONNECTING ROD		157. BEARING		158. SHAFT		159. GEAR	
160. BELT		161. PUMP		162. VALVE		163. PISTON		164. CYLINDER	
165. CRANK		166. CONNECTING ROD		167. BEARING		168. SHAFT		169. GEAR	
170. BELT		171. PUMP		172. VALVE		173. PISTON		174. CYLINDER	
175. CRANK		176. CONNECTING ROD		177. BEARING		178. SHAFT		179. GEAR	
180. BELT		181. PUMP		182. VALVE		183. PISTON		184. CYLINDER	
185. CRANK		186. CONNECTING ROD		187. BEARING		188. SHAFT		189. GEAR	
190. BELT		191. PUMP		192. VALVE		193. PISTON		194. CYLINDER	
195. CRANK		196. CONNECTING ROD		197. BEARING		198. SHAFT		199. GEAR	
200. BELT		201. PUMP		202. VALVE		203. PISTON		204. CYLINDER	
205. CRANK		206. CONNECTING ROD		207. BEARING		208. SHAFT		209. GEAR	
210. BELT		211. PUMP		212. VALVE		213. PISTON		214. CYLINDER	
215. CRANK		216. CONNECTING ROD		217. BEARING		218. SHAFT		219. GEAR	
220. BELT		221. PUMP		222. VALVE		223. PISTON		224. CYLINDER	
225. CRANK		226. CONNECTING ROD		227. BEARING		228. SHAFT		229. GEAR	
230. BELT		231. PUMP		232. VALVE		233. PISTON		234. CYLINDER	
235. CRANK		236. CONNECTING ROD		237. BEARING		238. SHAFT		239. GEAR	
240. BELT		241. PUMP		242. VALVE		243. PISTON		244. CYLINDER	
245. CRANK		246. CONNECTING ROD		247. BEARING		248. SHAFT		249. GEAR	
250. BELT		251. PUMP		252. VALVE		253. PISTON		254. CYLINDER	
255. CRANK		256. CONNECTING ROD		257. BEARING		258. SHAFT		259. GEAR	
260. BELT		261. PUMP		262. VALVE		263. PISTON		264. CYLINDER	
265. CRANK		266. CONNECTING ROD		267. BEARING		268. SHAFT		269. GEAR	
270. BELT		271. PUMP		272. VALVE		273. PISTON		274. CYLINDER	
275. CRANK		276. CONNECTING ROD		277. BEARING		278. SHAFT		279. GEAR	
280. BELT		281. PUMP		282. VALVE		283. PISTON		284. CYLINDER	
285. CRANK		286. CONNECTING ROD		287. BEARING		288. SHAFT		289. GEAR	
290. BELT		291. PUMP		292. VALVE		293. PISTON		294. CYLINDER	
295. CRANK		296. CONNECTING ROD		297. BEARING		298. SHAFT		299. GEAR	
300. BELT		301. PUMP		302. VALVE		303. PISTON		304. CYLINDER	
305. CRANK		306. CONNECTING ROD		307. BEARING		308. SHAFT		309. GEAR	
310. BELT		311. PUMP		312. VALVE		313. PISTON		314. CYLINDER	
315. CRANK		316. CONNECTING ROD		317. BEARING		318. SHAFT		319. GEAR	
320. BELT		321. PUMP		322. VALVE		323. PISTON		324. CYLINDER	
325. CRANK		326. CONNECTING ROD		327. BEARING		328. SHAFT		329. GEAR	
330. BELT		331. PUMP		332. VALVE		333. PISTON		334. CYLINDER	
335. CRANK		336. CONNECTING ROD		337. BEARING		338. SHAFT		339. GEAR	
340. BELT		341. PUMP		342. VALVE		343. PISTON		344. CYLINDER	
345. CRANK		346. CONNECTING ROD		347. BEARING		348. SHAFT		349. GEAR	
350. BELT		351. PUMP		352. VALVE		353. PISTON		354. CYLINDER	
355. CRANK		356. CONNECTING ROD		357. BEARING		358. SHAFT		359. GEAR	
360. BELT		361. PUMP		362. VALVE		363. PISTON		364. CYLINDER	
365. CRANK		366. CONNECTING ROD		367. BEARING		368. SHAFT		369. GEAR	
370. BELT		371. PUMP		372. VALVE		373. PISTON		374. CYLINDER	
375. CRANK		376. CONNECTING ROD		377. BEARING		378. SHAFT		379. GEAR	
380. BELT		381. PUMP		382. VALVE		383. PISTON		384. CYLINDER	
385. CRANK		386. CONNECTING ROD		387. BEARING		388. SHAFT		389. GEAR	
390. BELT		391. PUMP		392. VALVE		393. PISTON		394. CYLINDER	
395. CRANK		396. CONNECTING ROD		397. BEARING		398. SHAFT		399. GEAR	
400. BELT		401. PUMP		402. VALVE		403. PISTON		404. CYLINDER	
405. CRANK		406. CONNECTING ROD		407. BEARING		408. SHAFT		409. GEAR	
410. BELT		411. PUMP		412. VALVE		413. PISTON		414. CYLINDER	
415. CRANK		416. CONNECTING ROD		417. BEARING		418. SHAFT		419. GEAR	
420. BELT		421. PUMP		422. VALVE		423. PISTON		424. CYLINDER	
425. CRANK		426. CONNECTING ROD		427. BEARING		428. SHAFT		429. GEAR	
430. BELT		431. PUMP		432. VALVE		433. PISTON		434. CYLINDER	
435. CRANK		436. CONNECTING ROD		437. BEARING		438. SHAFT		439. GEAR	
440. BELT		441. PUMP		442. VALVE		443. PISTON		444. CYLINDER	
445. CRANK		446. CONNECTING ROD		447. BEARING		448. SHAFT		449. GEAR	
450. BELT		451. PUMP		452. VALVE		453. PISTON		454. CYLINDER	
455. CRANK		456. CONNECTING ROD		457. BEARING		458. SHAFT		459. GEAR	
460. BELT		461. PUMP		462. VALVE		463. PISTON		464. CYLINDER	
465. CRANK		466. CONNECTING ROD		467. BEARING		468. SHAFT		469. GEAR	
470. BELT		471. PUMP		472. VALVE		473. PISTON		474. CYLINDER	
475. CRANK		476. CONNECTING ROD		477. BEARING		478. SHAFT		479. GEAR	
480. BELT		481. PUMP		482. VALVE		483. PISTON		484. CYLINDER	
485. CRANK		486. CONNECTING ROD		487. BEARING		488. SHAFT		489. GEAR	
490. BELT		491. PUMP		492. VALVE		493. PISTON		494. CYLINDER	
495. CRANK		496. CONNECTING ROD		497. BEARING		498. SHAFT		499. GEAR	
500. BELT		501. PUMP		502. VALVE		503. PISTON		504. CYLINDER	
505. CRANK		506. CONNECTING ROD		507. BEARING		508. SHAFT		509. GEAR	
510. BELT		511. PUMP		512. VALVE		513. PISTON		514. CYLINDER	
515. CRANK		516. CONNECTING ROD		517. BEARING		518. SHAFT		519. GEAR	
520. BELT		521. PUMP		522. VALVE		523. PISTON		524. CYLINDER	
525. CRANK		526. CONNECTING ROD		527. BEARING		528. SHAFT		529. GEAR	
530. BELT		531. PUMP		532. VALVE		533. PISTON		534. CYLINDER	
535. CRANK		536. CONNECTING ROD		537. BEARING		538. SHAFT		539. GEAR	
540. BELT		541. PUMP		542. VALVE		543. PISTON		544. CYLINDER	
545. CRANK		546. CONNECTING ROD		547. BEARING		548. SHAFT		549. GEAR	
550. BELT		551. PUMP		552. VALVE		553. PISTON		554. CYLINDER	
555. CRANK		556. CONNECTING ROD		557. BEARING		558. SHAFT		559. GEAR	
560. BELT		561. PUMP		562. VALVE		563. PISTON		564. CYLINDER	
565. CRANK		566. CONNECTING ROD		567. BEARING		568. SHAFT		569. GEAR	
570. BELT		571. PUMP		572. VALVE		573. PISTON		574. CYLINDER	
575. CRANK		576. CONNECTING ROD		577. BEARING		578. SHAFT		579. GEAR	
580. BELT		581. PUMP		582. VALVE		583. PISTON		584. CYLINDER	
585. CRANK		586. CONNECTING ROD		587. BEARING		588. SHAFT		589. GEAR	
590. BELT		591. PUMP		592. VALVE		593. PISTON		594. CYLINDER	
595. CRANK		596. CONNECTING ROD		597. BEARING		598. SHAFT		599. GEAR	
600. BELT		601. PUMP		602. VALVE		603. PISTON		604. CYLINDER	
605. CRANK		606. CONNECTING ROD		607. BEARING		608. SHAFT		609. GEAR	
610. BELT		611. PUMP		612. VALVE		613. PISTON		614. CYLINDER	
615. CRANK		616. CONNECTING ROD		617. BEARING		618. SHAFT		619. GEAR	
620. BELT		621. PUMP		622. VALVE		623. PISTON		624. CYLINDER	
625. CRANK		626. CONNECTING ROD		627. BEARING		628. SHAFT		629. GEAR	
630. BELT		631. PUMP		632. VALVE		633. PISTON		634. CYLINDER	
635. CRANK		636. CONNECTING ROD		637. BEARING		638. SHAFT		639. GEAR	
640. BELT		641. PUMP		642. VALVE		643. PISTON		644. CYLINDER	
645. CRANK		646. CONNECTING ROD		647. BEARING		648. SHAFT		649. GEAR	
650. BELT		651. PUMP		652. VALVE		653. PISTON		654. CYLINDER	
655. CRANK		656. CONNECTING ROD		657. BEARING		658. SHAFT		659. GEAR	
660. BELT		661. PUMP		662. VALVE		663. PISTON		664. CYLINDER	
665. CRANK		666. CONNECTING ROD		667. BEARING		668. SHAFT		669. GEAR	
670. BELT		671. PUMP		672. VALVE		673. PISTON		674. CYLINDER	
675. CRANK		676. CONNECTING ROD		677. BEARING		678. SHAFT		679. GEAR	
680. BELT		681. PUMP		682. VALVE		683. PISTON		684. CYLINDER	
685. CRANK		686. CONNECTING ROD		687. BEARING		688. SHAFT		689. GEAR	
690. BELT		691. PUMP		692. VALVE		693. PISTON		694. CYLINDER	
695. CRANK		696. CONNECTING ROD		697. BEARING		698. SHAFT		699. GEAR	
700. BELT		701. PUMP		702. VALVE		703. PISTON		704. CYLINDER	
705. CRANK		706. CONNECTING ROD		707. BEARING		708. SHAFT		709. GEAR	
710. BELT		711. PUMP		712. VALVE		713. PISTON		714. CYLINDER	
715. CRANK		716. CONNECTING ROD		717. BEARING		718. SHAFT		719. GEAR	
720. BELT		721. PUMP		722. VALVE		723. PISTON		724. CYLINDER	
725. CRANK		726. CONNECTING ROD		727. BEARING		728. SHAFT		729. GEAR	
730. BELT		731. PUMP		732. VALVE		733. PISTON		734. CYLINDER	
735. CRANK		736. CONNECTING ROD		737. BEARING		738. SHAFT		739. GEAR	
740. BELT		741. PUMP		742. VALVE		743. PISTON		744. CYLINDER	
745. CRANK		746. CONNECTING ROD		747. BEARING		748. SHAFT		749. GEAR	
750. BELT		751. PUMP		752. VALVE		753. PISTON		754. CYLINDER	
755. CRANK		756. CONNECTING ROD		757. BEARING		758. SHAFT		759. GEAR	
760. BELT		761. PUMP		762. VALVE		763. PISTON		764. CYLINDER	
765. CRANK		766. CONNECTING ROD		767. BEARING		768. SHAFT		769. GEAR	
770. BELT		771. PUMP		772. VALVE		773. PISTON		774. CYLINDER	
775. CRANK		776. CONNECTING ROD		777. BEARING		778. SHAFT		779. GEAR	
780. BELT		781. PUMP		782. VALVE		783. PISTON		784. CYLINDER	
785. CRANK		786. CONNECTING ROD		787. BEARING		788. SHAFT		789. GEAR	
790. BELT		791. PUMP		792. VALVE		793. PISTON		794. CYLINDER	
795. CRANK		796. CONNECTING ROD		797. BEARING		798. SHAFT		799. GEAR	
800. BELT		801. PUMP		802. VALVE		803. PISTON		804. CYLINDER	
805. CRANK		806. CONNECTING ROD		807. BEARING		808. SHAFT		809. GEAR	
810. BELT		811. PUMP		812. VALVE		813. PISTON			



Westinghouse
Electric Corporation

940 Williams Avenue
Columbus Ohio 43212
(614) 297-6223
September 24, 1984

American Electric Power Service Corporation
One Riverside Plaza
P.O. Box 16631
Columbus, Ohio 43216-6631

Attn: Mr. Steve Hodge

Westinghouse LP Turbine at the
Zimmer Plant

Dear Steve:

In response to several questions raised by A.E.P. during our conference call discussion on September 5, the Westinghouse Steam Turbine Generator Division in Orlando, Florida has answered as follows:

- A. Case 1 - As installed LP design, pressure-flow at the entrance to the LP turbines -

6,675,928 lb./hr.
176 psia
1362.0 BTU/lb.
672.0 deg. F

- B. Case 2 - LP with first stage removed, pressure-flow at the entrance to the LP turbines -

6,520,000 lb./hr.
116 psia
1319.0 BTU/lb.
582.0 deg. F (2nd stage temp.)

Based on our engineering evaluation and experience, the use of 650°F at the turbine inlet is considered acceptable with one reservation. A shell analysis of the No. 1 disc under the first three stages should be performed to verify tightness at this elevated temperature. If loosening is indicated, a tightening procedure would be developed. This would require returning the rotors to Westinghouse, de-stacking the discs, tightening, re-stacking discs and returning the rotors to the Zimmer Plant. This analysis can be performed at a price of \$9,800.00 and will require about 2 months. An approximate price to work on the rotors at our facility in Charlotte, NC (if needed) is \$700,000.00.

American Electric Power Service Corporation
September 24, 1984
Page 2

Operation at 650°F with first stage removed would require that a study of the eccentric loading on the No. 1 disc be performed; this will take about 2 months and cost \$9,800.00. The shrink-fit analysis would not be needed.

Methods you might consider to reduce temperature to 650°F are:

- a) reduce IP inlet temperature about 40 deg. F -- pressure-flow would then be --

6,675,298 lb./hr.
174 psia
1350 BTU/lb.
650°F

- b) reduce the flow resistance of the LP turbine initial stages (Westinghouse to change gauging of first two rows of stationary stages) to allow hot reheat temperature to be maintained at 1000°F -- pressure-flow would then be --

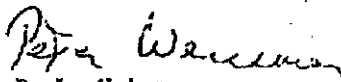
6,675,298 lb./hr.
160 psia
1350 BTU/lb.
650°F

NOTE: Approximate cost for two rows of stationary blading is \$153,000.00.

If operation at inlet temperatures greater than 650°F is to be considered Westinghouse will need to perform a finite element analysis of the No. 1 inner cylinder, bolting of the No. 1 inner cylinder and the rotor. This analysis can be completed in 8 months and will cost \$89,500.00 net.

Terms and conditions of sale for a study will be per Westinghouse Selling Policy 1270 dated November 1, 1982, copy enclosed. Please let us know which approach you will be considering.

Very truly yours,



P. L. Weissman
Special Sales Representative
Electric Utility Sales

PLW/d
Enclosure



Westinghouse
Electric Corporation

940 Williams Avenue
Columbus Ohio 43212

December 20, 1984
(614) 297-6223

American Electric Power Service Corp.
One Riverside Plaza
P.O. Box 16631
Columbus, Ohio 43216-6631

Subject: Zimmer Plant - Westinghouse LP Rotors
Shrink Fit and Eccentric Loading Studies

Attn: S. Hodge

Dear Steve:

The following is a summary of our work to date on the subject studies for AEP. Our final report will be available next week.

1. We have reviewed the stationary components and find them to be acceptable for operation at 700°F inlet temperature. Actual stress values were compared to temperature dependent allowable stresses that have been developed for the materials used. All values were well within our design limits.
2. The only concern that arose in the analysis of the rotating components was the shrink fit on the first disc on the LP shaft. The following highlights our findings:
 - a. The first disc has a .102 inch shrink fit on the diameter at zero RPM. The disc bore is 40 inches diameter nominal.
 - b. At 1800 RPM, the disc loses .062 inch fit due to CF which leaves .040 inch residual fit.
 - c. Our analysis concerned itself with the worst case condition which is a thermal gradient experienced during a cold start. Assuming a 672°F inlet temperature causes an additional loss of fit of .035 inch, this leaves .005 inch shrink fit which is acceptable (anything greater than .000 is acceptable). Assuming a 700°F inlet temperature causes a loss of fit of .0365 inch, this leaves .0035 inch shrink fit which is acceptable.
3. Regarding the removal of row 1R from the LP rotors, this increases the disc neck stresses due to eccentric loading. This was found to be acceptable. This shrink fit is also adversely impacted by approximately .0003 inch but this is no problem since the inlet temperature will be much lower in this case (approximately 582°F). This eliminates a concern regarding shrink fit.

- 2 -

In summary, operation at 672°F inlet temperature to the LP elements is acceptable to Westinghouse. It appears that operation at 700°F inlet temperature to the LP elements is also acceptable though the margin is decreased somewhat by the additional 28°F temperature. We are concerned that the .0035 inch fit remaining at 700°F may be within our calculation accuracy, particularly regarding projected thermal gradients. A more exacting calculation is available but this requires approximately four weeks to perform and was not possible to do given the time constraints imposed. This calculation also requires as input a time history of flows and temperatures.

Again, it should be emphasized that the analysis was done for the worst case of a cold startup condition. At steady state conditions, the shrink fit is approximately .015 inch. Therefore, a determination should be made by AEP as to what inlet conditions the rotor will see during startup. If the maximum is 672°F, then the rotors are acceptable and no further analysis is necessary. If the maximum is 700°F, we believe the rotors are acceptable but would require further analysis to produce a recommendation.

Our final report will be available next week. Until then, if you have any questions, please let us know.


P. L. Weissman
Special Sales Representative
Electric Utility Sales